EXPERIMENTAL INVESTIGATION ON THE APPLICABILITY OF FBRM IN THE CONTROL OF BATCH COOLING CRYSTALLIZATION

CHEW, JIA WEI

NATIONAL UNIVERSITY OF SINGAPORE

2006

EXPERIMENTAL INVESTIGATION ON THE APPLICABILITY OF FBRM IN THE CONTROL OF BATCH COOLING CRYSTALLIZATION

CHEW, JIA WEI
(B.Eng.(Hons.), NUS)

A THESIS SUBMITTED

FOR THE DEGREE OF MASTER OF ENGINEERING

DEPARTMENT OF CHEMICAL AND BIOMOLECULAR ENGINEERING

NATIONAL UNIVERSITY OF SINGAPORE

2006

Name : CHEW, Jia Wei

Degree : Master of Engineering (Chemical)

Department : Department of Chemical and Biomolecular Engineering

Thesis Title : Experimental Investigation on the Applicability of FBRM in the Control of Batch Cooling Crystallization

Abstract

Consistent particle properties are an important goal for industrial batch crystallizations. Several control strategies, from unseeded linear cooling to seeded supersaturation control, were evaluated for the cooling crystallization of glycine. Particle properties were assessed in-line using ATR-FTIR, FBRM, and PVM. Closed-loop supersaturation-control was not superior to open-loop temperature-control, and seeding was by far the most effective strategy in this comparison. Unseeded systems do not achieve consistency, because primary nucleation is unpredictable and do not occur at a fixed temperature. In this work, the FBRM was successfully used to detect primary nucleation, after which control strategies were automatically implemented in unseeded cooling crystallization systems. A novel technique to counter the problem of inconsistent crystal products due to randomness of primary nuclei was also proposed. This employs FBRM in a closed feedback loop, which involves adjusting the coefficient of variance (c.v.) of the primary nuclei. Consistent crystal products from unseeded systems were hence achievable.

Keywords: batch cooling crystallization, ATR-FTIR, FBRM, feedback loop, PAT

Acknowledgements

I would like to thank my advisor, Prof. Reginald Tan, for his patient guidance and relentless encouragement. I would also like to thank Dr. Ann Chow and Dr. Simon Black for rendering useful advice throughout this work. Without their advice and supervision, this work would not have been possible.

My sincere gratitude also goes to my colleagues at the Institute of Chemical and Engineering Sciences for their valuable technical insights and merry companionship.

Finally, I want to thank my family and friends for their unconditional love and support through the years.

Contents

Chapter 4   **Experimental Methods**

Chapter 5   **Results and Discussion**

Summary

Consistent particle properties are an important goal for industrial batch crystallizations. Several control strategies, from unseeded linear cooling to seeded supersaturation control, were evaluated for the cooling crystallization of glycine. Particle properties were assessed in-line, facilitating assessment of process consistency. Closed-loop supersaturation-control was not superior to open-loop temperature-control; and changing the pre-set cooling profile, or the pre-set supersaturation limit, showed limited benefits. Seeding was by far the most effective strategy in this comparison. The possible reason for this observed insensitivity to cooling modes is that crystal growth rates matched the rate of supersaturation increase for all cooling rates, so that seeded processes operated entirely within the metastable zone. In contrast, unseeded systems did not achieve consistency, because primary nucleation is unpredictable and do not occur at a fixed temperature.

Seeded systems are advantageous in producing consistent crystal products. However, in view of the constraints on the usage of ports available in the crystallization vessel, a trade-off exist between using a port for the insertion of an in-line probe for monitoring of the process or using it for the addition of seeds. The implementation of in-line instrumentation cannot be over-emphasized, hence this necessitates a means to internally generate the seeds.

The utilization of Focused Beam Reflectance Measurement (FBRM) probe has increased tremendously, as evident from the large number of recent publications. There has yet been any published record of closed-loop feedback technique involving FBRM. Primary nucleation is unpredictable and does not occur at a fixed temperature, hence, a means to improve automation of the process through a closed-loop feedback strategy using the FBRM would be beneficial. In this work, the FBRM was successfully used to detect nucleation, after which control strategies were automatically implemented in unseeded cooling crystallization systems. In addition, the randomness of primary nucleation produces inconsistent initial nuclei for different runs, thereby resulting in inconsistent product crystals. A method to counter this problem using FBRM closed-loop feedback control is also addressed in this thesis, which involves adjusting the coefficient of variance (c.v.) of the primary nuclei. Consistent crystal products from unseeded systems were thus achievable.

List of Tables

List of Figures

1) Introduction

Crystallization is of enormous economic importance in the chemical industry. Worldwide production rates of basic crystalline commodity products exceed 1 Mt/year (Tavare, 1995) and the demand is ever-increasing. In the manufacture of these chemicals, crystallization is an important step, which borders on multiple disciplines such as physical chemistry, chemical reaction engineering, and surface, material, mineral, and biological sciences. Crystallization is employed heavily as a separation technique in the inorganic bulk chemical industry in order to recover salts from their aqueous solution; while in the organic process industry, it is also used to recover crystalline product, to refine the intermediary, and to remove undesired salts. The crystallization processes range from the production of a bulk commodity crystalline chemical on a very large capacity to clean two-phase systems to complex multi-phase, multi-component systems involving multiple steps in a process sequence.

A key concern of the pharmaceutical industry is to maximize production efficiency while improving consistency and quality of the final products. Because many drugs are produced and marketed in the crystalline solid state for stability and convenience of handling, developments in the governing and regulating of crystallization have generated much interests in recent years (see Braatz et al.

(2002) and Yu et al. (2004) and references cited therein). The goal is to ensure product consistency and quality through controlling the performances of known critical steps and parameters in the manufacturing process.

The fundamental driving force for crystallization from solution is the difference between the chemical potential of the supersaturated solution and that of the solid crystal face. It is common to simplify this by representing the nucleation and growth kinetics in terms of the supersaturation, which is the difference between the solution concentration and the saturated concentration. Supersaturation is typically created in crystallizers by cooling, evaporation, and/or by adding a solvent by which the solute has a lower solubility, or by allowing two solutions to intermix.

Control of crystallization processes is critical in a number of industries, including microelectronics, food, and pharmaceuticals, which constitute a significant and growing fraction of the world economy (Braatz, 2002). Poor control of crystal size distribution (CSD) can completely halt the production of pharmaceuticals, certainly a serious concern for the patients needing the therapeutic benefit of the drug.

The challenges in controlling crystallization are significant. First, there are significant uncertainties associated with their kinetics (Braatz, 2002; Gunawan et al., 2002; Nagy and Braatz, 2002; Ma et al., 1999; Qiu and Rasmuson, 1994;

Nylvt, 1968;). Part of the difficulty is that the kinetic parameters can be highly sensitive to small concentrations of contaminating chemicals, which can result in kinetic parameters that vary over time. Also, many crystals are sufficiently fragile that the crystals break after formation (Kougoulos et al., 2005; Gahn and Mersmann, 1995), or the crystals can agglomerate (Yu et al., 2005; Paulaime et al., 2003; Fujiwara et al., 2002; Yin et al., 2001; Masy and Cournil, 1999) or erode or re-dissolve (Garcia et al., 2002, 1999; Prasad et al., 2001; Sherwood and Ristic, 2001) or other surface effects that are difficult to characterize. Another significant source of uncertainty in industrial crystallizers is associated with mixing. Although crystallization models usually assume perfect mixing, this assumption is rarely true for an industrial-scale crystallizer.

Crystallization processes are highly non-linear, and are modeled by coupled nonlinear algebraic integro-partial differential equations (Attarakih et al., 2002; Rawlings et al., 1992). The very large number of crystals is most efficiently described by a distribution. For the case of distribution in shape as well as overall size, there are at least three independent variables in the equations. Simulating these equations is challenging because the crystal size distribution can be extremely sharp in practice, and can span many orders of magnitude in crystal length scale and time scale (Hu et al., 2005; Puel et al., 2003; Monnier et al., 1997).

Another challenge in crystallization is associated with sensor limitations. The states in a crystallizer include the temperature, the solution concentration, and the crystal size and shape distribution. The solution concentration must be measured very accurately to specify the nucleation and growth kinetics.

1.1) Motivation and Objective

This thesis presents the work carried out in the control of batch cooling crystallization. The objective of this project is chiefly to evaluate the benefits of new methods for controlling crystallizations over conventional methods using temperature control. S-Control, the more common method of feedback control using in-line instrumentation Attenuated Total Reflection-Fourier Transform Infrared (ATR-FTIR), was evaluated. Then, a novel concept of using Focussed Beam Reflectance Measurement (FBRM) in a closed-loop feedback loop was investigated.

The reason for the prevalent use of the indirect approach is the lack of accurate in-line sensors for the measurement of particle size and solution concentrations. In recent years, accurate in-line sensors that are robust enough to be used in production environment have become available (see Yu et al. (2004) and Braatz (2002) and references cited therein). This opens up the possibility of using such measurements to control crystallizations interactively. The most commonly used feedback control method is the closed-loop supersaturation-control (S-control)

using ATR-FTIR technique in which supersaturation is controlled at a constant level. This control method has been implemented for a variety of cooling and more recently, anti-solvent crystallizations (Yu et al., 2006; Zhou et al., 2006). These past studies have shown that S-control is sensitive to the pre-set supersaturation value (S_{set}). A suitable S_{set} value should be one that will promote growth while suppress nucleation and ensure a reasonable batch time. To encourage growth relative to nucleation, S_{set} has to be somewhere between the solubility curve and metastable zone limit. A lower S_{set} is expected to give better quality product crystals with narrower CSD due to its increased suppression of secondary nucleation, but is disadvantageous in terms of increased batch time. On the other hand, a higher S_{set} is expected to generate more fines due to faster growth as a consequence of its proximity to the metastable limit, but is advantageous in terms of reduced batch time.

The claimed benefits for S-control approach include more consistent products in terms of CSD and improved robustness (Yu et al., 2006; Gron et al., 2003; Fujiawara et al., 2002). Therefore the aim of this study was to assess the benefits of in-line control, specifically S-control, over conventional control (T-control) for achieving consistent particle properties and avoiding fines in cooling crystallizations. Namely, the following hypotheses have been tested:

- Non-linear temperature profiles will give improvements over linear profiles.
- S-control is better than T-control.

- S-control is effective in unseeded as well as seeded crystallizations.

- S-control is sensitive to S_{set}.

FBRM has emerged as a widely used technique for the in situ characterization of crystallization systems (refer to Chapter 3.3). It has been used to develop and optimize crystallization processes (Doki et al., 2004; Worlitschek and Mazzotti, 2004; Tadayyon and Rohani, 2000), track and trouble-shoot crystallizer systems (Wang et al., 2006; Wang and Ching, 2006; Yu et al., 2006; O'Sullivan and Glennon, 2005; Deneau and Steele, 2005; Kougoulos et al., 2005; Heath et al., 2002; Abbas et al., 2002; Barrett and Glennon, 1999), to monitor polymorphic forms (Scholl et al., 2006; O'Sullivan et al., 2003), and in control of crystallization systems (Barthe and Rousseau, 2006; Barrett and Ward, 2003; Barrett and Becker, 2002). The objective of any process monitoring is to ultimately bring about control to the process. Yet, despite the proven useful applicability of FBRM in crystallization, there has not been any published work of implementation of closed-loop feedback control using FBRM to the best of the authors' knowledge.

In seeded crystallization processes, the point of seeding is pre-determined, hence ensuring consistency in the process. On the contrary, in unseeded systems, initial nuclei are generated by primary nucleation, which is unpredictable in that it may occur at different temperatures for different runs. Primary nucleation is deemed to have occurred when the fresh nuclei starts forming spontaneously from the clear solution. Parsons et al. (2003) termed this

the 'cloud point'. Since primary nucleation is unpredictable and do not occur at a fixed temperature, the usual practice is for an operator to be physically present to monitor the point of occurrence of nucleation then manually start the control profiles thereafter, subject to the discretion of the operator in defining the exact point of primary nucleation. Alternatively, the point of primary nucleation is simply deemed to have occurred at some point during the cooling profile, which is pre-determined despite the inability to predict the exact point of primary nucleation prior. This hence necessitates a means to detect nucleation, after which different cooling profiles are implemented. A closed-loop feedback control using the FBRM could improve automation of the process. As Barthe and Rousseau (2006) have pointed out, the onset of nucleation is clearly identified by the sudden increase in the chord counts by the FBRM. Barrett and Glennon (2002) have also used FBRM to successfully detect the metastable zone width (MZW). The feasibility and applicability of automating primary nucleation detection through the use of a feedback loop involving FBRM is investigated in this work.

In contrast to seeded systems in which the amount of seeds added is specific, the initial nuclei formed by primary nucleation in unseeded systems are random and irreproducible for different runs. Even with exactly the same initial conditions and cooling rate in approaching nucleation, primary nucleation gives different initial seeds; hence product consistency is not possible for every run. Seeding is known to be advantageous in ensuring product consistency because the size range of the seeds, whether the seeds are added dry or wet, the temperature at

which the seeds are added, and the amount of seeds are all pre-determined, thereby ensuring increased consistency in product crystals. However, the scarcity of ports in crystallization vessels in the industry makes the port requirement for seeding a disadvantage. Industries have to weigh the pros and cons of using a port of a crystallization vessel for the insertion of a probe for in-line monitoring or for the purpose of seeding. The trade-off for using the port for seeds addition instead of for insertion of a probe for in-line monitoring is the loss of useful data for constant monitoring of the crystallization process. On the contrary, if the port were to be used for probe insertion, the crystallization process has to be operated as unseeded systems, which subjects the system to the irreproducibility and randomness of primary nucleation. Oftentimes, a decision has to be made between seeding or the insertion of an in-line probe. This hence motivates a means to manipulate the nuclei generated by primary nucleation in unseeded systems to achieve consistent nuclei from primary nucleation in different runs, which thereby provides a viable alternative to external seeding and allows for in-line monitoring of the process through a probe (Yu et al., 2004; Sistare et al., 2005; Birch et al., 2005; and Barrett et al., 2005).

The strategy employed in this work is to manipulate the system temperature according the FBRM statistics to enforce consistency in the initial seeds generated by primary nucleation. Cerreta and Liebel (2000) have asserted that the FBRM provides the necessary and sufficiently accurate in-line assessment to return a deviation to a set-point. FBRM Control Interface gives users many

different statistics, and the paramount concern is which of these statistics should be controlled to bring about an improvement to a crystallization process. Controlling the absolute particle counts (Doki et al., 2004), in particular the fines particle counts, may seem like a good idea at first; however, such a control is not easily amenable for scale-up nor for a different system, hence is not as useful, although counts may be the most reliable statistic generated by FBRM.

A model system for such a study should have a suitable solubility curve for aqueous crystallizations, as well as being readily available and non-toxic. Glycine met these criteria. The potential disadvantage of known polymorphism was not relevant because unseeded crystallizations from water always give the metastable α-glycine, which is kinetically stable. Moscosa-Santillan et al. (2000) used a spectral turbidimetrc method for on-line crystal size measurement and simulation to devise an optimal temperature profile for seeded batch cooling crystallization of glycine. Doki et al. (2004) reported a process control strategy for the seeded production of glycine by manipulating the alternating temperature profile and the final termination temperature, resulting in the avoidance in the generation of fines. In their work, however, the ATR-FTIR was used only to monitor the system supersaturation, without the implementation of a closed-loop feedback control loop. Our current work considers the potential advantages of implementing an automated approach of supersaturation control (S-control) for controlling seeded and unseeded batch crystallization of glycine.

1.2) Thesis Overview

Fundamentals of crystallization, comprising of nucleation, metastable zone, and growth are first presented in Chapter 2.

Next, techniques and instruments measuring various aspects of crystallization in-line are discussed in Chapter 3. The Process Analytical Technology (PAT) initiative is discussed. The principles and applicability of ATR-FTIR, FBRM, and PVM, the instruments of interest in this work, are then elucidated.

Chapters 4 and 5 describe the control strategies used in batch cooling crystallization in this work. The benefits, or lack thereof, of closed-loop feedback Supersaturation Control (S-control) was analyzed against the conventional open-loop Temperature Control (T-control). Subsequently, two novel strategies involving closed-loop feedback using FBRM was proposed and investigated. In the first strategy, FBRM was used in the automatic detection of primary nucleation. The second strategy involves using FBRM to achieve consistent initial 'seeds' generated through primary nucleation, thereby superseding the advantage of external seeding.

Finally, the first section of chapter 6 gives an overall conclusion of the results in this work, while the second discusses compelling trends and potential future opportunities in the field of solution crystallization research.

2) Background

Crystallization from solution can be considered a two-step process. The first step is a phase separation, called nucleation, and the second step is the subsequent growth of nuclei to crystals. The prerequisite for crystallization to occur is a supersaturated solution, and supersaturated solutions are not at equilibrium. Since every system strives to reach equilibrium, supersaturated solutions finally crystallize. By crystallizing, the solutions move towards equilibrium and supersaturation is relieved by a combination of nucleation and crystal growth. Various nucleation mechanisms (Yin et al., 2001; Mersmann, 1996; Nyvlt, 1984) and crystal growth mechanisms (Mullin, 2001; Ulrich, 1989) have been proposed to explain these phenomenons.

The two kinetic steps - nucleation and crystal growth - dominate the production process of crystalline products. In industrial crystallization, crystal size distribution (CSD) and mean crystal size as well as external habit and internal structure are important characteristics for further use of the crystals. With regard to product characteristics, nucleation, as the first of the two kinetic steps, usually has a strongly predetermining influence on the second step crystal growth. Nucleation and growth are strongly interrelated to the width of the metastable zone or the metastability of a system set to crystallize.

The relation of the degree of nucleation to crystal growth determines important product properties, such as product crystal size and size distribution. But even the crystal shape (Hentschel and Page, 2003; Winn and Doherty, 2000) can be influenced distinctly by the conditions of growth, such as type of solvent used (Lahav and Leiserowitz, 2001; Li et al., 2000; Granberg et al., 1999) or presence of impurities (Li et al., 2001; Prasad et al., 2001; Hendriksen et al., 1998). A given crystal face can also be 'seeded' by exposing it to a particular nucleating surface (Yin et al., 2001). The crystalline form of the drug, as well as the characteristics of the particles, determine the end-use properties of the pharmaceutical product such as the in vivo dissolution rate, and the various transport properties involved in the delivery of the active ingredient. Furthermore, the purity of crystalline products strongly depends on the growth rate, since, for example, fast growth may lead to liquid inclusions. The above-mentioned aspects clarify the necessity for the control of crystallization processes. Without the control of crystallization processes no desired and reproducible product quality comprising crystal size distribution (CSD), shape and purity can be ensured.

This chapter presents the fundamentals of crystallization comprising of concepts of nucleation, metastable zone and growth.

2.1) Nucleation

Nucleation from solution is the generation of new crystalline phase, under conditions where a free energy barrier exists. Nuclei are the first formed embryos, which subsequently grow to produce visible tangible crystals. It occurs due to the clustering or aggregation of molecules or ions in a supersaturated melt, solution or vapor, to a size at which such entities become viable in that they will grow rather than re-dissolve.

Nucleation can be distinctly divided into two subsets – primary and secondary. Figure 2-1 summarizes the modes and mechanisms of nucleation aptly.
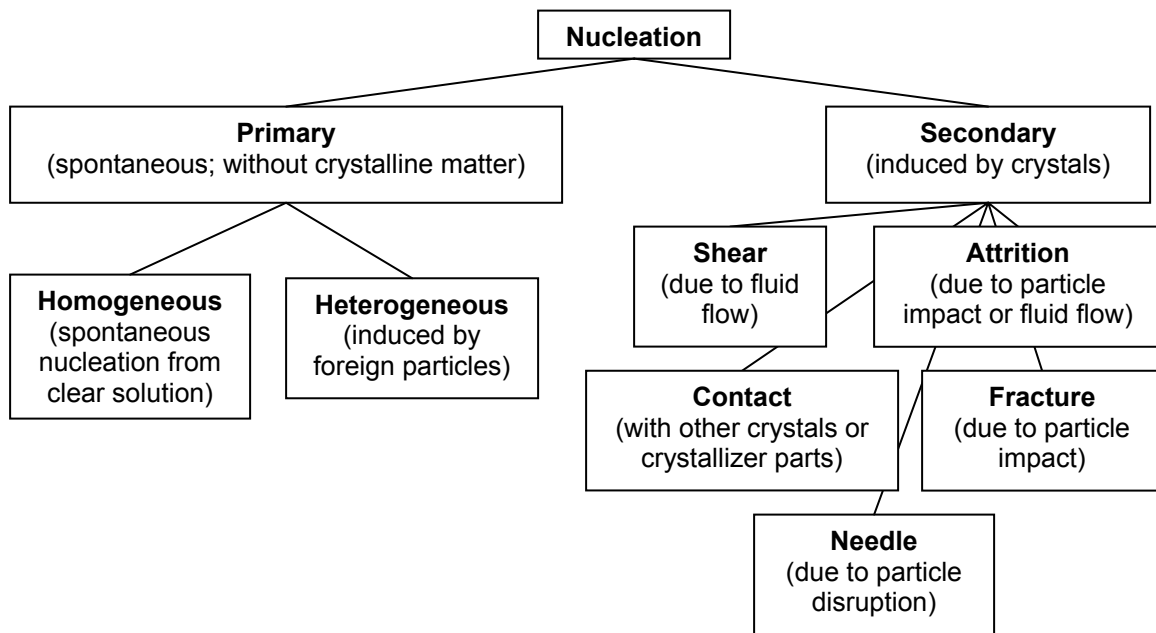
Figure 2-1: Modes and Mechanisms in Nucleation

The condition of supersaturation or supercooling alone is not sufficient for a system to begin to crystallize. Before crystals can develop there must exist in the solution a number of minute solid bodies, embryos, nuclei or seeds, which act as centers of crystallization. Nucleation may occur spontaneously or it may be induced artificially. It is not always possible, however, to determine whether a system has nucleated with or without the influence of some external stimulus.

Nucleation can often be induced by agitation, mechanical shock, friction and extreme pressures within solutions and melts. The erratic effects of external influences such as electric fields, spark discharges, ultra-violet light, X-rays, γ-rays, sonic and ultrasonic irradiation have also been studied, but none so far has found any significant application in large-scale crystallization practice (Jones, 2002).

2.1.1) Primary Nucleation

Primary nucleation occurs mainly at high levels of supersaturation and is thus most prevalent during unseeded crystallization or precipitation. This mode of nucleation may be subdivided into homogeneous (i.e. spontaneous nucleation from clear solution) and heterogeneous (i.e. nucleation due to the presence of foreign solid particles).

Homogeneous nucleation occurs when there are no special objects inside a phase which can cause nucleation (Figure 2-2). It involves forming a stable nucleus in a supersaturated solution. Not only have the constituent molecules to coagulate and resist the tendency to re-dissolve, but they also have to become oriented into a fixed lattice. The number of molecules in a stable crystal nucleus can vary from about ten to several thousands (Mullin, 2001). However, a stable nucleus could hardly result from simultaneous collision of the required number of molecules since this would constitute an extremely rare event. Gibbs considered the change of free energy during homogeneous nucleation, which leads to the classical nucleation theory and to the Gibbs-Thompson relationship in Eq. 1-1 (Mullin, 2001).

$$B^o = A \ \exp\left[-\frac{16\pi\gamma^3 v^2}{3k^3 T^3 (\ln S)^2}\right] \qquad \text{(Eq. 1-1)}$$

where γ is the interfacial tension, v is the molecular volume, k is the Boltzmann constant, S is the supersaturation ratio $\frac{c}{c^*}$, c is the solution concentration and c* is the equilibrium saturation concentration.

Crystal nucleus
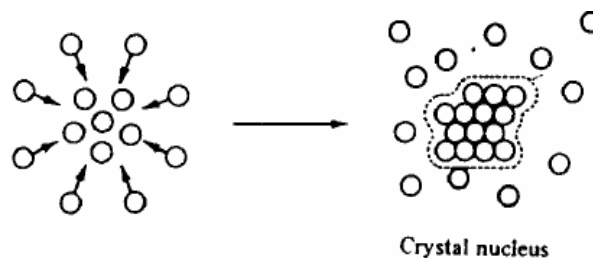
Figure 2-2: Schematic of Primary Homogeneous Nucleation

.

Heterogeneous nucleation, on the other hand, occurs when there are foreign particles or surfaces inside a phase which can cause nucleation. It becomes significant at lower supersaturation levels. Although most primary nucleation in practice is liable to be heterogeneous rather than homogeneous, it is difficult to distinguish between the two types. The functional form of the nucleation rate is similar to that in Eq. 1-1, but the overall effect is to reduce the critical level of supersaturation or metastable zone width.

2.1.2) Secondary Nucleation

Secondary nucleation takes place only because of the prior presence of crystals of the material being crystallized. A supersaturated solution nucleates much more readily, i.e. at a lower supersaturation, when crystals of the solute are already present or deliberately added. The crystal surface at the solid-liquid interface appears to play an important role in all the secondary nucleation processes. Most experimental observations tend to indicate that the secondary contact nucleation process provides an important source for producing nuclei and that in industrial practice the secondary nucleation has predominant influence on the overall performance (Tavare, 1995).

The nucleation rate may in general be represented by the semiempirical relation in Eq. 2-2. The nucleation rate constant k_b may be a function of many other variables, in particular, temperature, hydrodynamics, presence of impurities, and

crystal properties. The power law term μ_k^j represents the kth moment of the CSD in the crystallizer. Normally, the use of the third moment is found to be suitable to account for the secondary nucleation effects.

$$B' = k_b \mu_k^j \Delta c^b \qquad \text{(Eq. 2-2)}$$

2.2) Metastable Zone

The metastable zone is a region bounded by the equilibrium and metastable curves, where the solution is supersaturated while spontaneous crystallization does not occur. This constitutes the allowable supersaturation level during every crystallization process. Only by further increase of the supersaturation will a certain degree of supersaturation be reached at which spontaneous nucleation occurs: the metastable limit. This metastable limit is, in contrast to the saturation limit, thermodynamically not founded and kinetically not well defined. It depends on a number of parameters such as temperature level, rate of generating the supersaturation, solution history, impurities, fluid dynamics, reactor dimensions and configurations, etc.

The metastable zone width (MZW) results from the specific characteristics of nucleation in a supersaturated solution of soluble substances. The metastable zone width can be considered as a characteristic property of crystallization for each system. Also it is an important parameter to analyze the specifications of the products obtained from the industrial crystallization processes, such as

product crystal size, crystal size distribution (CSD) and crystal shape by its contribution to nucleation and crystal growth (Kim and Mersmann, 2001).

It is difficult to predict the metastable zone width (MZW) because it is difficult to pinpoint the exact type of nucleation acting in each system. Most of the parameters associated with MZW estimation are closely connected with the description of nucleation behavior in the solution. Figure 2-3 compares the metastable zone width for different modes of nucleations.
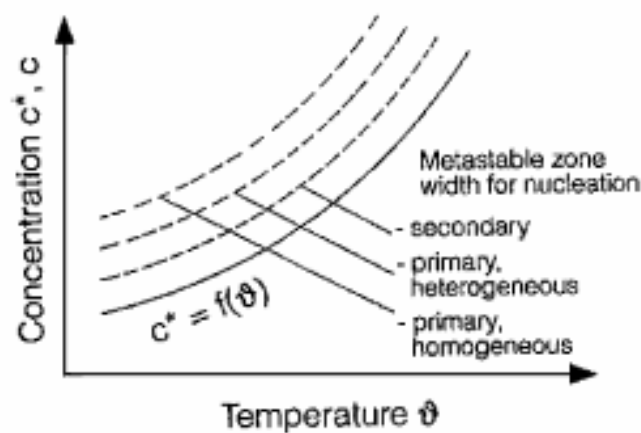
Figure 2-3: Metastable Zone Width for various types of Nucleation (Ulrich and Strege, 2001)

Many authors have tried to express the MZW with certain parameters as semi-empirical relationships (Kim and Ryu, 1997; Nyvlt et al., 1970). Mullin and Jancic (1979) and Nyvlt (1968) have published the experimental methods to measure the MZW and the procedure to interpret the nucleation order according to simple empirical nucleation equation. Regardless of the type of nucleation, the measurement of MZW is mainly carried out by the polythermal method, in which

nuclei are detected visually or instrumentally (Parsons et al., 2003; Barrett and Glennon, 2002; Fujiwara et al., 2002; Nyvlt et al., 1970). Little attention has been paid so far to the prediction of MZW because it is difficult to know what nucleation is contributing to metastability in each system. A simplified model based on integral growing of nucleus in nucleation was presented to predict the MZW, which was limited for seeded solutions (Mersmann and Bartosch, 1997). Kim and Mersmann (2001) attempted prediction of the MZW for several nucleation processes. Their study aimed at obtaining the relations which would enable a satisfactory estimate of MZW in the crystallizer acting with homogeneous nucleation, heterogeneous nucleation, and surface nucleation.

A control of the actual supersaturation is mandatory to be able to exert a targeted influence on nucleation and growth processes (Fujiwara et al., 2005). In order to design products by crystallization processes it is essential to measure on- and in-line supersaturation and metastability. Only optimum nucleation points as well as optimum growth rates throughout the process can ensure the desired product quality. In other words, optimum crystallization processes can only be accomplished if the metastable zone width and the actual operation point of the crystallizer within this zone is known and controlled during the entire process. This necessitates sensors and control strategies capable of serving that purpose.

2.3) Growth

Once a stable nuclei has been formed in a supersaturated or supercooled system, it begins to grow into crystals of visible size. Many theories have evolved to explain the mechanisms of crystal growth.

The diffusion theories presume that matter is deposited continuously on a crystal face at a rate proportional to the difference in concentration between the point of deposition and the bulk of the solution (Jones, 2002). The mathematical analysis is similar to that used for other diffusional and mass transfer processes. In this theory, crystal growth is a diffusion and integration process, modified by the effect of the solid surfaces on which it occurs. When a crystal surface is exposed to a supersaturated environment, the flux of growth units (atoms, ions, molecules) to the surface exceeds the equilibrium flux so that the number of growth units joining the surface is greater than that leaving. The adsorption-layer theories have received much attention too (Tai et al., 1992; Mullin, 2001). At the surface, the growth units must become organized into the space lattice through an adsorbed layer. This results in growth of the surface. The ability of a surface to capture arriving growth units and integrate them into the crystal lattice is dependent upon the strength and number of interactions that can form between the surface and the growth unit. This theory suggests that crystal growth is a discontinuation process, taking place by adsorption, layer by layer, on the crystal surface.

The rate of crystal growth can be expressed as the rate of displacement of a given crystal surface in the direction perpendicular to the face. Variations occur in the shape of the crystal when individual faces grow at different rates, the overall crystal habit being determined by the slowest growing face (Mullin, 2001). It has been proposed that crystal growth rates are particle size dependent.

Size-dependent growth theory is concerned with the growth rate change of a crystal solely on account of its size. In this theory, three effects cause larger crystals to grow faster:

- The effect of size is closely linked to the solution velocity: Larger particles have higher terminal velocities than those of smaller particles, hence in cases where diffusion plays a dominant role in the growth process, the larger the crystals the higher the growth rate.

- The Gibbs-Thomson effect exerts a powerful effect at sizes smaller than a few micrometers. Crystals at near-nucleic size may grow at extremely slow rates because of the lower supersaturation they experience owing to their higher solubility. Hence the smaller the crystals, the lower their growth rate.

- Surface integration kinetics is postulated to be size-dependent. The number of dislocations in a crystal increases with size due to mechanical stresses, incorporation of impurity species into the lattice, etc. In addition, the larger the

crystals the more energetically will they collide in agitated suspensions and the greater are the potential for surface damage. Both these effects favor faster surface integration kinetics and lead to higher growth rates with increasing crystal size.

In contrast, the growth rate dispersion theory refers to the fact that individual crystals, all initially of the same size, can grow at different rates, even if each apparently is subjected to exactly identical growth environments. Ulrich (1989) and Tavare (1991) have made excellent reviews on this topic. Growth rate dispersion stems mainly from different interfaces with the surface integration kinetics on different crystals. The less ductile the crystals, the more likely they are prone to growth rate dispersion.

Various growth rate measurements can be categorized in a number of ways (Garside et al., 2002).

- Measurements can either be made on single crystals, or on a population, i.e. a large number of crystals. The former are particularly valuable for fundamental studies of growth mechanisms and habit modification, while the latter are usually employed for purposes more directly related to design.

- Supersaturation and crystal size may be approximately constant during the growth period, or there may be significant variations in these parameters. In

the former case, point values of growth rate are obtained directly; in the latter, point values have to be extracted from the overall system responses. These two cases correspond to the differential and integral techniques respectively, as widely used in chemical reaction engineering.

- The measurement defining the growth rate can be obtained from changes in the crystals (e.g. increases in their size or mass) or changes in the solution concentration arising from the deposition of solute into the crystal. These two cases, depending on the 'solid side' and 'solution side' information respectively, are linked through a mass balance, as expressed follows:

$$-\frac{dw}{dt} = \frac{1}{\rho_L V_L} \frac{dM_c}{dt}$$ (Eq. 2-3)

Where w is the mass fraction solution concentration, M_c is the total mass of crystals in suspension, ρ_L is the solution density, and V_L is the volume of solution in the crystallizing system.

- Experiments can be carried out isothermally or non-isothermally. The former is the more common procedure, although the latter offers the possibility of determining activation energies of crystal growth directly.

2.4) Control Strategies for Batch Cooling Crystallization

The principal consequences of a bad control of crystallizers are the non-reproducibility and the low quality of the solids produced (Jones, 2002; Mullin, 2001). In uncontrolled crystallization processes, nucleation starts stochastically and as a result, product quality varies distinctively. Consequently, the feedback control of industrial crystallizers or at least the optimization of operating conditions is of potentially great importance.

Since the generation of supersaturation conditions in solution crystallization mainly depends on the cooling rate, substantial research activity has been devoted to the computation of optimal temperature trajectories (Jones, 1974; Jones and Mullin, 1974; Mullin and Nyvlt, 1971), or optimal operating policies (Ward et al., 2006; Rohani et al., 2005a, b; Yu et al., 2005; Takiyama et al., 2002). Most past studies in batch crystallization control have dealt with finding the open-loop temperature versus time trajectory that optimizes some characteristics of the desired crystal size distribution (CSD), as discussed in several papers (Braatz, 2002; Monnier et al., 1997; Matthews et al., 1996; Miller and Rawlings, 1994; Rawlings et al., 1993; Barrera and Evans, 1989). This classical approach requires the development of a first-principles model with accurate growth and nucleation kinetics, which can be obtained in a series of continuous or batch experiments. Uncertainties in the parameter estimates, nonidealities in the model assumptions, and disturbances have to be taken into account to ensure that this approach results in the expected optimized product

quality (Nagy and Braatz, 2004; Ma and Braatz, 2003; Togkalidou et al., 2002; Ma et al., 1999; Eaton and Rawlings, 1990).

However, the efficiency of such control policies strongly depends upon the accuracy of the nucleation and growth kinetic parameters which are required to calculate optimal temperature profile (Nagy and Braatz, 2004; Ma et al., 1999). Moreover, the assessment of these parameters requires cautious and complex experimental work, which is impractical in the context of industrial development. The optimal strategies in question are basically "open-loop", which means no in-line or on-line measurement of the crystallization process is necessary. As such, deviations of the process conditions, quality, productivity and reproducibility are almost inevitable due to industrial disturbances (e.g. batch-to-batch variations of Impurities). An immediately conceivable solution to this problem lies in the "closed-loop" control of crystallizers, which has recently been an active field of research. Several review papers have been published on this topic (Fujiwara et al., 2005; Braatz, 2002; Miller and Rawlings, 1994; Eaton and Rawlings, 1990).

Usually the main objective of batch crystallization is to produce large uniform crystals (to ease downstream processing) within a given time. Since a large number of nuclei form if the supersaturation crosses the metastable limit, most crystallizers are operated by adding seeds near the start of the batch and maintaining the supersaturation within the metastable zone, where the nucleation and growth processes compete for the solute molecules. Both the nucleation and

growth rates are positively correlated with supersaturation. An optimal control strategy should have a high enough supersaturation that the growth rate is significant (so that the batch runs are not too long) but low enough supersaturation to keep the rate of nucleation low. Seeding reduces the productivity of each batch, but can lead to more consistent crystals when the crystallizer is poorly controlled (Chung et al., 1999). An alternative unseeded method creates the seed inside the crystallizer. Figure 2-4 shows typical operating lines for each method, in the concentration versus temperature diagram. For seeded operation, the seed is introduced shortly after the solubility curve is crossed and the operating line should remain within the metastable zone. For unseeded operation, the operating line first reaches the metastable limit to generate primary nucleation and then the supersaturation should be kept below the metastable limit similar to the seeded system.
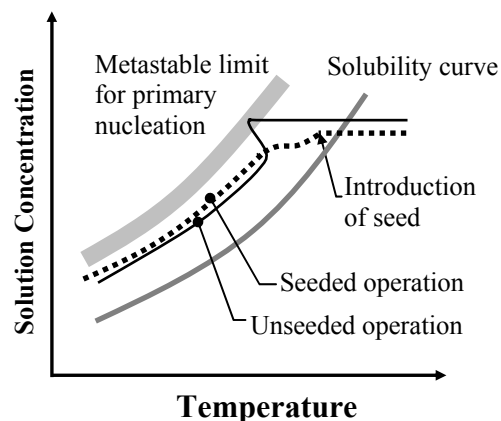
Figure 2-4: Concept of seeded and unseeded batch cooling crystallization (Fujiwara et al., 2005).

Fujiwara et al. (2005) reviewed the recent technological advances in the in-situ control of pharmaceutical crystallization processes. First principles and direct design approaches were compared and their relative merits and demerits were discussed. First principles approach provides more insight into crystallization process through simulation but parameter uncertainties and non-idealities in the model assumptions hamper its effectiveness in controlling crystallization. Direct design approach circumvents such modeling issues and is simpler to design and implement. The authors also compared T- and S-control strategies and concluded that S-control is less sensitive to most practical disturbances and to variations in nucleation and growth kinetics.

3) In-Line Monitoring Techniques

Crystallization is one of the most critical and least understood pharmaceutical manufacturing processes. Many process and product failure can be traced to a poor understanding and control of the crystallization process.

Most crystallization processes in the pharmaceutical industry are designed and controlled based on trial-and-error experimentation, which can be time consuming and expensive. Recent advances in process sensor technologies have improved the monitoring capabilities during the operation of crystallization processes (see Braatz, 2002 and references cited therein). And the whole objective of monitoring the process in-situ is so that some form of control can be brought about in the event that the process has veered away from product specifications.

Faster computers and advances in sensor technologies and simulation and control algorithms are removing the main bottlenecks that limited progress in crystallization control. Recently, in-line sensors have enabled the development of systematic first-principles (model-based) and direct design (measurement-based) approaches for the control of industrial crystallization processes (Fujiwara et al., 2005). Pharmaceutical processes are increasingly making use of in-line sensors

to monitor in real time and bring about enhanced control of the crystallization process. Further advances are expected to lead to even more utilization of these techniques to reduce time-to-market and increase productivity, which are key industrial ideals.

A few examples of in-line sensors that have received much attention are as ATR-FTIR (Chapter 3.2), FBRM (Chapter 3.3), and PVM (Chapter 3.4). In addition, both near-infrared (NIR) spectroscopy (Norris et al., 1997) and Raman spectroscopy coupled with fiber optics have been used for the in situ detection and optimization of various polymorphs (Scholl et al., 2006; Ono et al., 2004; Starbuck et al., 2004; Agarwal and Berglund, 2003). Raman spectroscopy has been also used for monitoring solution concentration during protein crystallization (Schwartz and Berglund, 2002, 2000; Tamagawa et al., 2002).

Even with these advances in in-line sensors and a better understanding of the crystallization mechanisms at the molecular level (Winn and Doherty, 2002), pharmaceutical crystallization processes can be challenging to control due to variations in solution thermodynamics and kinetics due to small concentrations of contaminating chemicals, complex nonlinear dynamics associated with non-ideal mixing and dendritic growth, and unexpected polymorphic phase transformations (Rodriguez-Hornedo and Murphy, 1999).

In this chapter, the Process Analytical Technology (PAT) concept is first introduced. Then, the three main instruments – ATR-FTIR, FBRM, and PVM - used in this work is reviewed. The principles belying and their applications will be presented.

3.1) Process Analytical Technology (PAT)

The Food and Drug Administration's (FDA) process analytical technology (PAT) initiative is a collaborative effort with industry to introduce new and efficient manufacturing technologies into the pharmaceutical industry. Although PAT has been widely used in the chemical industry, its application in the pharmaceutical industry is still at its infant stage (Yu et al., 2004). PAT's are systems for design, analysis, and control of manufacturing processes, based on timely measurements of critical quality and performance attributes of raw and in-process materials and products, to assure high quality of products at the completion of manufacturing. The application of PAT to crystallization is currently an area of high interest for both the chemical development and manufacturing arenas. This scenario is partly due to the growing emphasis on PAT as a tool for "21st Century Manufacturing" as described in the guideline document "PAT – A Framework for Innovative Pharmaceutical Development, manufacturing, and Quality Assurance" issued by the U.S. FDA in 2004[①]. This effort, however, is also a reflection of the increasing awareness within the chemical industry that

---

[①] FDA guidelines on PAT: http://www.fda.gov/cder/guidance/6419fnl.htm

crystallization processes are often poorly understood and poorly controlled (Birch et al., 2005).

Implementation of PAT involves scientifically based process design and optimization, appropriate sensor technologies, statistical and information tools (chemometrics), and feedback process control strategies working together to produce quality products (Yu et al., 2004; Sistare et al., 2005; Barrett et al., 2005). There are many current and new tools available that enable scientific, risk-managed pharmaceutical development, manufacture, and quality assurance. These tools, when used within a system can provide effective and efficient means for acquiring information to facilitate process understanding, develop risk-mitigation strategies, achieve continuous improvement, and share information and knowledge. In the PAT framework, these tools can be categorized as[2]:

- Multivariate data acquisition and analysis tools
- Modern process analyzers or process analytical chemistry tools
- Process and endpoint monitoring and control tools
- Continuous improvement and knowledge management tools

An appropriate combination of some, or all, of these tools may be applicable to a single-unit operation, or to an entire manufacturing process and its quality assurance.

---

[2] FDA's PAT initiative: http://www.fda.gov/cder/OPS/PAT.htm#Introduction

Yu et al. (2004) gave a review on the application of PAT to crystallization processes and discussed the various in-situ analytical tools available. A few case studies were used to illustrate the use of the PAT concept to control important aspects of product quality, e.g. particle size, shape and polymorphic form. FTIR-ATR, FBRM and PVM, which are used in this work, have been highlighted as the three major tools in the monitoring and control of particle size and shape. Barrett et al. (2005) also presented a review on the use of PAT for the understanding and optimization of batch crystallization process. This review, however, concentrates only on discussing the ability of FBRM in monitoring the change in PSD in different crystallization systems. Other authors presented industrial case studies on how PAT was employed to provide insights into crystallization processes (Scott and Black, 2005).

Applications of PAT to crystallization processes can be broadly classified into four categories as follows (Birch et al., 2005):

- The use of in-line sensors to monitor and control solution concentration throughout the crystallization process. Dunuwila et al. (1994) was the first to propose and demonstrate the applicability of ATR-FTIR for monitoring solution concentration in-line (refer to Chapter 3.2). FTIR spectroscopy has since garnered widespread interest from industry and academia, sprouting several publications of its application for the control of crystallization (Gron et al., 2003; Fevotte, 2002; Liotta and Sabesan, 2002; Togkalidou et al., 2001).

- The use of PAT to monitor polymorph or pseudo polymorph conversion in real time, with a view to understand the kinetics of the transition and gain knowledge necessary to develop a robust process (Ono et al., 2004; Agarwal and Berglund, 2003; Starbuck et al., 2002).

- Applications to a control strategy based on first principles, as described in Togkalidou et al. (2004).

- Particle engineering through monitoring and control of the CSD via a PAT tool. FBRM[3] has been the instrument at the forefront of research in this field (refer to Chapter 3.3).

A goal of the PAT initiative is to encourage the application of process engineering expertise in pharmaceutical manufacturing and regulatory assessment (Yu et al., 2004). The results of PAT are a depth of process knowledge leading to optimized operation with control systems that ensure quality outcomes. While models analyzing the information obtained from process measurements provide a framework for representing process knowledge, PAT enables such measurements and modeling to be performed in real-time and on-line. Quality-control using PAT is based on in-process electronic data rather than laboratory testing on a subset of the final product. Thus, PAT holds the potential for

---

[3] Details of FBRM can be found at Mettler-Toledo's website: http://www.mt.com/lasentec.

improving efficiency and quality. Some of the benefits PAT bestows on pharmaceutical manufacturing include:

- Enhancing process understanding and reducing process failures

- Ensuring quality through optimal design, continuous monitoring, and feedback control

- Reducing cycle time to improve manufacturing efficiency

- Identifying the root causes of process deviations

- Basing regulatory scrutiny on process knowledge and scientifically based risk assessment

Production crystallizations can be difficult processes to characterize and improve. Traditionally, pharmaceutical crystallization processes have been developed empirically. Thus, there is much to be gained in applying PAT to these systems. Aspects of PAT applied to crystallization include identification of critical variables, sensor technologies to observe these variables, chemometrics tools to manage and interpret data, and process control schemes.

3.2) Attenuated Total Reflection-Fourier Transform Infrared (ATR-FTIR)

ATR-FTIR spectroscopy enables accurate measurement of solution concentrations for crystallization processes (Liotta and Sabesan, 2004; Fujiwara et al., 2002; Groen and Roberts, 2001; Lewiner et al., 2001; Dunuwila and Berglund, 1997), including the multi-solvent multi-solute organic systems

commonly encountered during pharmaceutical crystallization. A significant advantage of ATR-FTIR spectroscopy over most other methods for solution measurement is the ability to provide simultaneous measurement of multiple chemical species. ATR-FTIR spectroscopy has also been applied to the detection of the metastable limit (Barrett and Glennon, 1999), monitoring during polymorphic transitions (O'Sullivan et al., 2003; Aldridge et al., 1996; Buckton et al., 1998; Salari and Young, 1998; Skrdla et al., 2001), and evaluation of impurities (Otte et al., 1997) during crystallization.

In ATR-FTIR spectroscopy, the infrared spectrum is characteristic of the vibrational structure of the substance in immediate contact with the ATR immersion probe. IR Spectroscopy is well suited to provide real-time structural and kinetic data about dissolved organic molecules or particles in suspension during solid/liquid operations (e.g. crystallization processes) without complicated hardware developments. The MIR (Mid IR) region is the region of fundamental stretching modes i.e. for C-C, C-H; while NIR reflects anharmonic overtones, and is mostly seen for highly energetic excitations of groups such as O-H, N-H. But the information from MIR tends to be more selective so that the calibration procedures allowing the quantitative measurement of chemical species from the recorded spectra require less tedious and less time-consuming tasks than using NIR data (Hu et al., 2001; Fevotte, 2002). Most pharmaceutical applications of IR spectroscopy have so far been focused on the off-line characterization of raw materials and manufactured products, and in particular to the detection of "off-

specification" products. Recently, several groups (Dunuwila and Berglund, 1997; Braatz et al., 2002; Fevotte, 2002; Fujiwara et al., 2002; Lewiner et al., 2001, 2001a; Togkalidou et al., 2001; Feng and Berglund, 2002; Grön et al., 2003) have shown that the in situ ATR FTIR technique can be successfully applied to the in-line measurement of supersaturation during the solution crystallization of organic products and, consequently, of drugs.

3.2.1) Principle of ATR-FTIR Technique

Currently applied methods for measurement of solubility and supersaturation based on viscometry, refractometry, interferometry and density require the separation of phases prior to measurement. ATR-FTIR Spectroscopy provides a unique configuration in which the infrared spectrum of a liquid phase can be obtained in a slurry in-situ without phase separation. Infrared spectroscopy is essentially a non-destructive method for providing chemical information on organic and some inorganic materials. ATR-FTIR uses the principle of total internal reflection. Infrared light is passed through an appropriate infrared transparent crystal in contact with the sample. The evanescent field penetrates the surface, probing the infrared absorption of chemical species.

ATR spectroscopy is based on the presence of an evanescent field in an optically rarer medium (the sample) in contact with an optically denser medium (the ATR probe crystal) within which radiation is propagated due to internal reflection. The

depth of penetration of the evanescent wave is the order of the wavelength, so one can postulate that the interaction of this field is limited to the solution phase. That is why such technique allows the measurement of the solute concentration in the slurry without being disturbed by the solid particles. The crystal of the ATR probe is chosen such that the depth of penetration of the infrared energy into the solution is smaller than the liquid phase barrier between the probe and the solid crystal particles. Hence when the ATR probe is inserted into a crystal slurry, the substance in immediate contact with the probe will be the liquid solution of the slurry, with negligible interference from the solid crystals. That the crystals do not significantly affect the infrared spectra collected using the ATR probe has been verified experimentally (Dunuwila and Berglund, 1997; Dunuwila et al., 1994). The depth of penetration is given as follows:

$$d_p = \frac{\lambda}{2\pi n_1 [\sin^2 \theta - (\frac{n_2}{n_1})^2]^{\frac{1}{2}}}$$

(Eq. 3-1)

where λ is the wavelength of the incident radiation, *n1* and *n2* are, respectively, the refractive indices of the crystal and of the solution, and θ is the angle of incidence of the propagating radiation.

Figure 3-1 is a schematic representation of path of a ray of light for total internal reflection. The ray penetrates a fraction of a wavelength (*dp*) beyond the reflecting surface into the optically rarer medium of refractive index n_2 and there is a certain displacement (*D*) upon reflection.

Internal
Reflection
Element

n_1

d_p

Sample → $n_2 < n_1$ D
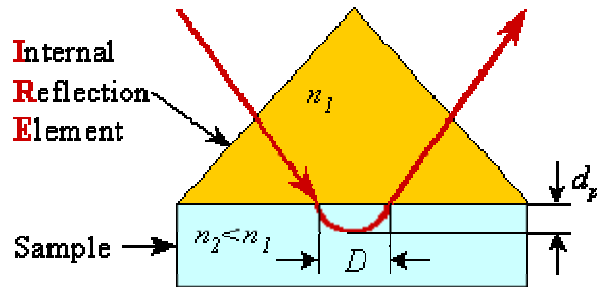
Figure 3-1: Diagram illustrating travel path of ray of light

The possibility of designing immersion probes with various ATR element materials (i.e. crystal of high refractive index) offers unique advantages for the monitoring of crystallization processes (Lewiner et al., 2001):

- No external sampling is necessary. Consequently, many problems related to the use of temperature-controlled external sampling loops, and phase separation devices are avoided.

- The technique is insensitive to the presence of solid particles in the crystallizing medium. ATR is not affected by scattering in the presence of particles, bubbles or dispersed droplets.

- FTIR spectroscopy provides real-time information on the time variations of many chemical species present in the solution, including impurities. Further developments of the technique could therefore allow new control strategies taking into account, for example, batch-to-batch variations due to the impurities content.

However, from an industrial standpoint, several concerns arise from the use of ATR probes, which have to be carefully examined.

- Potential for performance variation results from the fact that the effective path length depends on θ. Therefore, any mechanical change is likely to result in a change in the measured absorbance, thus impairing the calibration used to monitor the dissolved solid concentration.

- Any operating condition allowing a non-uniform distribution of chemical composition in the neighborhood of the ATR crystal, such as adhesion or imperfect mixing, can lead to inaccurate measurements. For example, encrustation of the probe can easily occur and appropriate solutions have to be developed.

- Chemical deterioration of the ATR elements will take place in strongly aggressive chemical media, in particular when strong acids and oxidizing agents are present in solution.

- Due to unknown reasons, possibly mechanical and/or thermal stress, the short lifetime of the ATR immersion probes is sometimes incompatible with industrial applications; while the choice of hard materials is not always possible.

- As Eq. 3-1 shows, in the case of products absorbing at high values of λ, the depth of penetration is increased and it is therefore important to check that no drift in the spectra is observed during the crystallization of industrial slurries with high solids content.

3.2.2) Chemometrics

Chemometrics is defined as the use of multivariate data analysis and mathematical tools to extract information from chemical data. Modern in-line or on-line sensors are capable of collecting huge amounts of data from chemical processes. The application or development of chemometric tools to this wealth of process data is termed "process chemometrics" and seeks to provide additional insights into the chemical process through monitoring, modeling and control (Workman et al., 1999). Chemometric tools are useful in both the design stage of crystallization processes when experimental design methods aid in the optimization of the many operating variables and in the interpretation of the multivariate data collected by process sensors (Yu et al., 2005).

ATR-FTIR spectroscopy has been coupled with chemometrics to provide highly accurate in situ solution concentration measurement in dense crystal slurries (Togkalidou et al., 2002, 2001; Dunuwila and Berglund, 1997, 1994). Transformation of the spectra data to concentration information is a critical step towards obtaining reliable and accurate results. Traditional regression methods can be applied by correlating the heights or areas of specific peaks, or alternatively a ratio of specific peaks to a concentration of the measured constituent can be used (Dunuwila and Berglund, 1997; Fevotte, 2002; Lewiner et al., 2002). However, traditional regression methods should not be applied to correlated variables, which the spectral variables typically represent (Pollanen et

al., 2006). In complex chemical systems, the bands in the IR spectrum from different constituents often overlap one another, the absorbencies of specific compounds of interest can be low and, consequently, no single peak can be found to correlate reliably with concentration. In addition, random variation, in part due to instrument drift, is an inherent feature, which makes for error if a specific peak is relied on for concentration data.

Multivariate methods, e.g. partial least squares (PLS) regression and principal component regression (PCR) calibration models, can be applied to solute concentration prediction from crystallization systems (Pollanen et al., 2005; Togkalidou et al., 2001, 2002; Feng and Berglund, 2002; Profir et al., 2002). PLS enables the linear modeling of correlated variables. A large number of variables, in this case spectra points, can be included in the model. PLS reduces the dimensions of the original data and simultaneously reduces the noise level. The PLS calibration can be improved by careful data collection and selection, model validation steps, and using an appropriate data preprocessing technique.

When predicting solution concentration, including multiple absorbances in the calibration model averages measurement noise over multiple spectral frequencies and allows the explicit consideration of peak shifts. The strong correlations within the data make it impossible to construct an ordinary least squares (OLS) model between the multiple absorbances and the solution concentration. The ability of the chemometrics methods of Principal Component

Regression (PCR) and Partial Least Squares (PLS) to handle highly correlated

data allows these chemometrics methods to construct calibration models based

on multiple absorbances. The calibration model used in this work has the form

$$y = b^T x \qquad \text{(Eq. 3-2)}$$

where y is the output prediction (a solution concentration), x is the vector of

inputs (the IR absorbances from the ATR-FTIR and temperature), b is the vector

of regression coefficients.

There are numerous chemometrics methods, most being variations of PLS or

PCR, which can give very different calibration models for data sets (Togkalidou,

2001). The robust chemometrics approach is to apply several chemometrics

methods and then to select the calibration model which gives the most accurate

predictions. The six different methods considered in this work were:

- Top-down Selection PCR (TPCR)

- Correlation PCR (CPCR)

- Forward Selection PCR 1 (FPCR1)

- Forward Selection PCR 2 (FPCR2)

- Confidence Interval PCR (CIPCR)

- Partial Least Squares (PLS)

The mean width of the prediction interval was used as a criterion to select

amongst the calibration models. All chemometric calculations were performed

using MATLAB codes (generated in Braatz group at the University of Illinois at

Urbana-Champaign), except for the PLS algorithm which is featured in MATLAB itself.

3.2.3) Applicability of ATR-FTIR to the monitoring and control of batch crystallizations

ATR-FTIR technique has continued to be the method for in-situ monitoring of concentration. A variety of calibration methods have been developed in the literature. Groen and Roberts (2004) used transmittance ratio of peak intensities characteristics of methanol and urea as calibration parameter for urea-water-methanol system. Peak shift was observed in aqueous urea solutions due to the high degree of hydrogen bonding. Borissova et al. (2004) set up a calibration routine that can choose up to eight wavenumbers within the spectral range of $4000 - 650 \text{ cm}^{-1}$ and the intensity of the corresponding peaks are read into the control software. The absorbance peak ratio was calculated based on two peak heights. Three different calibration models (exponential, linear and power) were then computed. The wavenumbers and the calibration models that gave the best prediction were chosen. These calibration methods, despite being simpler and more straightforward, are often unable to account for peak drift due to a change of solvent content especially in mixed solvent systems. The calibration method based on range of wavenumbers and advanced chemometrics have been shown to be more reliable and accurate (Fujiwara et al., 2002). Besides measuring concentration of different molecular components, Schöll et al. (2006) extended

the application of FTIR-ATR to monitoring the speciation of L-glutamic acid during pH-shift precipitation. The identification of different L-glutamic acid species is possible because different ionic species exhibit different characteristics absorbance bands. Using FTIR-ATR information in combination with FBRM data, the nucleation kinetics of the precipitation of L-glutamic acid were determined in-situ.

The evaluation of solubility and metastability curves is required to design any industrial solution crystallization operation. In usual industrial practice, little time may be devoted to such an evaluation, and only few data points of the curves in question are generally available. In order to shorten and to refine the determination of the solubility curve, a procedure using ATR-FTIR has been developed (Fujiwara et al., 2002). Under supersaturated conditions, if the cooling rate remains moderate and/or if the growth rate is high, the concentration profile quickly reaches the solubility curve, and therefore provides a way to measure it. Such an experimental determination of the solubility can be referred to as a "supersaturated approach". In opposition to usual solubility determinations, this new method provides continuous solubility curves which offer attractive potential advantages:

- Continuous data have richer information content than usual discrete data obtained from samples, and might be used to improve the knowledge of the crystallization system.

- The solute concentration profiles allow the user to know with assurance when the equilibrium has been reached. Such information represents significant benefit in terms of saving of time during the determination of the solubility curve.

- The measured solute concentration profiles can provide valuable information about the dissolution mechanisms and kinetics, especially in the field of pharmacy.

The evaluation of the limits of the metastable zone is also an important issue of crystallization processes. It is well known that many practical and fundamental aspects of nucleation phenomena arise from the variability of the limit of metastability curves which have to be investigated in relationship with operating conditions such as the method of cooling, the rate of temperature decrease, the effect of the hydrodynamic conditions in the crystallizer or of potential impurities, etc. To assess the limits of metastable zone, a solution of known concentration is maintained under undersaturated conditions at a given temperature. The temperature is then decreased according to a pre-set cooling rate while the FTIR spectrometer monitors in-line the evolution of solute concentration. When nucleation occurs, the concentration decreases significantly and the corresponding temperature is recorded. The use of both the calibration procedure and the solubility curve of the system under consideration is a straightforward exercise to compute in-line the time variations of supersaturation (Lewiner et al., 2001).

Liotta and Sabesan (2004) implemented real time feedback Supersaturation-Control (S-Control) on the cooling crystallization of a Schering-Plough API drug candidate using FTIR-ATR and FBRM. FTIR-ATR was calibrated using partial least square (PLS) method across a range of wavenumbers. A cascaded control structure was set up where the primary loop minimized error between the measured supersaturation and set-point supersaturation by manipulating the cooling rate set-point. The secondary loop adjusted the heater/chiller performance to ensure that the new temperature set-point specified by the primary loop was achieved. S-control was shown to be effective in avoiding secondary nucleation and thereby producing large crystals as long as an appropriate supersaturation set-point was used. Although cascade control structure may give faster response, it requires tuning of feedback controller parameters, whose values are dependent on the unknown crystallization kinetics, to follow the set-point supersaturation. In contrast, the control structure used in this work does not require controller tuning except the initial tuning of the heating/refrigerated circulator.

By using rigorous calibration procedures accounting for the temperature dependence of MIR spectra, the in situ ATR-FTIR technique can be successfully applied to the investigating and monitoring of crystallization processes. The design of automatic procedures for the acquisition of fundamental data such as solubility or MZW has been shown to be convenient and time-saving for process development purposes. In addition, the in-line ATR-FTIR technique also offers a

practical means of monitoring polymorphism, and therefore a new tool to better investigate phase transition phenomena. The absence of metastability with respect to the undesired polymorphic form throughout the crystallization process was confirmed by applying ATR-FTIR in Muller et al. (2006).

3.3) Focused Beam Reflectance Measurement (FBRM)

Off-line sensors for the measurement of CSD have long delay times, because physical processes such as sedimentation, sieving, and centrifugation are required before measurement can be taken. In situ CSD sensors are needed for efficient control of crystallization. Forward light scattering is not feasible as it cannot be applied in dense suspensions. In industrial crystallization processes, laser backscattering is the technique most commonly employed.

In recent years, Lasentec FBRM has emerged as a widely used technique for the in situ characterization of high-concentration particulate slurries. FBRM is a probe-based measurement tool, which is installed directly into the system without the need for sample dilution or manipulation. The Lasentec FBRM probe offers the potential for monitoring in situ changes in particle characterization (particle size and structure) over a wide range of suspension concentrations and applications. Some applications involving FBRM includes the field of crystallization (Wang et al., 2006; Kougoulous et al., 2006, 2005a and b; Scholl et al., 2006a and b; Wang and Ching, 2006; Barthe and Rousseau, 2006; Yu et

al., 2006, 2005; Shaikh et al., 2005; O'Sullivan and Glennon, 2005; Scott and Black, 2005; Deneau and Steele, 2005; Worlitschek et al., 2005, 2004; Kougoulos et al., 2005; Kim et al., 2005; Doki et al., 2004; Barrett and Ward, 2003; O'Sullivan et al., 2003; Barrett and Gennon, 2002; Barrett and Becker, 2002; Abbas et al., 2002; Loan et al., 2002; Ruf et al., 2000; Tadayyon and Rohani, 2000; Barrett and Glennon, 1999), polymerization (Hukkanen and Braatz, 2003; Heath et al., 2006a and b; Negro et al., 2006; Yoon and Deng, 2004; Swift et al., 2004; Shi et al., 2003; Owen et al., 2002), fermentation (Ge et al., 2006), papermaking (Ravnjak et al., 2006; Dunham et al., 2000), fiber cement production (Negro et al., 2006), emulsion (Dowding et al., 2001), biological systems (Pearson et al., 2004, 2003; Jeffers et al., 2003; Choi and Morgenroth, 2003; McDonald et al., 2001), waste water treatment (de Clercq et al., 2004;), reaction systems (Custers et al., 2002), and other particulate processes (Clarke and Bishnoi, 2005; Li et al., 2005; Bagusat et al., 2005; Benesch et al., 2004; Heath et al., 2002; Alfano et al., 2000; Richmond et al., 1998).

3.3.1) Principle of FBRM Technique

The FBRM probe utilizes laser light backscattering technology to supply, in real time, a chord length distribution (CLD) as the laser light randomly traverses particles passing through the measurement zone. The CLD measured is a function of the number, size, and shape of particles under investigation (Barrett and Glennon, 1999). As the beam crosses the surface of a particle or particle

structure, light from the beam is backscattered into the probe. The duration of each reflection is multiplied by the velocity of the scanning beam, resulting in a chord length. The measurement range is 1 to 1000µm, with the distribution sorted by chord length into various linear or logarithmic channel distributions. Typically, many thousands of chord lengths are measured per second, with the numbers of counts dependent on the concentration of solids present in the suspension. Hence, the number of chords reported and their measured length will be intimately related to both the particle diameter and shape. Spherical particles will give chord lengths closer to the average particle size than rod-like crystals, for which the dominant chord length may be closer to the minor axis length.

An FBRM probe is inserted into a flowing medium of any concentration or viscosity. A laser beam is projected through the sapphire window of the FBRM probe and highly focused just outside the window surface. This focused beam is then moved so it follows a path around the circumference of the probe window. The focused beam is moving at a high speed (2 m/s to 6 m/s, depending on the application) so that particle motion is insignificant to the measurement. As particles pass by the window surface, the focused beam will intersect the edge of a particle. The particle will then begin to backscatter laser light. The particle will continue to backscatter the light until the focused beam has reached the particle's opposite edge. The backscatter is collected by the FBRM optics and

converted into an electronic signal. Figure 3-2 shows the schematic illustration of the FBRM probe.
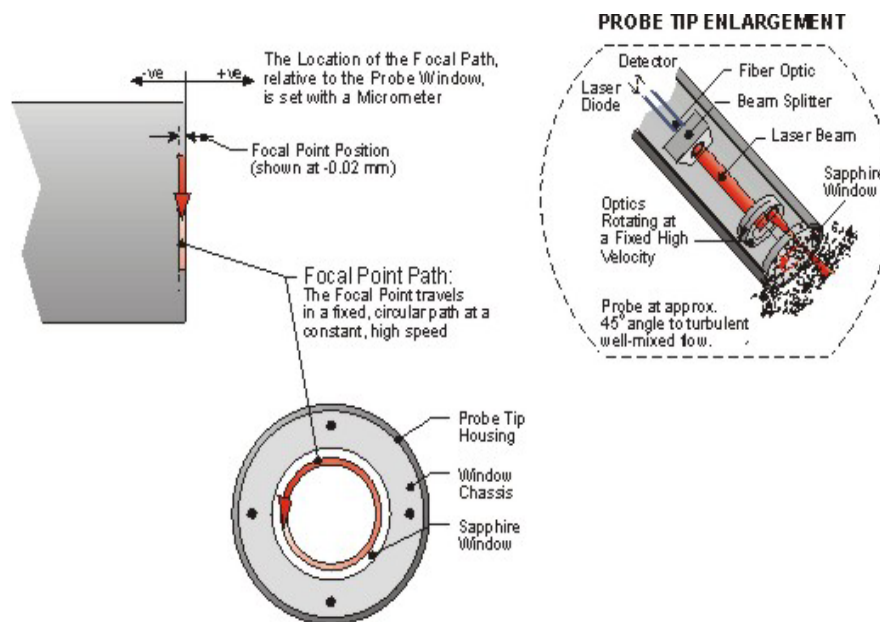
Figure 3-2: Schematic Diagram of FBRM Probe Tip

FBRM uses a unique discrimination circuit to isolate the time period of backscatter from one edge of an individual particle to its opposite edge. This time period is multiplied by the scan speed and the result is a distance, which is the chord length of the particle. A chord length (see Figure 3-3) is a straight line between any two points on the edge of a particle or particle structure (agglomerate). FBRM typically measures tens of thousands of chords per second, resulting in a robust number-by-chord-length distribution (number of counts per second sorted by chord length into 90 logarithmic size bins).
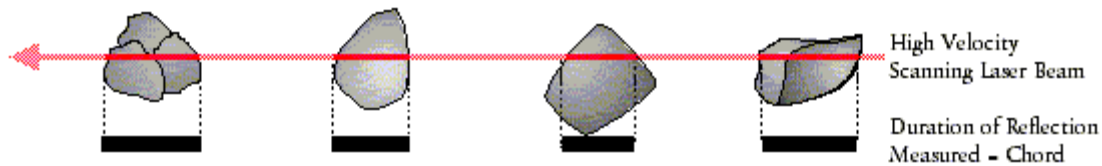
Figure 3-3: Chord length measurements

The data generated by FBRM is a chord-length distribution (CLD), which is a highly precise and sensitive means of tracking changes in both particle dimension and particle population. In addition, with a number-per-length-per-second distribution, specific regions of the distribution can be isolated to enhance resolution to change (i.e., number of fine particles or number of coarse particles in a given dimensional range). Because no particle shape is assumed, the CLD is essentially unique for any given particle size and shape distribution, which means CLDs of different systems cannot be compared per se. Assuming the average particle shape is constant over millions of particles, changes to the CLD are solely a function of the change in particle dimension and particle number. Where shape is also changing, this information can typically be filtered out or enhanced, depending on the goal of the application. An important caveat to note is that materials that do not backscatter (e.g., materials that only produce specular reflection such as optical-grade glass beads, optically clear polystyrene, and pure oils in pure water) cannot be measured with FBRM.

Probe location and orientation is crucial to ensure the successful implementation of the FBRM in optimal measurement of the particles in the system. The side-mounted positions generally allow better sample presentation to the window, at

least for a radial impeller. These positions provide higher counts, and thus the collected data may be regarded as more statistically robust than the data collected in the top-mounted positions. With the probe mounted from the side, the liquid and the suspended particles impinge directly on the window, whereas, with the probe mounted from the top, there is less direct flow impingement. Therefore, the side-mounted positions allow the receipt of a better sample for measurement (Barrett and Glennon, 1999). While it is not always possible to mount the probe at a perfect orientation to the flow, probe location is important for the best possible presentation of material to the probe window (Figure 3-4). As shown in Figure 3-4(a), (b), and (c), flow of particles to the probe window is obstructed. Figure 3-4(d) is the only probe orientation that allows the flow of particles to be adequately impinging on the window surface. The flow carries particles close to the window for the best measurement presentation. The action of the particles against the window prevents buildup of scale on the window surface. The best orientation is achieved when the angle of the probe window is between 30° and 60° to the flow, though 45° is the optimum angle.

    (a)   (b)   (c)   (d)
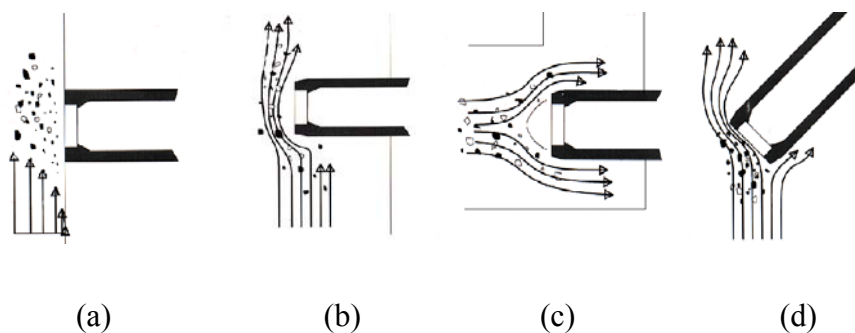
Figure 3-4: Different Orientations of FBRM probe

In general, probe location becomes more important with:

- Extremes in individual particle density (i.e., very low or very high) vs. the carrying solution.

- Lower solids concentration.

- Lower carrying-solution viscosity.

- Larger median particle size.

- Wider particle size distribution.

- Greater particle shape deviation from a sphere.

3.3.2) Applicability of FBRM to the monitoring and control of batch crystallizations

The FBRM probe requires no sample dilution, which has important industrial implications. Rapid in-line data collection allows for the possibility of real time process control, thereby enabling an immediate response to any process change, presenting the potential for minimizing waste and maximizing in-specification production. The FBRM output can be related to changes in particle shape, solids concentration and rheological behavior of fluid suspensions. Overall, the FBRM probe is ideal for industrial utilization as a quality and process control device, providing rapid and accurate data accumulation, with the collected information requiring minimal attention from the plant operators (Barrett and Glennon, 1999). Work published to date on the FBRM system has attempted to either directly

relate the measured chord length data to the particle size data or, more successfully, to simply correlate it to properties dependent on particle size (Bloemen and De Kroon, 2005; Worlitschek et al., 2005, 2004; Li et al., 2005; Hukkanen and Braatz, 2003; Wynn, 2003; Heath et al., 2002; Ruf et al., 2000). Others have investigated some of the relevant operating issues associated with its use (O'Sullivan and Glennon, 2005; Sistare et al., 2005; Worlitschek and Mazzotti, 2003; Barrett, 2003).

FBRM has emerged as a widely used technique for the in situ characterization of crystallization systems. Chord length distributions (CLD) recorded by FBRM are generally used for qualitative analysis and are difficult to compare with particle size distribution (PSD) measured by other techniques. Li et al. (2005a) compared the different particle sizing techniques and cautioned the use of CLD to describe PSD because CLD result is complex, depending not only on the PSD, but also on particle optical properties and shape. Despite the apparent difficulties, several researchers have devoted efforts into restoring PSD from CLD through complicated mathematical modelling (Bloemen and De Kroon, 2005; Li and Wilkinson, 2005; Li et al., 2005b; Worlitschek et al., 2005; Barthe and Rousseau, 2006). Although these authors were able to verify their models with experimental data, their algorithms are only applicable to well defined systems with known shape and optical properties and may not be extendable to systems in general.

FBRM can be used to dynamically quantify and control the effect of process variables (reaction rate, temperature, addition rates, residence time, mixing speed, etc.) on a particulate system, as well as to quantify the effect of the particulate system on downstream performance (separation, reactivity, dispersability, formulations, etc.). Also, FBRM data can be correlated directly with any upstream or downstream process variable or final product specification (size, rheology, zeta potential, etc.) that is a function of the particle shape, dimension, and/or number of particles in the particle system. The typical parameters evaluated with FBRM are particle behavior (including primary growth, agglomeration, dispersion, dissolution, breakage, attrition, and morphology shift), and particle count in isolated regions of the distribution[④].

In addition to process optimization and control, the FBRM measurement is unique in its ability to "fingerprint" each batch at its process concentration based on particle size, particle shape, and particle population. System data is collected at regular intervals in-line and in real time, hence processes can be tracked throughout the run. This makes FBRM an excellent tool to monitor batch-to-batch consistency.

FBRM has been used to develop and optimize crystallization processes (Tadayyon and Rohani, 2000; Worlitschek and Mazzotti, 2004; Doki et al., 2004), track and trouble-shoot crystallizer systems (Wang et al., 2006; Wang and Ching, 2006; Yu et al., 2006; O'Sullivan and Glennon, 2005; Deneau and Steele, 2005;

[④] Refer to Lasentec FBRM Hardware Manual

Kougoulos et al., 2005; Heath et al., 2002; Abbas et al., 2002; Barrett and Glennon, 1999), to monitor polymorphic forms (O'Sullivan et al. , 2003; Scholl et al., 2006), and in control of crystallization systems (Barthe and Rousseau, 2006; Barrett and Ward, 2003; Barrett and Becker, 2002). The objective of any process monitoring is to ultimately bring about control to the process. Yet, despite the proven useful applicability of FBRM in crystallization, there has not been any published work of automated closed-loop feedback control using FBRM, which is what is attempted in this work. Barthe and Rousseau (2006), Doki et al. (2004), and Tadayyon and Rohani (2000) have presented work involving usage of FBRM as a means of controlling crystallization process, but these are not carried out in a closed-loop feedback loop, as in this work.

The main topic of study in Barthe and Rousseau (2006) was to control the distribution in a batch crystallizer. Estimates of the CSD in the batch crystallizer were obtained by applying a model of the octahedral paractamol crystals to a CLD obtained from FBRM. Equipped with process data from FBRM, preferential fines removal was implemented, which led to larger crystal sizes but significantly wider distributions. A peristaltic pump drew fines-rich stream upwards so that larger crystals, whose terminal velocity was greater than the upward liquid velocity, fell back into the well-mixed region of the crystallizer. The rate of removal of fines from the crystallizer was determined by the speed of the pump, and the fines are subsequently dissolved in a separate heating bath before the solution is channeled back to the crystallizer. Fines were removed at a fixed rate,

and FBRM was only used as a monitoring tool to investigate the optimal cooling rate.

Doki et al. (2004) presented T-control strategy for α-glycine using ATR-FTIR and FBRM. Fines were eliminated from the product by repeated temperature-cycling. When the FBRM count increased to a certain point, of which a value was chosen on-site, heating was started until the crystal count returned to the value of the original seed crystals and then the cooling was started again and continued at the same cooling rate. Intermittent heating was repeated during the course of cooling until the final temperature was reached. ATR-FTIR was only used for monitoring purpose rather than for control. Such control method is straightforward but suffer from the drawback of being system dependent and the count number at which heating should be activated requires determination on site.

Tadayyon and Rohani (2000) investigated cooling crystallization of KCl using fines dissolution rate as the manipulated variable. One control variable was the 125 μm chord length count rate measured by FBRM. Control of fines suspension density was accomplished using the FBRM technique. The cooling rate was forced to reach its setpoint by manipulating fines dissolution rate. The control loop could successfully reject disturbance in the fines density and handle the step increase in the feed flow rate.

In short, Lasentec FBRM instruments provide in-process, real-time, particle size and high solids concentration particle count. The benefits inferred by the FBRM are as follows:

- Does not assume spherical particles.

- Provides both the size distribution and count in each size range at regular intervals.

- Enables monitoring of particle count in specific size regions (fines, coarse, etc.) to increase precision, sensitivity, and early warning to process dynamics.

- Can be used to fingerprint batch endpoint based on particle size, shape, and count.

In this work, automation of the entire unseeded crystallization process was brought about, making use of signals from the FBRM. Furnished with FBRM data, automatic detection of primary nucleation and subsequent heating to achieve consistency in the internally-generated seeds was brought about, superseding the advantage of external seeding. Chapter 5 details this work.

3.4) Particle Vision and Measurement (PVM)

An alternative method for measuring the CSD is through periodic sampling, video microscopy, and image analysis (Puel et al., 1997; Patience and Rawlings, 2001). Sampling can be problematic in an industrial environment. A commercial

instrument that has become available is the Lasentec Particle and Vision Measurement (PVM) system, in which images of crystals in solution are obtained using a probe inserted directly into the dense crystal slurry.

Process video microscopy (PVM) is becoming increasingly used to image the crystals as they grow in solution, to visualize the extent of agglomeration and changes in crystal size and shape (Braatz, 2002). In recent years most of these techniques have been used to design new pharmaceuticals crystallization processes, and to troubleshoot problems with existing processes.

PVM instruments are in-process video microscopes built for lab and production environments. They are typically used in applications where the solids concentration is between 1 % and 40 %. Minimum particle size resolution is particle-system dependent, but valuable information usually starts between 5 µm and 10 µm. On the upper end, the practical limit is 1 mm. The enabling of direct observation of crystals, which allow for shape information to be obtained is a major advantage.

PVM's high-resolution imaging at up to 50% solids provides a unique qualitative understanding of the process especially in the following cases:

- Where system sampling is difficult.

- The process is not well understood.

- Multiphase particle systems are under investigation.

- In-depth shape analysis is required.

In-line imaging microscopy has the advantage that the crystals are directly observed. PVM allows a rapid collection of data of 10-30 frames per second, providing two-dimensional snapshots of the crystals in real-time. Although the contrast of the images is insufficient for direct image analysis, the specific shape of the crystals can be obtained through image data reduction and robust chemometrics. A significant weakness of the PVM is that it can only image crystals not smaller than 5 μm (Pacek et al., 1994). Filtration efficiency as well as the behavior of the crystallization process however depends on crystals smaller than 5 μm. If crystals of smaller sizes can be imaged, then imaging could have significant advantage over laser backscattering for the in-line measurement of crystal size distribution.

The PVM is a rugged instrument suitable for use in industrial applications. The main use of in-line video microscopy today is for qualitative troubleshooting (Wang et al., 2006b; Scholl et al., 2006a; Barrett and Glennon, 2002). The on-line estimation of characteristics of the CSD has been demonstrated using a combination of PVM, FBRM, and robust chemometrics (Togkalidou et al., 2001b). Given the importance of crystal shape in pharmaceutical applications, and that progress becomes easier as computers continue to increase in speed, the accuracy of such predictions can be expected to improve in future years (Braatz, 2002).

4) Experimental Method

4.1) Experimental Set-Up

A photograph of the experimental set-up for crystallization experiments is shown in Figure 4-1.
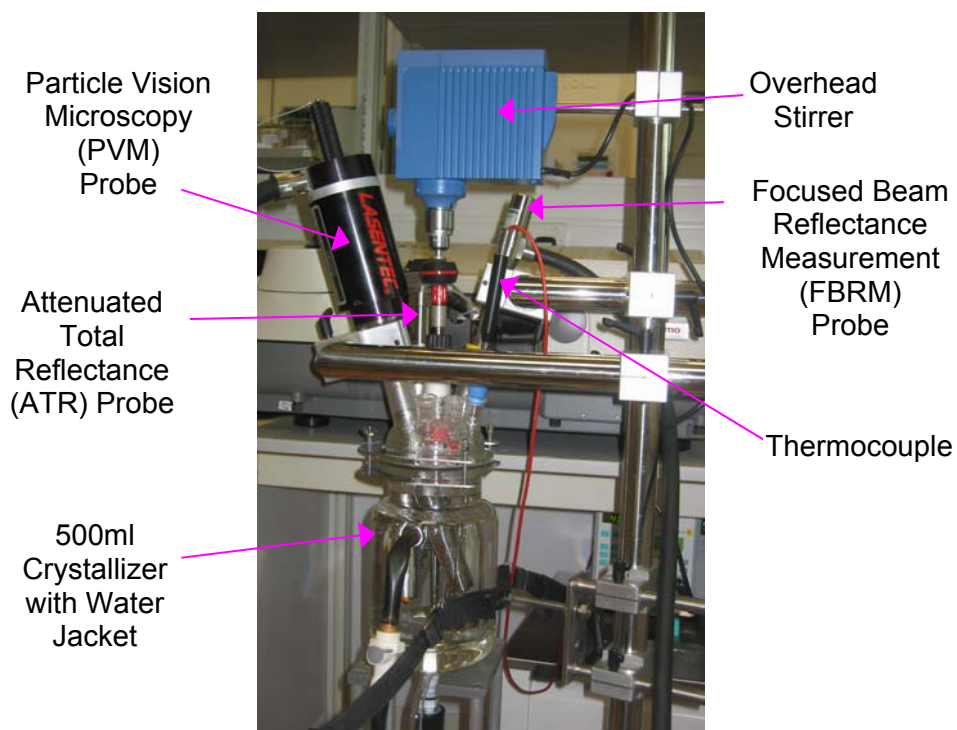
Figure 4-1: Experimental set-up for crystallization experiments. In-line instruments used include the ATR-FTIR, FBRM, and PVM.

Crystallization experiments were performed using glycine (≥99% purity, Sigma) in a 500 ml jacketed baffled flat bottom crystallizer. An overhead stirrer with a four-bladed Teflon impeller was used to agitate the system at 550 rpm. De-ionized water was used to prepare the solutions. The same experimental set-up was used for all experiments.

A FBRM probe (Model D600L, Lasentec) was inserted into the turbulent zone of the suspension. Chord length distributions (CLD) were obtained every 10 seconds using the Control Interface Software version 6.0b16. Data acquired were analyzed using the Data Review Software version 6.0b16, which displays CLD and related statistics.

Absorbance spectra were collected every minute using a Nicolet Nexus 4700 FTIR equipped with a Dipper-210 Axiom Analytical Attenuated Total Reflectance (ATR) probe. Zinc Selenide was the internal reflectance element.A spectral resolution of 4 cm^{-1} was used and every spectrum was the average of 32 scans in the range of 650-4000 cm^{-1}. Deionized water at room temperature was used for the background measurement. The spectrometer is continuously being purged with purified air supplied through a purge gas generator (Parker Balston, model 75-52-12VDC).

The system temperature was controlled by a Julabo FP50-HL circulator and measured every two seconds using a stainless steel Pt100 thermocouple.

The Lasentec Particle Vision and Measurement (PVM) probe was inserted into the system for visual monitoring of the evolution of the crystals, mainly to detect any significant attrition, agglomeration, secondary nucleation or any change in habit.

4.2) Calibration for In-Line Solution Concentration Measurement

Specific amounts of glycine and deionized water were added into the 500 ml crystallizer. With the overhead stirrer agitating the system, the slurry was heated to about 15 ^oC above the saturation temperature and maintained at this elevated temperature for at least 30 minutes to ensure that all crystals have dissolved. Absorbance spectra were collected every minute while the solution was cooled at 0.5 ^oC/min. Data acquisition was stopped once nucleation occurred because the solute concentration would not be the same as the starting concentration. The spectra acquired after first crystals appeared were excluded from the calibration set. Absorbance spectra were collected for six different solution concentrations in the range from 0.20 to 0.40 g/g-water, while temperatures span the range from 15 to 70 ^oC. These ranges are inclusive of concentration and temperature values required in all the experiments.

4.3) Solubility Measurements

The solubility of α-glycine in the temperature range 20-60 ^{o}C was measured using the calibrated ATR-FTIR. Glycine was dissolved in excess into de-ionized water in the 500 ml crystallizer. The slurry was equilibrated at each temperature for about an hour before spectral data were acquired at that temperature. Solubility values were calculated using the calibration model described later on in this paper. Glycine crystals were taken from the slurry after equilibration at each temperature and X-ray powder diffraction (XRPD) analysis was carried out to verify the polymorphic form.

4.4) Metastable Zone Widths (MZW) Measurements

The Metastable Zone is the region where the solution is supersaturated but spontaneous nucleation does not occur. The measurement of the MZW was necessary to provide an estimation of the point of nucleation for unseeded systems, and to give an indication of the temperature at which seeds should be added for seeded systems.

MZWs of glycine were investigated in the temperature range of 20-70 ^{o}C. Glycine of various concentrations was prepared in a 500 ml crystallizer. The solution was heated to and maintained at 10 ^{o}C above the saturation temperature for at least 30 minutes, then cooled at various constant rates (0.5 ^{o}C/min, 1 ^{o}C/min and 1.5

^{o}C/min) until nuclei formed via primary nucleation were detected by the FBRM. FBRM D600 probe has previously been employed to detect nucleation by other researchers (Fujiwara et al., 2002; Barrett and Glennon, 2002). Fujiwara et al.(2002) have further provided a thorough comparison of MZW determination by FBRM with that by visual observation and by ATR-FTIR, and found that FBRM detected nucleation the earliest amongst the three methods.

4.5) Correlation between CLD and PSD

Data from FBRM were relied on in the comparison analysis of our product crystals; hence verification of the validity of FBRM statistics is essential. PSD measured under an optical microscope was used to compare with CLD obtained from FBRM. Images of product crystals were captured with an Olympus BX51 polarizing light microscope. The images were converted into digital images through a color video camera (JVC KY-F55B 3-CCD) and were processed by an image analysis software (AnalySIS). The length of the longest dimension of each crystal was recorded as the geometric crystal size. More than 1000 product crystals from each batch were measured.

4.6) Temperature-Control (T-control) Crystallization

Both seeded and unseeded systems were used in T-control experiments.

An appropriate amount of glycine corresponding to a saturation temperature of 50 ^{o}C was dissolved in de-ionized water in the 500 ml crystallizer. The system was then heated to and maintained at 60 ^{o}C for at least 30 minutes before a cooling ramp of 0.5 ^{o}C/min was imposed to approach the onset of nucleation (unseeded systems) or the point of seeding (seeded systems). A cooling rate of 0.5 ^{o}C/min was chosen because slower rates give fewer initial nuclei and longer batch time, while faster rates result in excessive nucleation and fine crystals. The final temperatures for all experiments were 20 ^{o}C.

For seeded systems, the system was cooled at 0.5 ^{o}C/min to a point midway between the solubility curve of α-glycine and the metastable limit (which corresponded to 45 ^{o}C in this case) before seeds were added dry. This was to ensure that the seeds would not dissolve and that spontaneous nucleation would be avoided. The solubility of α-glycine was used to determine the point of seed addition because XRPD data showed that the product crystals crystallized from water in our experiments were consistently the α form. Seeds were product crystals from previous batches in the sieve fraction of 125-212 μm. Amount of seeds added corresponded to 2 % of the total mass of raw glycine used. The temperature was held at 45 ^{o}C for 10 minutes after seed addition, to allow time for adequate dispersion of seeds, before T-control was activated

In unseeded systems, to avoid the need for manual observation, the system was cooled to 35 ^{o}C at 0.5 ^{o}C/min and held for 20 minutes. Primary nucleation was

always observed although the temperature at which nucleation occurs varied due to the stochastic nature of nucleation. The CLDs of the self-nucleated seeds were recorded at the end of the 20 minutes, after which T-control was activated. Pre-determined temperature profiles include linear, concave, and convex cooling. Various linear cooling rates were implemented. The convex profile was determined by the cubic formula in Eq. 4-1, derived by Mayrhofer and Nyvlt (1988) for a batch system with negligible nucleation rate and constant growth rate, while the concave profile was the mirror image of the convex profile.

$$T_{set} = T_0 - (\frac{t}{t_{total}})^3 (T_0 - T_f) \qquad \text{(Eq. 4-1)}$$

where T_{set}, T_0, and T_f denote set-point, initial and final temperatures respectively, t represents time and t_{total} represents the duration of the convex profile.

4.7) Supersaturation-Control (S-control) Crystallization

The experimental procedures for S-control crystallization are the same as that for T-control crystallization. The set-point supersaturation profile is the result of a compromise between the desire for fast crystal growth and low nucleation rate (Fujiwara et al., 2005). In our case, a constant S_{set} was used and a closed-loop feedback control was implemented to manipulate the system temperature to match the set-point. A program was written in Microsoft Visual Basic 6.0 to implement the S-control, reading the system concentration as computed from the

absorbance data acquired by the ATR-FTIR and then manipulating the system temperature by sending signals to the circulator.

4.8) Detection of Primary Nucleation in Unseeded Crystallization Systems Using FBRM

An appropriate amount of glycine corresponding to a saturation temperature of 50 $^{\circ}$C was dissolved in de-ionized water in the 500 ml crystallizer. The system was then heated to and maintained at 60 $^{\circ}$C for at least 30 minutes before a cooling ramp of 0.5 $^{\circ}$C/min was imposed to approach the onset of primary nucleation. The FBRM was used to detect the point at which primary nucleation occurs, after which the decreasing temperature ramp in approaching primary nucleation was then halted automatically.

4.9) Feedback Loop employing FBRM in Unseeded Batch Cooling Crystallization

After the decreasing temperature ramp is halted automatically upon detection of primary nucleation, the system is held at that temperature for 15 minutes to allow for the primary nucleation to complete and the system statistics to stabilize. Subsequently, an increasing temperature ramp is imposed to adjust the coefficient of variance (c.v.) of the crystals to a pre-determined setpoint to

achieve consistency in the nuclei generated by primary nucleation in different runs. Thereafter, T-Control is implemented.

4.10) Investigation on the applicability of the FBRM Feedback Loop techniques on an alternative system

Exactly the same methods that was used for the glycine-water system was tested on paracetamol-water system.

An appropriate amount of paracetamol corresponding to a saturation temperature of 50 $^{\circ}$C was dissolved in de-ionized water in the 500 ml crystallizer. The system was then heated to and maintained at 60 $^{\circ}$C for at least 30 minutes before a cooling ramp of 0.5 $^{\circ}$C/min was imposed to approach the onset of primary nucleation. The FBRM was used to detect the point at which primary nucleation occurs, and the decreasing temperature ramp in approaching primary nucleation is then halted automatically.

After the decreasing temperature ramp is halted automatically upon detection of primary nucleation, the system is held at that temperature for 15 minutes to allow for the primary nucleation to complete and the system statistics to stabilize. Subsequently, an increasing temperature ramp of 0.3 $^{\circ}$C/min is imposed to adjust the coefficient of variance (c.v.) of the CLDs to a pre-determined setpoint to

achieve consistency in the nuclei generated by primary nucleation in different runs.

FBRM data for paracetamol crystals so formed were validated, via comparison with results from sieve analysis (Sonic sifter, model L3P from ATM Co.). The smallest aperture used was 150 µm and the largest 1000 µm. All particles retained on one sieve were assumed to have the same size, which is the arithmetic mean aperture size of two adjacent sieves. Crystal products were filtered and washed repeatedly with mother liquor. Then the crystals were left to dry at room temperature for a day before sieve analysis was carried out.

5) Results and Discussion

This chapter presents the results of experiments carried out in the investigation of the optimal control strategy for batch cooling crystallization.

5.1) Overview

Consistent particle properties are an important goal for industrial batch crystallizations. Several control strategies, from unseeded open-loop T-control to seeded S-control, were evaluated for the cooling crystallization of glycine. Particle properties were assessed in-line using ATR-FTIR, FBRM, and PVM, facilitating investigations of process consistency. Surprisingly, the more sophisticated closed-loop feedback S-control did not give better crystal quality over the simple traditional T-control. Changing the pre-set cooling profile, or the pre-set supersaturation limit, showed limited benefits. In this comparison, seeding was by far the most effective strategy.

The prime reason for crystal product inconsistency in unseeded systems is that primary nucleation is unpredictable and do not occur at a fixed temperature. This hence necessitates a means for automated detection of the onset of primary

nucleation and a strategy to tune the primary nuclei so formed to achieve consistency as per external seeding.

In this work, a novel concept of using FBRM in a feedback control loop has been developed and investigated. FBRM was successfully used to detect primary nucleation, after which control strategies were automatically implemented in unseeded cooling crystallization systems. Another disadvantage of unseeded systems is that the randomness of primary nucleation produces inconsistent initial nuclei for different runs, thereby resulting in inconsistent product crystals. A method to counter this problem employing FBRM in a closed feedback loop is also addressed in this thesis, which involves adjusting the c.v. of the primary nuclei. Consistent crystal products from unseeded systems were hence achievable. A further validation of these two new techniques proposed was observed in the successful implementation in a more challenging system, paracetamol-water.

5.2) Calibration Model

Temperature and the absorbance spectra in the range of 650 to 1800 cm^{-1} were correlated with glycine concentration through chemometric methods, as detailed by Togkalidou et al. (2001, 2002). Their chemometric approach takes into account spectra over a wide range of wavenumbers, producing calibration models that are an order-of-magnitude more accurate than methods based on

absorbances at peaks. A significant advantage of using chemometrics to construct the calibration model is its ability to automatically factor in the relative signal-to-noise ratios as well as the magnitude of absorbances, and its ability to average the effect of noise over many absorbances (Fujiwara et al., 2002). Fujiwara et al. (2002) has shown that their chemometric approach measures concentration accurately even for a low concentration system like paracetamol-water.

As shown in Figure 5-1, the relative error of our calibration model is about 1 % with respect to the lowest concentration used (lowest required concentration is 0.23 g/g-water, which is the solubility of α-glycine at our lowest temperature of 20 ^{o}C). The sensitivity to the measured temperature is approximately 1 % per 1 ^{o}C according to the calibration model. Since the solubility of glycine in water is high, the contribution of noise becomes insignificant, and accurate solution concentration is attained. Systems with high solubilities are more amenable to use with ATR-FTIR as the effects of instrument drift becomes less significant. Such instrument drift is inherent in the IR system due to source instability and configuration changes in the optical conduits (Feng and Berglund, 2002).
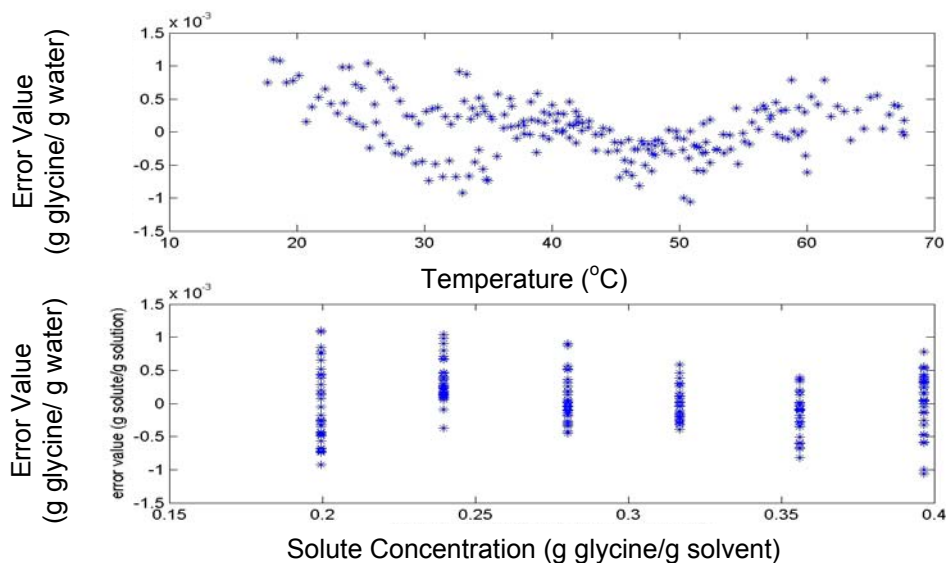
Figure 5-1: Calibration of the ATR-FTIR for α-glycine-water using robust chemometrics (Togkalidou et al., 2001, 2002) gave a relative error of less than 1% with respect to our lowest concentration measurement.

5.3) Solubility Curve and Metastable Zone Width (MZW) Determination

Figure 5-2 shows the solubility data of α-glycine obtained together with the reference data from Mullin (2001). It can be seen that our measurements are in good agreement with the reference data. This verifies the accuracy of our ATR-FTIR calibration model.
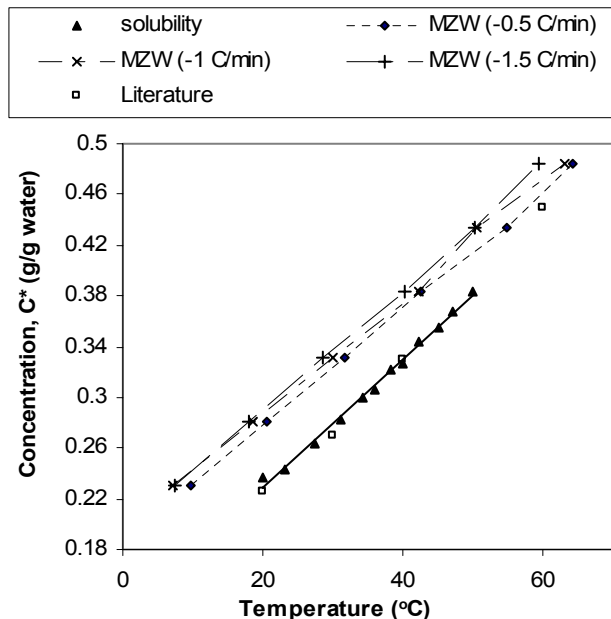
Figure 5-2: Solubility and metastable zone width of α-glycine measured. Reference solubility data were taken from Mullin (2001).

Figure 5-2 shows also the MZW measured by FBRM. As expected, the slower the cooling rate, the higher the temperature at which nucleation occurred and hence the narrower the MZW. The magnitude of the MZW is about 0.04 g-glycine/g-water. In this case, MZW is calculated with respect to the solubility curve of α-glycine because product crystals formed were consistently the α-polymorph.

5.4) Correlation between CLD and PSD (Glycine)

A typical microphotograph of the crystals is shown in Figure 5-3. In-situ observation using PVM showed that agglomeration and attrition were insignificant during crystallization. Therefore, the product crystals harvested are

mainly single crystals which made measurement under the microscope relatively easy. The length of the longest dimension of each crystal was recorded as the geometric crystal size.
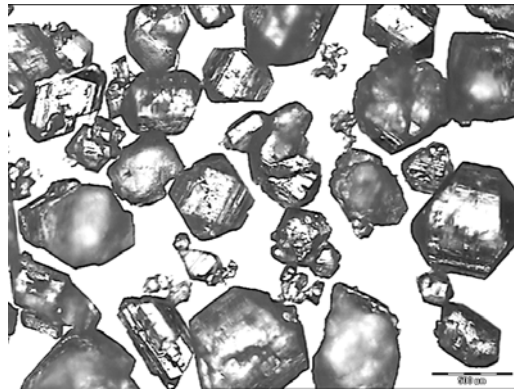
Figure 5-3: Typical microphotograph of glycine crystals obtained from crystallization experiments. Scale bar represents 500 μm.

Figure 5-4 compares the measured PSD with non-weighted and square-weighted CLDs. It is obvious that square-weighted CLD corresponds more closely to the PSD measured. Hence square-weighted CLDs are used for subsequent analysis in this work. Heath et al. (2002) have also found the square-weighted CLD of the FBRM to have closer resemblance to conventional laser diffraction distribution. Considering the critical parameters of standard deviation and mean, our results (Figure 5-5) show that the correlation between the FBRM square-weighted data and the measurements obtained by the microscope gave a R^2 value of 0.9. This implies that the FBRM measurements give a reliable reflection of the width of the PSD and crystal sizes in the system. Because the longest dimension was measured under the microscope, the gradient of the correlation between FBRM square-weighted mean and microscopic mean is less than 1.0. Numerically the

FBRM data do not correspond exactly to microscopy data as they are based on different principles of measurement; but trends could be observed and analyzed to give an understanding of the progress of the crystallization process.
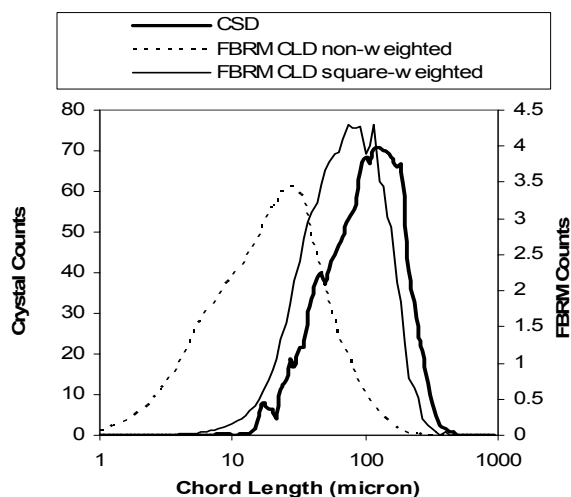
Figure 5-4: Comparison of PSD measured with the microscope and FBRM square-weighted and non-weighted CLDs for glycine.
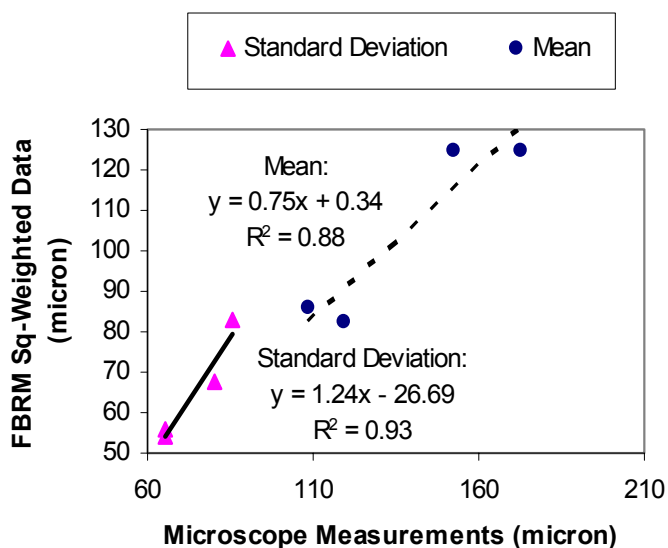
Figure 5-5: Plot of FBRM square-weighted data vs microscope measurements of the product crystals of four different runs for glycine.

For the CSD derived from microscopic measurements, horizontal displacements of the plots were observed as compared with the FBRM CLD (Figure 5-4). Such is expected; the position of this distribution depends on how the crystals were measured. Crystals are 3-dimensional, but measurements can only be made 2-dimensionally. Since glycine crystals are not spherical (Figure 5-3), different measured dimensions will result in different positions on the horizontal axis of the distribution (see Figure 5-6). If, as in this case, the longest dimension of each crystal was measured, a rightward shift of the microscopic distribution would be expected. Because the FBRM measures chord lengths randomly, the longest dimension of each crystal is not always captured.
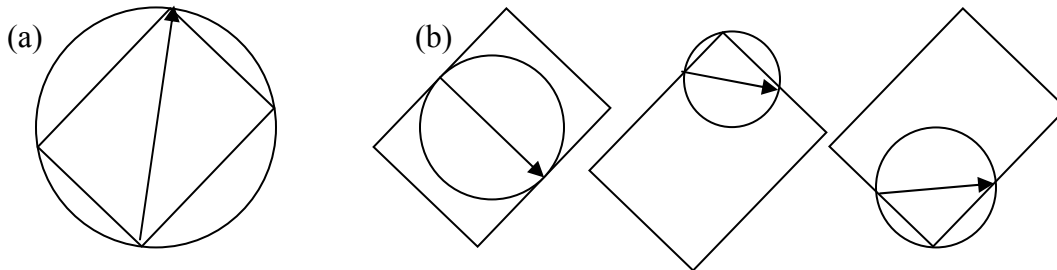
Figure 5-6: (a) Sphere corresponding to the longest chord length; (b) Sphere corresponding to the other chord lengths

5.5) Case Study 1: Open-Loop Temperature Control (T-control) - Seeded

Figure 5-7 shows the user-friendly control interface developed in Visual Basic for T-control, S-control and FBRM-control.
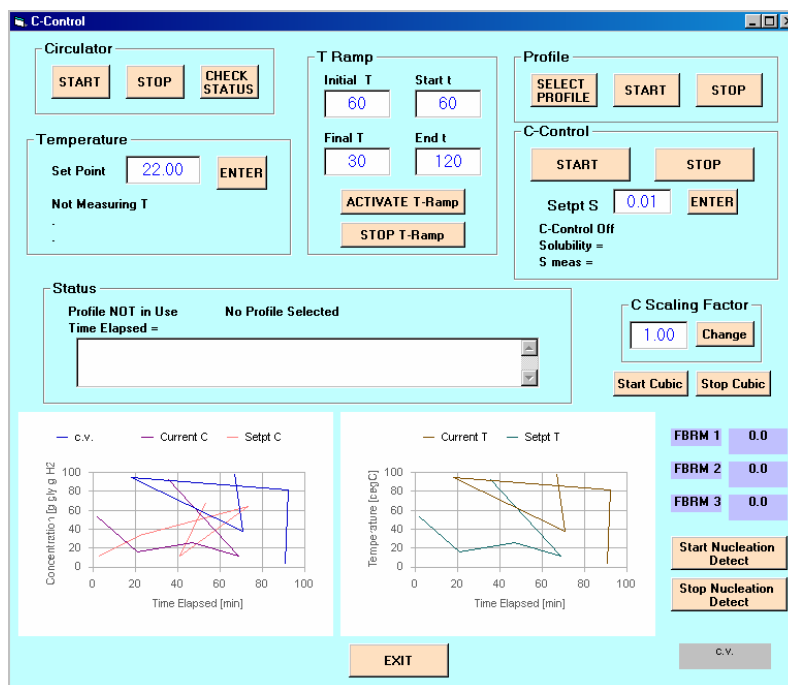
Figure 5-7: User-Friendly Control Interface developed in Visual Basic.

The temperature profiles implemented in the T-control experiments are shown in Figure 5-8. For seeded systems, the product crystal CLDs were similar (Figure 5-9(a)) despite the significant differences in the various temperature profiles. The convex profile, widely regarded as the optimal cooling profile, did not yield better crystal products compared to the other profiles; the concave profile, akin to natural cooling, gave crystal products of the same quality. The different linear cooling rates of 1 ^{o}C/min and 0.3 ^{o}C/min also did not result in any variations in product crystal quality, although the faster cooling rate was expected to generate more fines and should result in wider CLD. This observation of similarity of CLDs is further quantified by the FBRM statistics in Table 5-1(a). Mean and standard deviations agree closely for the different runs. This suggests that the product CLD is not affected by different cooling profiles. The supersaturation and FBRM

particle counts profiles of the linear 0.3 $^\circ$C/min run are illustrated in Figure 5-10, showing that the supersaturation was kept below 0.02 g/g-water and the particle counts remained quite constant for the entire run. Other T-control runs show similar profiles. A closer inspection of the supersaturation profiles of all four runs show that the supersaturation were all kept below 0.025 g/g-water, which is well below the metastable limit of 0.04 g/g-water shown in Figure 5-2, further verifying the absence of secondary nucleation observed. The wide MZW allows for a greater range of controls without violating the metastable limit, resulting in similar product crystal quality from all seeded runs. These data show that for seeded crystallizations, variations in crystallization trajectory within the metastable zone have little effect on the product particle size. Extremes of cooling rates may have more prominent effects on the CLDs, but such extremes may not be attainable at industrial scales.
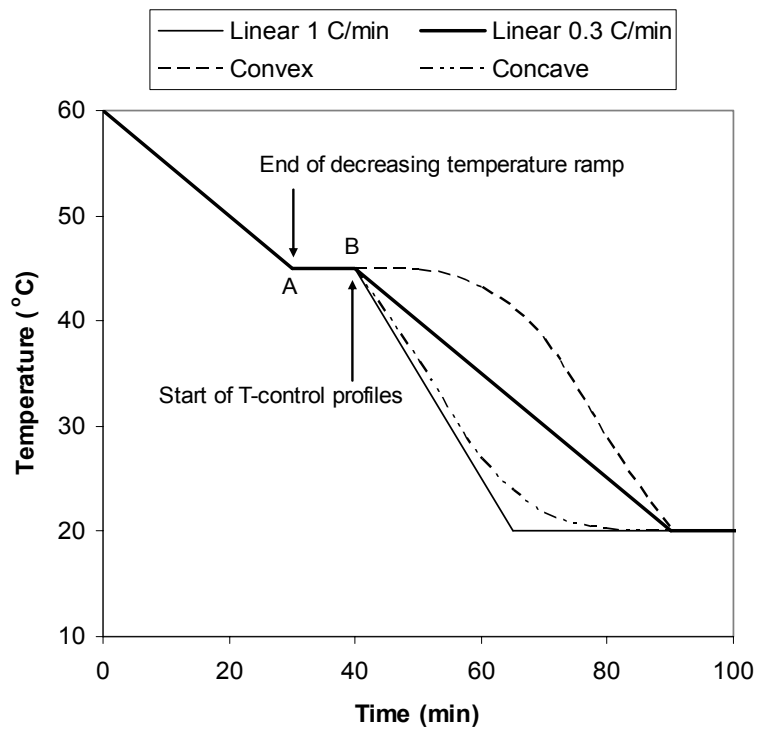
Figure 5-8: Temperature profiles implemented in T-control experiments for glycine system.
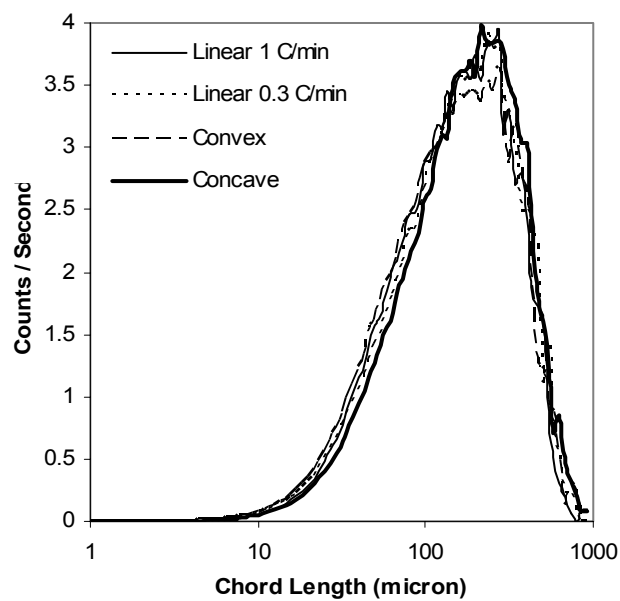
(a)
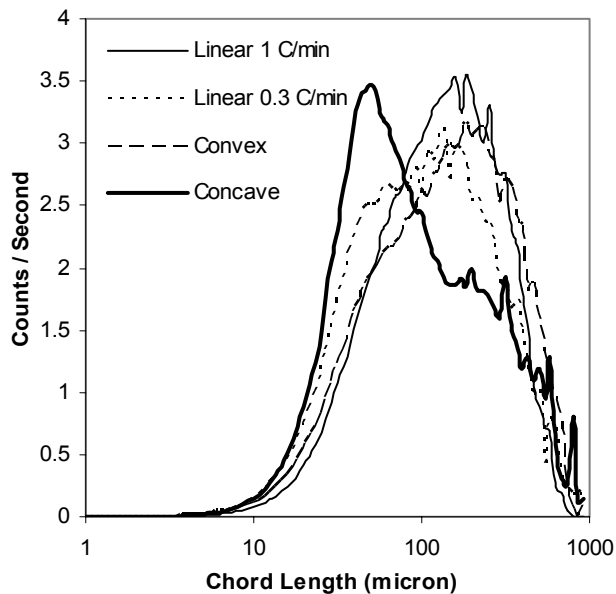
(b)
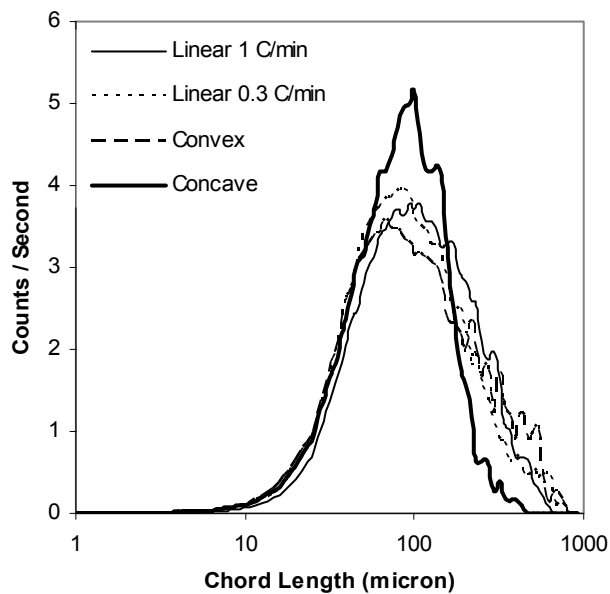
(c)

Figure 5-9: Glycine system: Normalized square-weighted CLDs of product crystals obtained from (a) seeded and (b) unseeded T-control experiments. (c): initial CLDs of primary nuclei before the implementation of various temperature profiles, of which the product crystals are shown in (b).

Table 5-1: Glycine system: FBRM statistics (in the 1-1000 μm range) for final product crystals obtained from various temperature profiles implemented on (a) seeded and (b) unseeded systems.

(a)

FBRM Statistics	Linear 1 ^{o}C/min	Linear 0.3 ^{o}C/min	Convex	Concave
Mean	196.3	216.8	208.3	195.2
Standard Deviation	143.7	152.5	148.0	138.0

(b)

FBRM Statistics	Linear 1 ^{o}C/min	Linear 0.3 ^{o}C/min	Convex	Concave
Mean	175.75	153.05	186.57	149.48
Standard Deviation	132.35	142.63	155.29	165.87
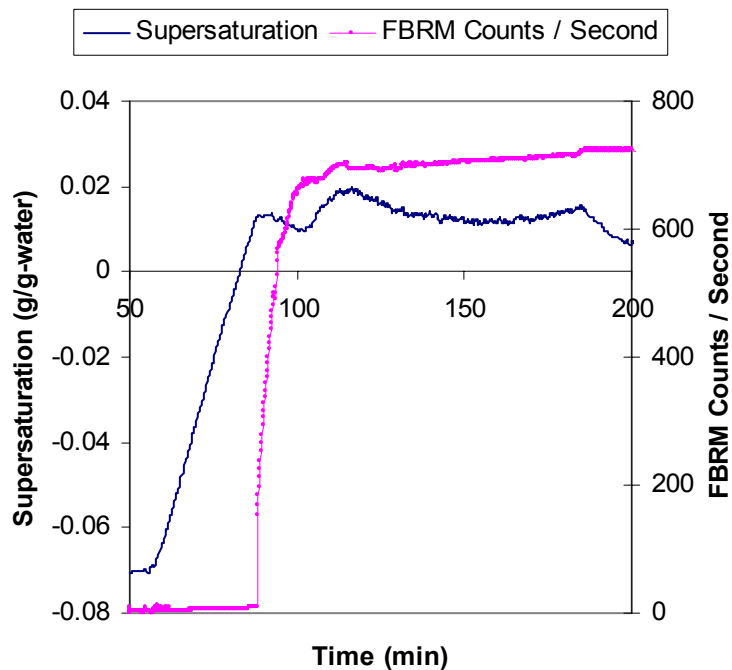
Figure 5-10: Supersaturation and FBRM particle counts profiles of a seeded T-control (linear 0.3 ^{o}C/min) run for glycine.

5.6) Case Study 2: Open-Loop Temperature Control (T-control) - Unseeded

Unseeded crystallizations were carried out with the same temperature profiles shown in Figure 5-8. In contrast to the seeded case, Figure 5-9(b) and Table 5-1(b) show that the product CLDs obtained from unseeded systems were considerably different when different temperature profiles were employed. One advantage of in-line technology is that the source of such variability can be investigated. The difference in product crystal quality is a consequence of the inherently disparate CLDs of self-nucleated seeds, rather than the effect of the different cooling profiles. Figure 5-9(c) shows the CLDs of the primary nuclei (point B in Figure 5-8), after holding for 20 minutes at 35 ^{o}C and before the implementation of the various temperature profiles. It is obvious that the discrepancies in the primary nuclei generated (Figure 5-9(c)) is the cause for the differences in the product CLDs (Figure 5-9(b)). This supports the hypothesis that the major source of variability in unseeded crystallizations is primary nucleation.

Figure 5-11 shows that CLDs of self-nucleated seeds from eight different runs varied considerably even though nucleation was approached at the same cooling rate before the activation of T-control. The CLDs were taken after holding the system at 35 ^{o}C for 20 minutes, and before the implementation of T-control or S-control (point B in Figure 5-8). The FBRM statistics of the self-nucleated seeds are listed in Table 5-2, giving a quantitative analysis of the variations in the CLDs. The average variabilities (numbers after the ± signs) are significant, indicating the substantial differences in the initial seeds formed. Square-weighted

mean vary by up to 30%, and square-weighted standard deviation varies by nearly 40% with respect to the average of the eight runs. Lack of control of size distribution in the self-nucleated seeds produced by spontaneous nucleation is a key feature in unseeded systems, as primary nucleation is random and irreproducible. In view of this, comparing the product CLDs of unseeded systems as a means of drawing a conclusion as to which profile is superior is thus not substantial, as higher variations in product CLDs obtained in unseeded systems may be attributed to the higher variations of the initial CLDs formed by primary nucleation. The observation here also demonstrates the power of in-line technique. The inconsistencies in the initial CLDs due to spontaneous nucleation would not have been detected if FBRM had not been used and the differences in product CLDs would have been attributed to the different temperature profiles used.
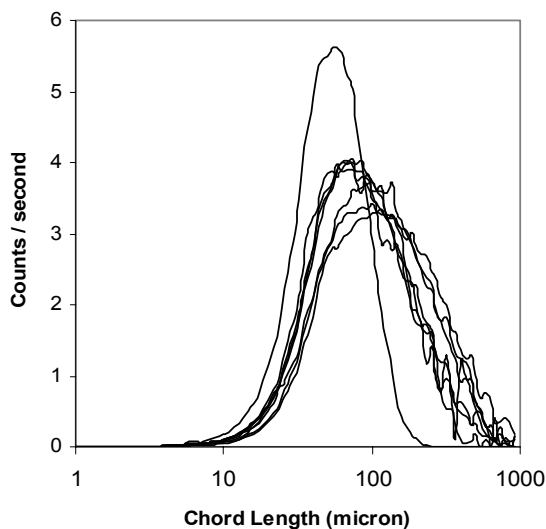
Figure 5-11: Normalized square-weighted CLDs of self-nucleated seeds from eight unseeded crystallization experiments for glycine system.

Table 5-2: Glycine system: Averaged FBRM statistics (in the 1-1000 μm range) for the CLDs of self-nucleated seeds in eight unseeded experiments.

FBRM Statistics	Averaged
Mean	122.76 ± 35.75
Standard Deviation	106.49 ± 40.28

5.7) Case Study 3: Closed-Loop Supersaturation-Control (S-control) – Seeded

After calibrating the ATR-FTIR, the next step in S-control is to determine a suitable set-point supersaturation value (S_{set}). To attain a compromise between fast growth and low nucleation, a set-point half-way between the solubility curve and metastable limit was chosen. Analysis of the solubility and MZW chart (Figure 5-2) gives this value to be approximately 0.02 g/g-water, corresponding to an undercooling of about 4 ^{o}C.

Here, supersaturation (S) is represented as the difference between the solution concentration (C) and the saturated concentration (C^*) at the same temperature (S = C-C*) instead of as a concentration ratio ($S = \dfrac{C - C^*}{C^*}$). This is primarily because of the greater errors associated with the latter, especially at lower values of C* (Liotta and Sabesan, 2004). In view of our calibration error of $\pm$ 0.001 g/g-water and the noise inherent in the ATR-FTIR measurement of concentration, set-point supersaturation value of two decimal places was used. A lower S_{set} was expected to bring about better crystal product quality because the concentration-temperature trajectory would be further away from the

metastable limit leading to a narrower PSD. To investigate if a lower S_{set} is beneficial towards better crystal product quality, S_{set} = 0.01 g/g-water was implemented in a seeded system. A notable feature of S-control is the lack of any time constraint on the system. The duration of S-control in this case was three hours. In another experiment, S_{set} = 0.02 g/g-water, which is half-way between the solubility and metastable limit curves was implemented, resulted in a batch time of one hour. The reason for the difference in duration is that, for a higher S_{set}, the concentration of the system has to decrease at a faster rate to generate higher supersaturation in the system to match the set-point. This hence forces the system temperature to decrease at a faster rate. The temperature profiles for these two runs are shown in Figure 5-12. The cooling ramps are almost linear, with rates of 0.15 ^{o}C/min and 0.45 ^{o}C/min respectively for S_{set} = 0.01 g/g-water and S_{set} = 0.02 g/g-water. No secondary nucleation was observed in both cases.
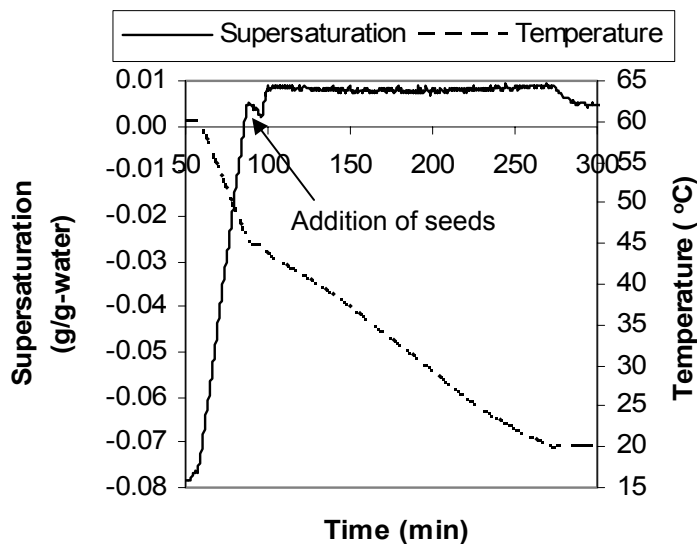
(a)
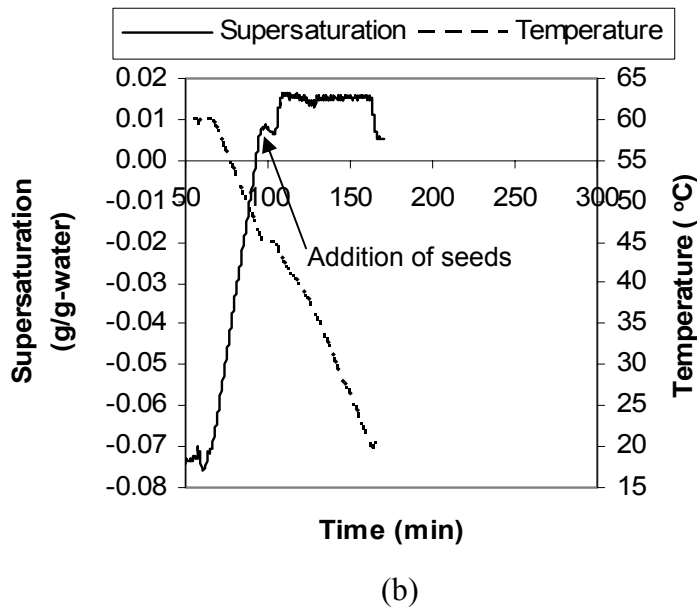
Figure 5-12: Supersaturation and temperature profiles of seeded crystallization under S-control at (a) S_{set} = 0.01 g/g-water and (b) S_{set} = 0.02 g/g-water for glycine system.

The supersaturation profiles of the two runs are shown in Figure 5-12. In both cases, the measured supersaturation never reached the set-point supersaturation value. For the case of S_{set} = 0.01 g/g-water, the measured supersaturation followed quite closely at approximately 0.009 g/g-water. However, for the case when S_{set} = 0.02 g/g-water, the system was maintained at approximately S= 0.016 g/g-water for most of the duration of S-control. The supersaturation offsets are due to inherent instrumentation constraints. Because the system concentration was measured at one-minute intervals, the calculated setpoint temperature was unable to respond fast enough to correspond to the decreasing concentration in the system. The difference between the system and set-point temperatures increases as set-point supersaturation increases because of the faster cooling rate required. A shorter measurement interval was not

feasible in this case for a couple of reasons. Firstly, the acquisition of every FTIR spectrum, which was the average of 32 scans, took about 25 seconds. Secondly, the control program was not robust at shorter time intervals due to the very large amount of data collected each time. Despite the instrumentation limit, the supersaturation was controlled to the same relatively constant level in all runs at the same S_{set}. The supersaturation offsets are due to the inability of the circulator to adjust the system temperature to the set-point temperature fast enough during cooling. The difference between the system and set-point temperatures increases as set-point supersaturation increases because of the faster cooling rate required. Despite the instrumentation limit, the supersaturation was controlled to the same relatively constant level in all runs at the same S_{set}.

The experiment with S_{set} = 0.02 g/g-water is expected to generate more fines and result in a wider CLD because of the increased possibility of secondary nucleation at higher supersaturation. However, this was not observed. As shown in Figure 5-13, the product CLDs obtained from the two experiments were very similar in terms of width of CLD and mean chord length. To further substantiate this observation, a quantitative comparison was carried out using FBRM statistics (Table 5-3(a)). The means and standard deviations are in good agreement, indicating that smaller S_{set} was not superior in giving higher quality product crystals. It can thus be concluded that S_{set} = 0.02 g/g-water is more efficient than S_{set} = 0.01 g/g-water for obtaining the same crystal quality but requiring only a third of the batch time.
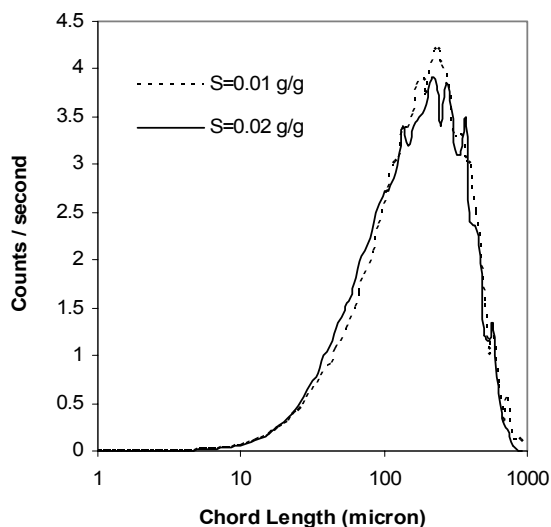
Figure 5-13: Normalized square-weighted product crystal CLDs obtained from seeded systems when S_{set} = 0.01 g/g-water and S_{set} = 0.02 g/g-water for glycine system.

Table 5-3: Glycine system: FBRM statistics (in the 1-1000 μm range) for final product crystals of (a) seeded experiments at two S_{set} values (0.01 and 0.02 g/g-water), (b) five seeded and (c) five unseeded S-control performed with S_{set} = 0.02 g/g-water.

(a)

FBRM Statistics	$S_{set} = 0.01$ g/g-water	$S_{set} = 0.02$ g/g-water
Mean	219.4	207.4
Standard Deviation	153.5	149.0

(b)

FBRM Statistics	Averaged
Mean	201.6 ± 5.27
Standard Deviation	143.5 ± 3.86

(c)

FBRM Statistics	Averaged
Mean	175.0 ± 25.8
Standard Deviation	160.7 ± 11.6

The next step was to check the reproducibility, which is an important concern in industries. Reproducibility in terms of both product crystal quality and batch time was investigated. The set-point supersaturation of 0.02 g/g-water was used for five runs of S-control. There are two reasons for using set-point supersaturation of 0.02 g/g-water instead of 0.01 g/g-water: firstly, it gives a shorter batch time; secondly, a S_{set} lower than the system supersaturation will cause the control system to increase the temperature to match the set-point temperature, resulting eventually in complete dissolution of the crystals if not properly monitored. The product CLDs of five seeded runs, as shown in Figure 5-14(a), are very similar, hence providing evidence of the high reproducibility of S-control systems. The duration of S-control for each run fell within the narrow range of 50 minutes and an hour, another indication of reproducibility. The temperature profiles obtained for these five runs are shown in Figure 5-15(a). It is observed that the temperature profiles are almost linear, with cooling rates between 0.43 ^{o}C/min and 0.50 ^{o}C/min. The FBRM statistics in Table 5-3(b) shows quantitatively that the variations of mean and standard deviations are within 3% of the average, another evidence of the high reproducibility. Linearity in the temperature profiles is in contrast to the observation of Liotta and Sabasen (2004) and our expectation of a cubic temperature profile. The probable explanation is that the solubility curve of glycine is approximately linear in the temperature range studied.
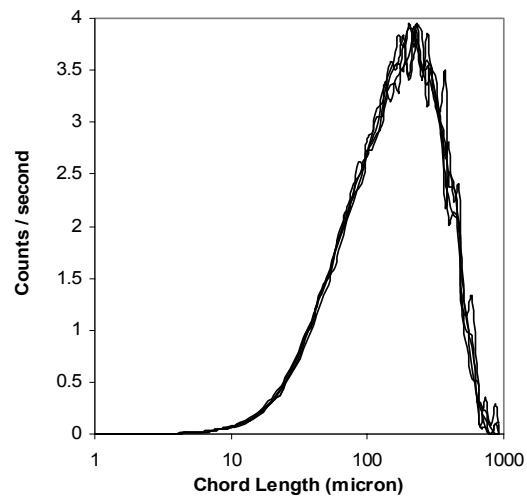
(a)
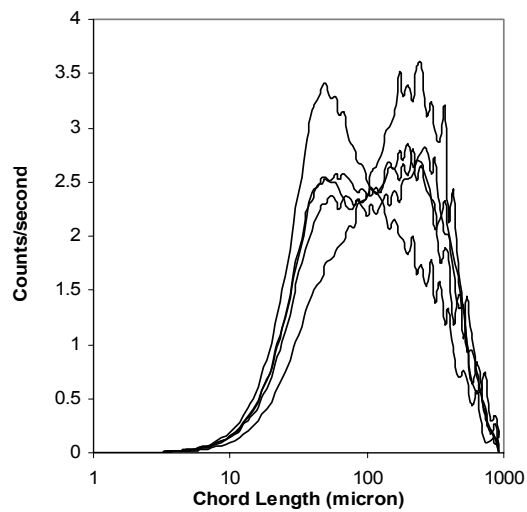
(b)

Figure 5-14: Normalized square-weighted product crystal CLDs of (a) five seeded and (b) five unseeded S-control experiments at $S_{set} = 0.02$ g/g-water for glycine system.
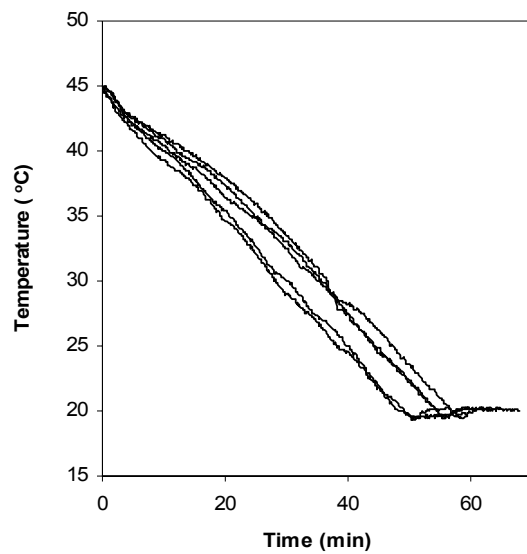
(a)
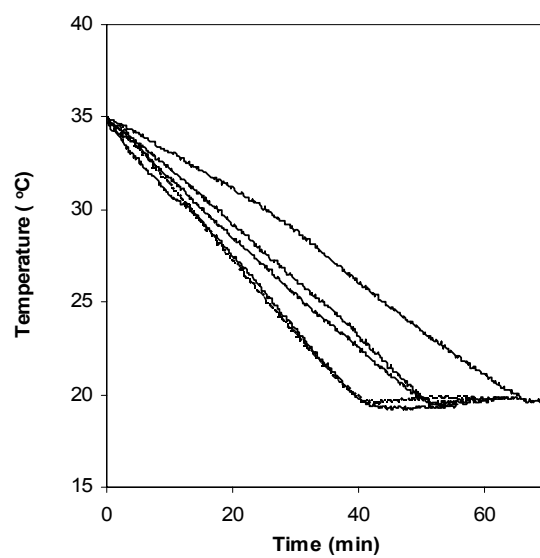
(b)

Figure 5-15: Temperature profiles obtained from (a) five seeded and (b) five unseeded S-control experiments at S_{set} = 0.02 g/g-water for glycine system.

5.8) Case Study 4: Closed-Loop Supersaturation-Control (S-control) – Unseeded

Unseeded systems have irreproducible initial CLDs when nucleation occurs, hence the final product CLDs are unlikely to be similar. This is evident from the product crystal CLDs shown in Figure 5-14(b) and FBRM statistics shown in Table 5-3(c). At the same set-point supersaturation value, the variability (quantities after the ± sign) of the product crystal CLDs for five different runs are at least three times greater than for the seeded systems. The duration of S-control ranged from 40 to 70 minutes. The temperature profiles obtained from unseeded runs (Figure 5-15(b)) were almost linear as in the seeded runs but the cooling rates span a larger range of $0.22 - 0.37$ ^{o}C/min. These observations suggest that reproducibility or batch-to-batch consistency is hard to achieve in self-seeded crystallizations and even the most sophisticated closed loop S-control is unable to overcome the variability of primary nucleation.

5.9) Comparison between T-control and S-control

Comparing the results from seeded T-control and S-control experiments (Table 5-1(a) and Table 5-3(b)), S-control did not display any advantage over T-control in terms of product quality since the standard deviations of the CLDs are similar. The insignificant difference between the effectiveness of S-control and T-control may be due to the fast growth rate of glycine. The average linear growth rate at cooling rate of 0.3 ^{o}C/min is estimated to be 62 nm/s by optical microscopy, and that is equivalent to at least 124 molecules being incorporated onto the crystal

per second. As a result, the controlling factor in glycine crystallization is the nucleation step. Once nuclei are formed (or seeds are introduced), the magnitude of the cooling rate will not make a significant difference because of the rapid growth rate. This also explains why seeding is important for glycine crystallization from water if reproducibility of product quality and process conditions are of prime concern.

Thus far, it has been shown that large variability in product crystal CLDs was observed in unseeded crystallization experiments regardless of whether open-loop or closed-loop control was implemented. This is primarily due to the unpredictable nature of primary nucleation. Product crystal quality became more consistent and reproducible when seeds were employed for both S- and T-control experiments. However, S-control did not demonstrate any significant advantage over T-control in terms of product crystal quality. S-control has been found to be insensitive towards the pre-set supersaturation values tested in this work of cooling crystallization of glycine from water. Insignificant attrition and agglomeration were observed. It can be concluded that sophisticated S-control was unnecessary for glycine. The possible reason for the insensitivity of product quality to the control strategy could be the fast growth rate of glycine. A similar conclusion was reached in a separate study on a well-behaved pharmaceutical compound (Black et al., 2006). This conclusion may be generally valid for all fast-growing systems.

Moscosa-Santillan et al. (2000) have used turbidimetry as a control tool in cooling crystallization of glycine, and showed that the alternative temperature-time profiles so obtained improves product crystal quality of seeded systems. Moreover, the convex profile was observed to yield larger crystal product with lower coefficient of variation than the linear profile. However, in our present work, S-control and different variations of T-control profiles yielded similar crystal product quality. As shown in Figure 5-10, secondary nucleation was negligible, which was not the case for Moscosa-Santillan et al. (2000) whereby significant secondary nucleation was observed. The dissolution of fines through an alternating temperature profile would hence undoubtedly prove advantageous in giving higher quality crystal products in their case. The most probable explanation for the apparent inconsistency with the data presented here is that secondary nucleation occurred during the work of Moscosa-Santillan et al. (2000), whereas it was specifically excluded here (Figure 5-10). This may be because the supersaturations were larger in the previous work, or that the MZW's were smaller. One advantage of the in-line technologies deployed here is they would be capable of distinguishing between these two phenomena.

The differences in secondary nucleation rate may be due to the different agitator used, different stirring speed, different hydrodynamics within the crystallizer and other differences in operating conditions. The success of crystallization control hinges on control of the operation within the MZW. This metastable limit is, in contrast to the saturation limit, thermodynamically not founded and kinetically not

well defined. It depends on a number of parameters such as temperature level, rate of generating the supersaturation, solution history, impurities, fluid dynamics, etc. Because of the wide MZW (Figure 5-2) in our chosen model system and conditions, a wider range of controls that do not violate the metastable or solubility limits was possible which resulted in similar product crystals.

Consistent particle properties are an important goal for industrial batch crystallizations. Several control strategies, from unseeded linear cooling to seeded supersaturation control, were evaluated for the cooling crystallization of glycine. Particle properties were assessed in-line, facilitating investigations of process consistency. External seeding was by far the most effective strategy. Changing the pre-set cooling profile, or the pre-set supersaturation limit, showed limited benefits. Primary nucleation is unpredictable and do not occur at a fixed temperature, which nullifies the impact of any types of control in giving consistent product crystal.

5.10) Feedback Loop Involving FBRM

The control program was implemented using Microsoft Visual Basic 6.0 (Figure 5-7), which is hosted on a Pentium IV computer. FBRM statistics are transmitted to the computer to be analyzed at 60 s interval, and then a signal is sent to the circulator to adjust the crystallizer temperature, which in turn affects the FBRM

statistics. A schematic of this flow of information is shown in Figure 5-16. In this work, a fairly large measurement interval of 60 s was used because the control program was not robust at shorter time intervals due to the very large amount of data collected each time.
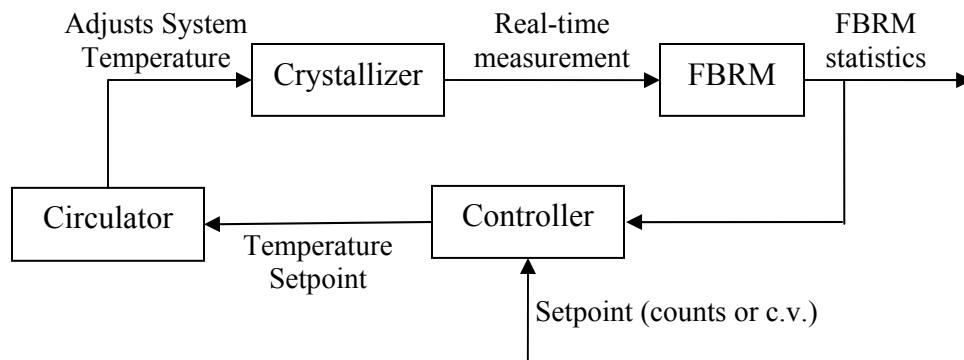
Figure 5-16: Schematic Diagram showing the Flow of Information in a Feedback Loop.

5.11) Detection of Primary Nucleation in Unseeded Systems Using FBRM

The appearance of crystals from the clear supersaturated solution is the definition for the occurrence of primary nucleation (Mullin, 2002). Since an increase in particle counts from its baseline level is a sure indication of the onset of primary nucleation, the FBRM's ability to track particle counts in-line facilitates the detection of primary nucleation. Jeffers et al. (2003) and Barrett and Glennon (1999) have found that the chord lengths measured per unit time recorded by the FBRM can be linearly correlated with solids density within a certain range, hence verifying FBRM's ability to monitor particle counts in the system.

A caveat to note is that to simply define an absolute number of particle counts above which primary nucleation is deemed to have occurred may lead to errors. Noise is inherent in FBRM measurements, and occasional spikes in measurement would lead to false detection of nucleation. Also, in view of potential fouling of FBRM probe even in clear solution, this strategy makes for errors in nucleation detection. More importantly, the absolute particle counts statistic is not amenable to scale-up nor to a different system, hence is not useful as a universal benchmark.

In this work, to override the fluctuation due to noise or fouling in the detection of primary nucleation, nucleation is deemed to have occurred only when there is a monotonous increase in the consecutive number of counts measured by the FBRM. At the onset of primary nucleation, the increase in counts is very steep, ensuring that successive readings of particle counts would show an increase in spite of fluctuation caused by noises in the measurement (Figure 5-17).
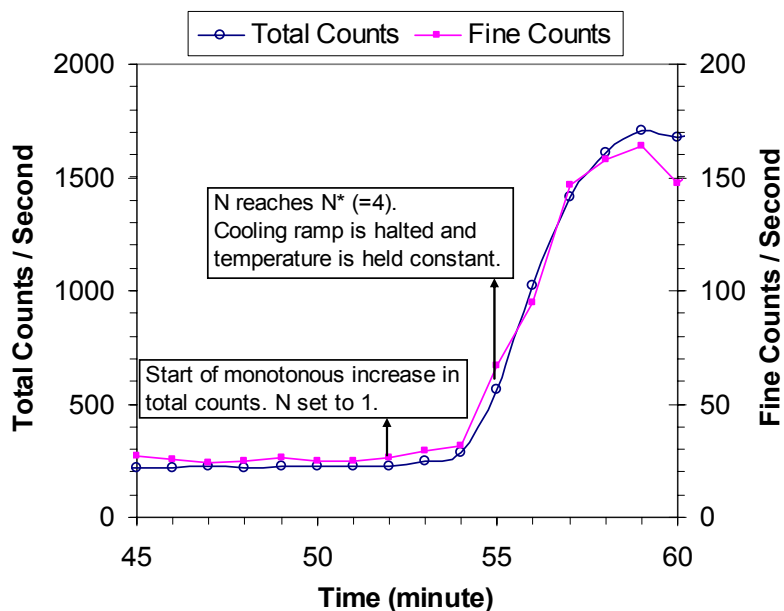
Figure 5-17: Detection of the onset of nucleation using FBRM by monitoring the number of successive readings showing positive increase in Total Counts.

If successive increase in the counts measured by FBRM is to be used as an indication of primary nucleation detection, a reasonable number of successive readings has to be pre-set as the threshold number of consecutive monotonously increasing readings of FBRM counts (N*) above which primary nucleation would definitely have occurred. If N* is set too low (e.g. N* = 3 or below), false detection of nucleation may result due to fouling or noise. On the other hand, if N* is set too high (e.g. N* = 10), the time lag between the onset of nucleation and subsequent control action could be unacceptably large.

For our experiments on the glycine-water system, with a measurement interval of 60 s, it was found that a value of N* = 4 was effective in detecting primary nucleation unambiguously. Figure 5-17 shows the measured values of Total

Counts in a typical experimental run. When the system detects a positive increase in Total Counts over the previous reading, an internal counter N is set to the value of 1. Only if the next and immediately subsequent readings continue to show an increase, then N is incremented by 1 at each time step. Otherwise, N is reset to 0. If N reaches the value of N* (= 4), then nucleation is deemed to have occurred, and the system is sent a signal to take subsequent control action as described earlier.

Figure 5-17 also shows the Fines Counts as an alternative statistic to Total Counts. It can be seen that for our system, the relative profile of Fines Counts follows very closely to that of Total Counts, and therefore it would be feasible to base our nucleation detection technique on either statistic. However, Total Counts was preferred since our experience indicates that Fines Counts were more susceptible to systematic fluctuations.

Our technique is expected to work for different models of the FBRM probe. Three models of FBRM probes (S400, D600L, and D600P) are available in our lab, and all worked equally well for this method of nucleation detection. The different models of probes are catered for different vessel dimensions, but operate on the same principle. That primary nucleation causes a rapid successive increment of Total Counts measurements is true regardless of scale.

5.12) Case Study 5: Using FBRM in a Feedback Loop to Improve Consistency in Unseeded Crystallization Systems

As concluded in Section 5.9, the randomness and unpredictability of primary nucleation in unseeded systems is the prime cause for the lack of reproducibility in product crystals, even when sophisticated controls like S-Control was implemented. The objective here is thus to manipulate the primary nuclei of different runs to achieve consistency in the beginning, before various modes of controls are implemented. Also, in view of the fact that many industrial players are reluctant to implement the ATR-FTIR in the production systems due to its vulnerabilities (Chapter 3.2), the ability to solely rely on FBRM for reproducibility in product crystals would be a great advantage.

The temperature profile for a typical experimental run is shown in Figure 5-18. The saturated solution (Point A) is cooled at a pre-set rate until nucleation is detected by the FBRM (Point B). The system is allowed to stabilize at the temperature of Point B for a fixed time (15 minutes), by which time primary nucleation is completed as shown by the counts profile in Figure 5-17. Then, the temperature is raised at a constant rate while using the FBRM to monitor the particle size distribution (PSD) of the "seed" crystals. The heating gradually re-dissolves the fines, thereby narrowing the PSD. When the desired quality of these internally generated "seeds" is achieved (Point D), the system is cooled at a constant rate to allow the crystals to grow until the final yield is attained (Point E).
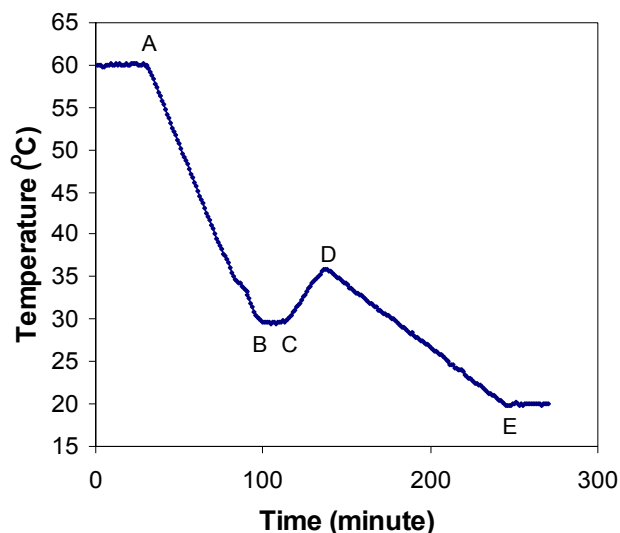
Figure 5-18: Temperature Profile of a typical run for glycine system.

In Figure 5-11, it has been shown that spontaneous primary nucleation arising from unseeded cooling crystallizations produced initial crystal nuclei with inconsistent PSD from batch to batch. This is hardly surprising, given the random and irreproducible nature of the nucleation process. In seeded crystallization processes, on the other hand, it is fairly simple to ensure that the PSD of the initial seeds is consistent. This difference is amply illustrated in the contrast between Figure 5-19(a) and Figure 5-19(b) for the case of sample data from several unseeded and seeded systems respectively. It is demonstrated in this work that it is possible to obtain consistency from internally-generated primary nuclei by manipulating the CLDs in Figure 5-19(a) to achieve that in Figure 5-19(c) through a closed-loop feedback technique involving FBRM.
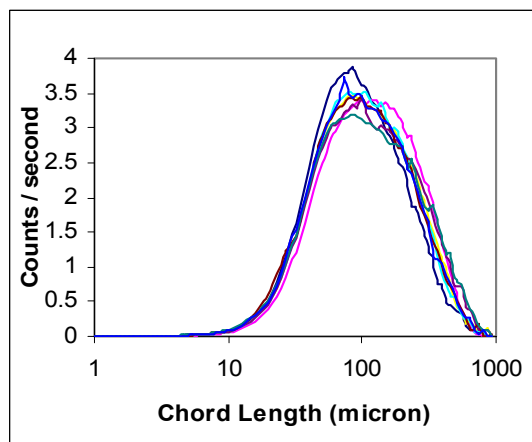
(a)
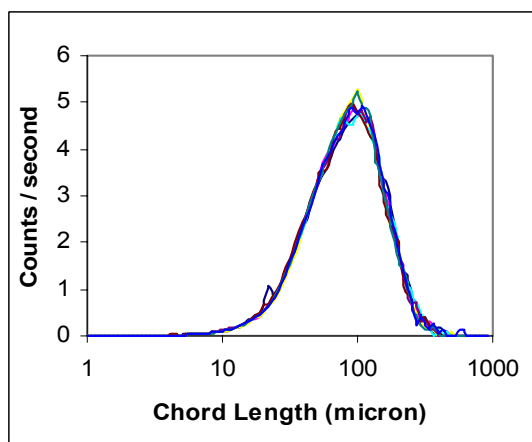
(b)
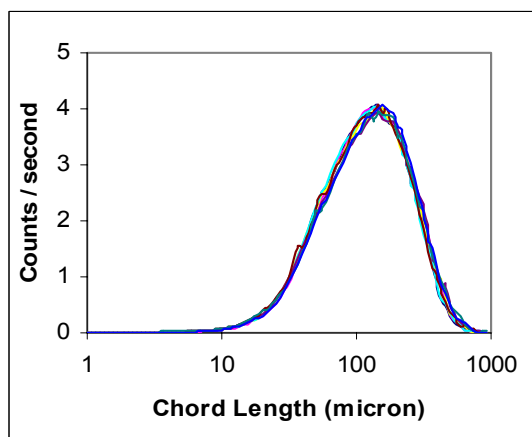
(c)

Figure 5-19: Normalized square-weighted initial CLDs (i.e. CLDs were taken just prior to the implementation of any control strategies) from eight (a) unseeded, (b) seeded and (c) unseeded with FBRM-Control crystallization experiments for glycine system.

The FBRM data (Figure 5-19) shown are in the form of normalized square-weighted chord length distributions (CLDs) Although FBRM-measured chord lengths are never equivalent to actual particle sizes, it has been demonstrated square-weighted CLD correlates well with the microscopic CSD (Section 5.4) for glycine crystals, and therefore we have used this statistic in the present work.

The complete mathematical definition of a particle size distribution (PSD) is often cumbersome, and it is more convenient to use one or two single numbers representing say the mean and spread of the distribution (Jones, 2002). For example, the mean particle size enables a distribution to be represented by a single dimension, while its standard deviation indicates its spread about its mean. The coefficient of variance (c.v.), which quantifies the width of the distribution function with respect to its mean, and is defined as the ratio of the standard deviation to the mean, has been reported to be useful for description and comparison of experimental results (Warstat and Ulrich, 2006). In the present work, a target value of the c.v. is used as the objective in the FBRM feedback loop.

Upon the detection of nucleation, an increasing temperature ramp of 0.3 $^{\circ}$C/min was used to manipulate the c.v. of the internally-generated "seed" crystals. A slower heating rate gives tighter control but increases batch time, while a faster heating rate gives coarser control but reduces batch time; hence an intermediate heating rate of 0.3 $^{\circ}$C/min is chosen. A set-point value of 0.7 was used to

determine the end of this heating stage of the process; the value 0.7 is based on a typical PSD of external seeds (Figure 5-19(b)). To ensure robust operation, an upper temperature limit was set (45 ^{o}C in this case) to avoid total dissolution. If this temperature is reached, the final cooling phase (D – E in Figure 5-18) is initiated even though the c.v. has not reached its set-point. For all the runs, the c.v. attained the set-point value without violating this temperature constraint.

A foreseeable problem that the practical implementation of FBRM-Control faces is related to the usually noisy FBRM data especially in systems with low solids concentrations. It can be seen in Figure 5-20 that despite the relatively high solids concentration of glycine crystals in our experiment, the raw c.v. measurement is very noisy, which could cause erroneous control action.
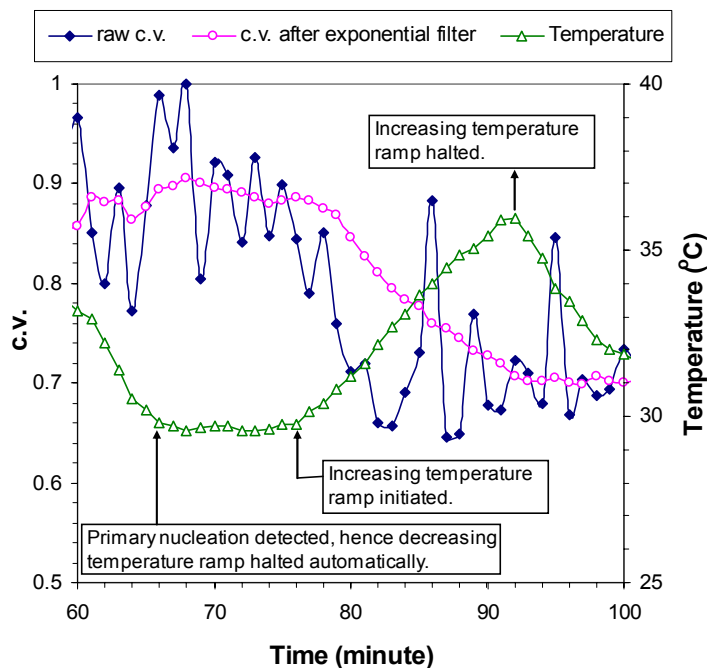
Figure 5-20: Plot of coefficient of variance (c.v.) vs time in the presence and absence of exponential filter for glycine system.

In this work, an exponential filter, which is a time-averaging feature of the FBRM Control Interface Software, was used to smoothen out the noisy FBRM data. Unlike the moving-average filter, the exponential filter does not give equal weight to past measurements, but gives exponentially declining weight to measurements further back in time. Figure 5-20 shows the FBRM data for c.v. with and without exponential filter (α = 0.1) applied, and it is clear that the filtered data are much more amenable to be used for control.

Figure 5-19(c) shows the measured FBRM CLDs of internally-generated seeds from eight different runs after manipulation by heating to attain a c.v. of 0.7. The CLDs are remarkably similar, demonstrating that automatic internal generation of seeds with high consistency can be achieved using this technique. After the desired quality of seeds is obtained (Point D in Figure 5-18), the system is cooled at a constant rate to allow steady crystal growth, until the desired yield is obtained (Point E in Figure 5-18). One could also apply more sophisticated control strategies at this stage (Point D), for example, constant supersaturation control with in-line ATR-FTIR measurements (Yu et al., 2006, Zhou et al., 2006; Fujiwara et al., 2005; Liotta and Sabesan, 2004).

Results for the CLDs of the final crystal product (five different runs) after linear cooling are shown in Figure 5-21(c). This can be compared with equivalent final product CLDs from previous work on unseeded (Figure 5-21(a)) and externally seeded (Figure 5-21(b)) crystallizations. The results clearly demonstrate that the

final product consistency from our fully automated FBRM technique for nucleation detection and internal seed conditioning is much better than for unseeded systems in terms of product consistency.
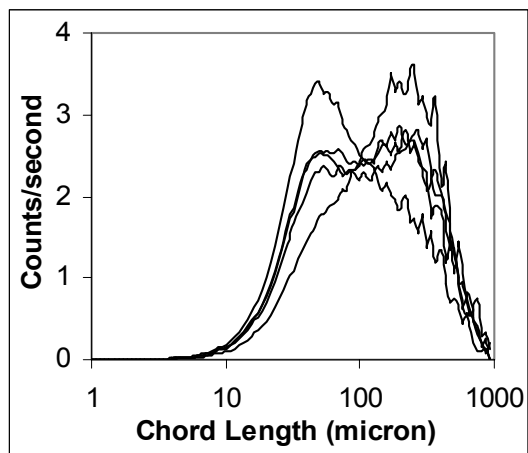
(a)
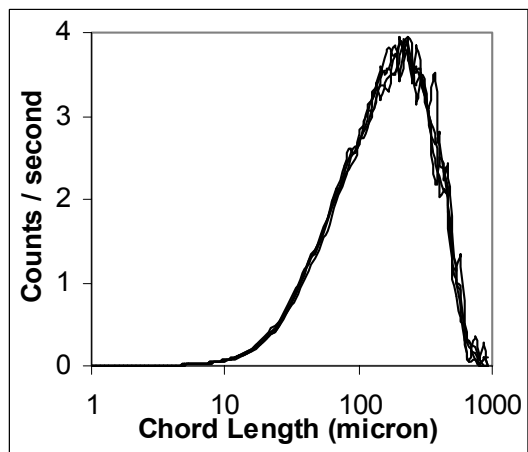
(b)
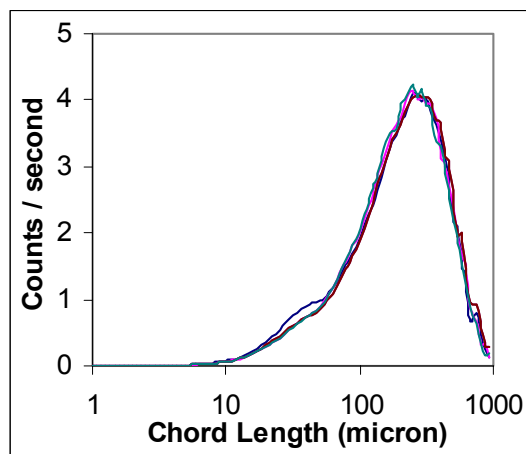
(c)

Figure 5-21: Normalized square-weighted product crystal CLDs of five (a) unseeded, (b) seeded, and (c) unseeded with FBRM-Control S-control experiments at S_{set} = 0.02 g/g-water for glycine system.

A closer inspection of Figure 5-21(b) and Figure 5-21(c) also shows that even external seeding (with its attendant operational complexities) produces marginally less consistent product as compared with our automated technique.

5.13) Sensitivity Analysis through In-Line Monitoring of the Crystallization Process using FBRM

In the event that the temperature-control of the system fails and extremes of temperature ramps (cooling / heating) are encountered, a robust feedback loop should still be able to detect primary nucleation and adjust the system c.v. without fail. This section shows the usefulness of the FBRM as an in-line instrument for monitoring crystallization processes.

In the detection of primary nucleation, extreme cooling rates of 0.1 $^{\circ}$C/min and 1 $^{\circ}$C/min were investigated. N* was similarly set to 4. Detection of primary nucleation was successful in both cases. Table 5-4 shows the stoppage temperature upon nucleation detection and duration of cooling temperature ramp. For a slower cooling rate, the batch time is too much longer despite the narrower metastable zone width. A cooling rate of 0.5 $^{\circ}$C/min was chosen for our runs in the previous sections in view of the batch time and stoppage temperature upon detection of primary nucleation. Figure 5-22 shows the square-weighted CLDs of the primary nucleation (Point C in Figure 5-18), implying that more nuclei were formed for faster cooling rates due to the higher supersaturation generated.

Table 5-4: Glycine system: Duration of cooling temperature ramp and stoppage temperature upon detection of primary nucleation for various cooling temperature ramps.

	Duration of cooling temperature ramp (min)	Stoppage temperature upon detection of primary nucleation ($^{\circ}$C)
0.1 $^{\circ}$C/min	216.3	38.4
0.3 $^{\circ}$C/min	57.7	31.2
1 $^{\circ}$C/min	36.6	23.4
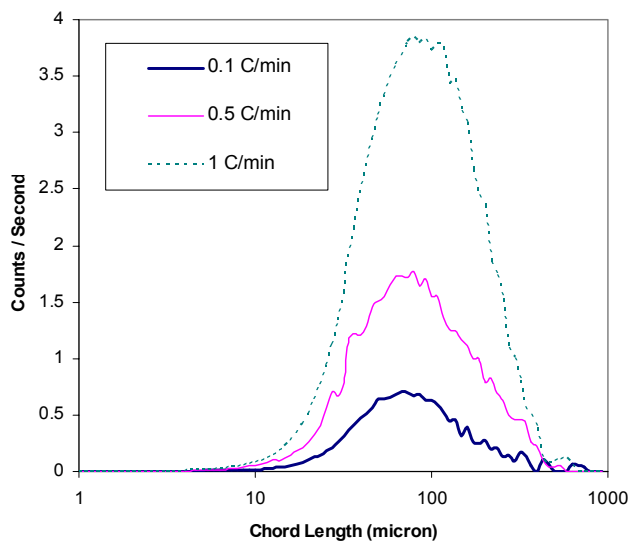
Figure 5-22: Square-weighted CLDs after the detection of primary nucleation for glycine system.

Extreme heating rates of 0.1 ^{o}C/min and 1 ^{o}C/min in the adjustment of c.v. of the primary nuclei were investigated too. The cooling rate in approaching nucleation was a constant 0.5 ^{o}C/min for the three different runs. It is seen in Figure 5-23(a) that it was possible to use a wide range of heating rates to achieve similar consistency in the CLDs, but using the same heating rate enhanced the consistency more (Figure 5-19(c)). As seen in Table 5-4, a lower heating rate results in longer batch time, which is hence less efficient. However, a higher heating rate results in a rapid decrease in c.v., making control more tricky. Also, higher heating rate causes rapid dissolution of nuclei, resulting in noisier CLDs due to lower solids concentration. In view of this, an intermediate heating rate of 0.3 ^{o}C/min was chosen in the previous sections.
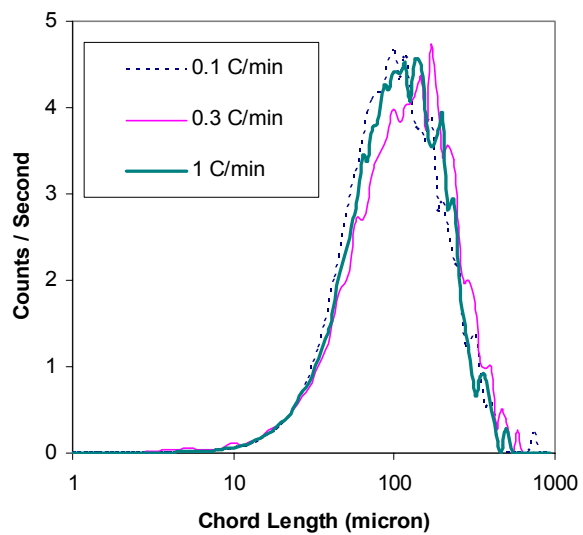
(a)
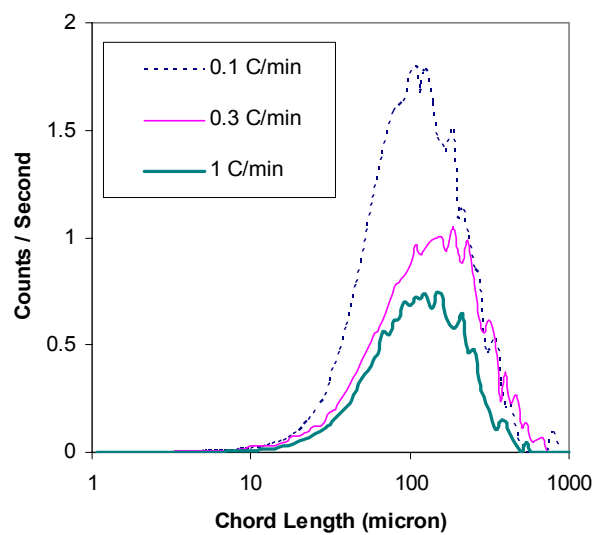
(b)

Figure 5-23: (a) Normalized and (b) Non-normalized Square-weighted CLDs after adjusting the c.v. for glycine system

5.14) Investigation of applicability of FBRM Feedback Loop on Paracetamol-Water System

Unlike S-Control, whereby it has been tested on several systems and proven to work, the technique involving the FBRM feedback loop proposed here is new. Hence, it is necessary to investigate its effectiveness in an alternative system. Paracetamol-water system was chosen for this, as it has been known to be a challenging system to measure the characteristics of the particle size distribution of (Fujiwara et al., 2002) due to its low solubility. Moreover, agglomeration, which is a common problem in the crystallization of pharmaceuticals, is prevalent in this system (Alander et al., 2003, 2004; Yu et al., 2005), and hence serves as a useful benchmark for the applicability of this technique. Accurate interpretation of size distribution measurements from particle size analyzers is much more difficult for agglomerating systems. Also, there is ample literature on the crystallization of this system (del Rio and Rousseau, 2006; Zhou et al., 2006; Granberg and Rasmuson, 2005; Worlitschek and Mazzotti, 2004; Femi-Oyewo and Spring, 1994; Yu et al., 2006; Chew et al., 2004; Al-Zoubi et al., 2002; Prasad et al., 2001; Rodriguez-Hornedo and Murphy, 1999).

The primary nucleation detection technique was successfully implemented for the paracetamol-water system. $N^* = 4$ was similarly used in this case. Although probe fouling was a severe problem, the fact that primary nucleation causes a rapid successive increment of Total Counts measurement overrides the distortion

of FBRM data due to fouling. FBRM signals and CLDs were noisier in this case, but such was not an obstacle for this technique.

The second new technique proposed served to improve consistency in unseeded crystallization systems through ensuring consistency in the internally-generated seeds from primary nucleation. The objective was for the primary nuclei generated to achieve a setpoint c.v. The temperature scheme used here is similar to that in Figure 5-18.

FBRM data were first validated against results obtained from sieve analysis (Yu et al., 2006). A typical micrograph of paracetamol crystals obtained from crystallization experiments is shown in Figure 5-24. As shown in Figure 5-25, FBRM square-weighted and sieve analysis mean and c.v. are well-correlated, with R^2 values of 0.86 and 0.97 respectively. However, absolute FBRM value is only about one-fifth of sieve analysis data. Sieve analysis measures the second longest chord length, while FBRM measures random chord lengths. Agglomeration is postulated to be the prime reason for the huge discrepancy in the absolute values between that obtained via sieve analysis and FBRM. This is a testament to the reliability of FBRM as a means to observe trends but not for absolute values. Since this work does not require absolute values from FBRM, such high R^2 values are sufficient grounds for dependence on FBRM data directly for this system.

Figure 5-24: Typical micrograph of paracetamol crystals obtained from crystallization experiments. Scale bar represents 500 μm.

$y = 0.27x + 2.74$
$R^2 = 0.86$
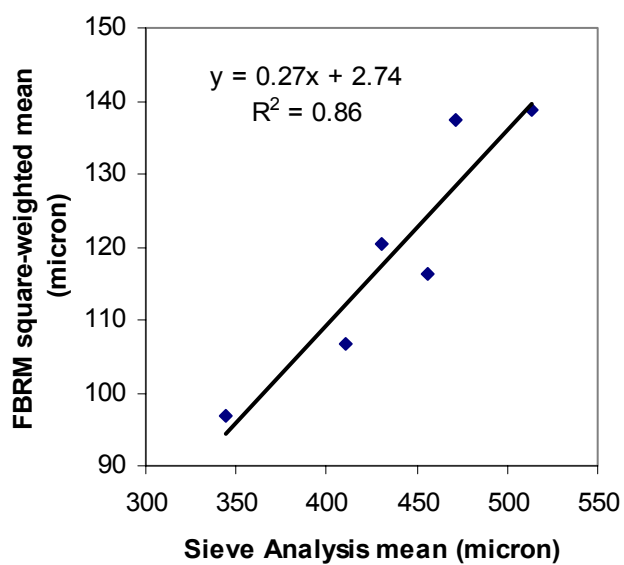
(a)
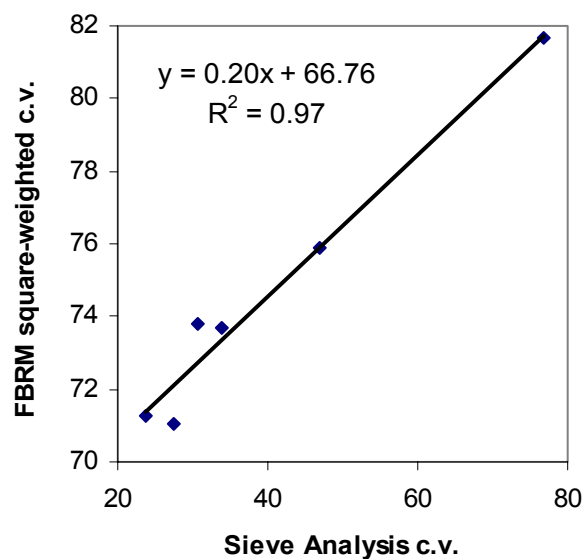
(b)

Figure 5-25: Plot of FBRM Square-weighted Data vs Sieve Analysis Data of product crystals for paracetamol system.

For the paracetamol-water system, the FBRM signals were very noisy, despite the implementation of exponential filter as before to smooth out the data obtained. Figure 5-26 shows the c.v. derived from FBRM signals after the application of exponential filter. In contrast to Figure 5-20 for the glycine-water system, it is shown that although the exponential filter lessens the noise, the signals obtained still fluctuates much, complicating control using FBRM. The deterioration of FBRM signal quality in this system is due to several reasons. Firstly, probe fouling is a very prevalent problem for this system. For all the experiments, the FBRM probe has to be withdrawn from the system for cleaning due to severe fouling upon the onset of primary nucleation. That the FBRM probe is connected to a fiber optic makes for convenient removal and re-insertion of the probe. Secondly, since FBRM measures chord length (Figure 3-3 in chapter 3),

agglomeration which results in jagged edges increases the noise in the FBRM signals. Paracetamol crystals are known to agglomerate to a large extent, especially in water (Fujiwara et al., 2002).
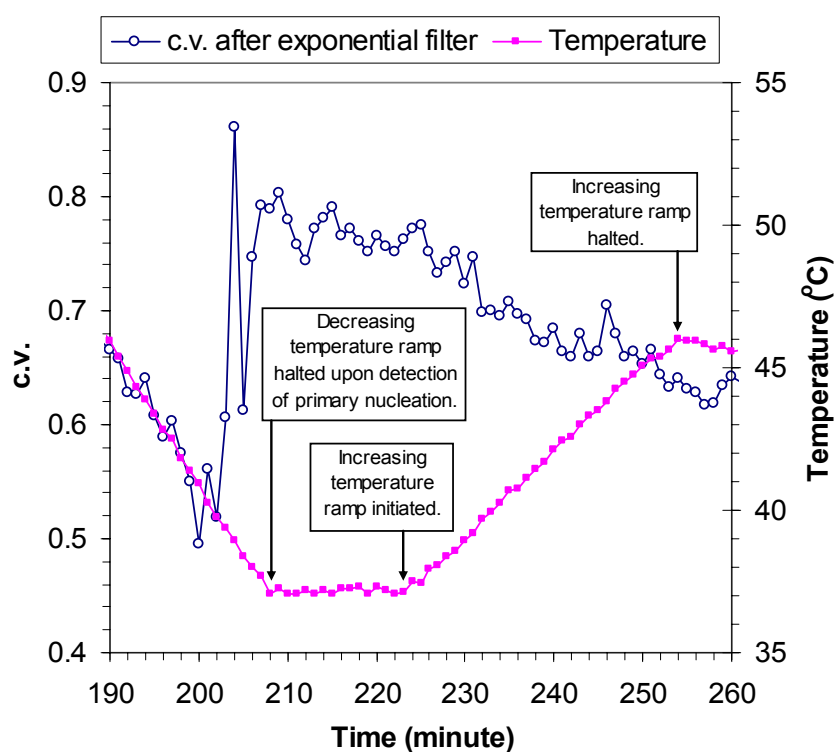
Figure 5-26: Plot of coefficient of variance (c.v.) vs time in the presence and absence of exponential filter for paracetamol system.

Figure 5-26 also shows that heating does not decrease the c.v. as much as it does in Figure 5-20. While the glycine system's c.v. decreased by up to 0.2 over a temperature increase of 6 ^{o}C (Figure 5-20), the paracetamol system's c.v. only decreased by 0.1 over a temperature increase of 11 ^{o}C. Compounded with the fluctuations, it makes for difficult attainment of a setpoint c.v. The setpoint c.v. in this case was determined to be 0.65, which was chosen based on a few observations of primary nucleation c.v. and the decrease in c.v. achievable by

heating. Since consistency is of prime consideration here, the concern was to ensure this c.v. setpoint is attainable for all runs. To circumvent the problem of fluctuations, the increasing temperature ramp was halted only after the system c.v. is lower than the setpoint for three consecutive times.

The CLDs obtained through FBRM upon primary nucleation (point C on Figure 5-18) and after heating (point D on Figure 5-18) are shown in Figure 5-27(a) and Figure 5-27(b) respectively. Hence, the technique proposed in this work has been successfully implemented for the paracetamol-system too, to achieve consistent internally-generated seeds, and hence improving batch-to-batch consistency in unseeded systems. It is observed in Figure 5-27(b) that, in comparison with Figure 5-19(c), the CLDs do not superimpose on one another as closely. A few factors contribute to this. Firstly, the noisy FBRM signals hamper the monitoring of system c.v., causing difficulties in the determination of the point at which the setpoint is attained. Secondly, the magnitude of c.v. decrease upon heating is smaller than for the glycine system, posing a restriction to the extent of adjustment of c.v. Thirdly, the greater extent of agglomeration damper the dissolution of fines during the heating process, again deterring the attainment of the setpoint c.v.
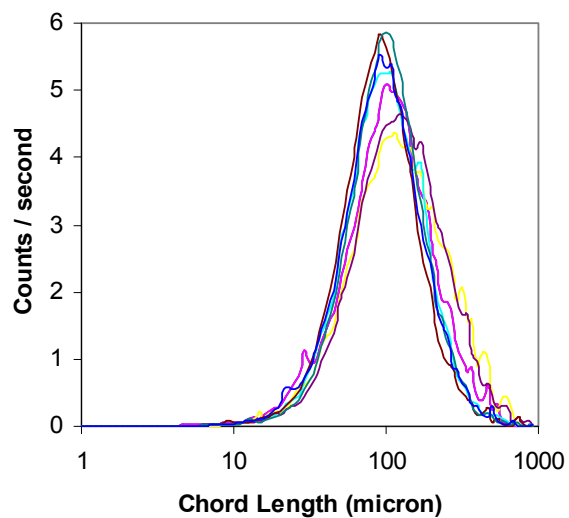
(a)
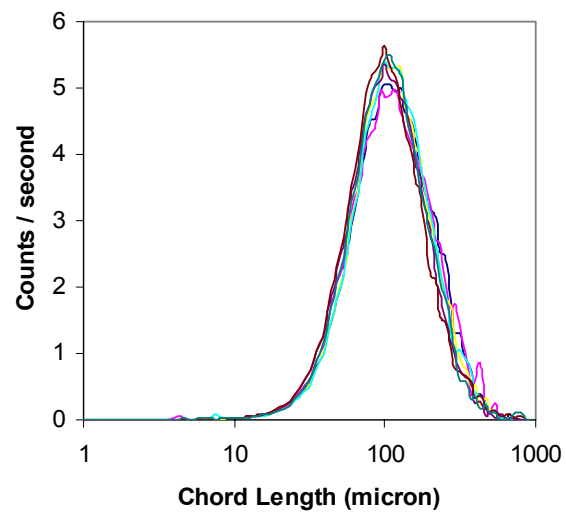
(b)

Figure 5-27: Normalized square-weighted CLDs (a) upon primary nucleation and (b) after heating to attain setpoint c.v. for paracetamol system.

5.15) FBRM as In-Line Instrumentation in a Closed Feedback Loop

Closed-loop feedback control involving FBRM has been implemented on unseeded crystallization of glycine crystals and paracetamol crystals from water to improve the consistency of product crystals.

The FBRM has proven to be useful in the detection of primary nucleation in unseeded systems, hence making it possible to accurately define the point of nucleation automatically. This allows for enhanced control in unseeded systems. Primary nucleation is defined to have occurred after four successive increases in counts measurement, after which the temperature ramp used in approaching primary nucleation is automatically stopped.

This work has also shown that it is possible to manipulate the c.v. of the self-nucleated seeds generated by primary nucleation in unseeded systems using closed-loop feedback control of FBRM to ensure reproducibility in the initial nuclei CLDs, superseding a prime advantage of seeding. Since product crystal consistency hinges on consistency at the start of spontaneous seeding by primary nucleation in unseeded systems, the successful implementation of FBRM-Control allows for unseeded systems to be used for producing consistent product crystals that was hitherto only possible for seeded systems.

5.16) FBRM Data Evaluation (Glycine)

This section serves to give a critical evaluation of FBRM data.

In analyzing the FBRM data, it is necessary to choose a common basis (for example, similar particle counts) to ensure valid comparison, and a suitable agitation speed to ensure suspension of particles at the probe window.

Seeds of the same size (product crystals in the sieve fraction of 125-212 µm) were added into separate systems in different amounts (1g and 5g). Figure 5-28(a) and Figure 5-28(b) show the CLDs of different seed masses, with the latter showing the percentage of counts per chord length to reflect the similarity of the two CLDs. It is obvious in Figure 5-28(a) that the area under the square-weighted CLD for the 5g seeds is larger, reflecting the higher mass of particles in the system. Heath et al. (2002) showed that FBRM measures the first diameter weighting (moment) of the chord distribution, which means that applying a square-weighting is effectively a cube (volume) weighting, hence the square-weighted CLD reflects the mass of the particles in the system. Since the seeds are of the same size, a five times increase in seed mass should result in a five times increase in the number of particles in the system. The FBRM counts per second statistic is expected to be five times more, but, in Table 5-5, there is only an approximately two times difference between the two runs. Jeffers et al. (2003) showed in their work there is a strong linear relationship between FBRM counts and mass in the system. However, in this work, this was not the case. This

seeming inconsistency in the results is not surprising, as the FBRM system measures a particular chord length instead of a specific dimension, and results are sensitive to both particle shape and particle size. Heath et al. (2002) and Barrett and Glennon (1999) have shown similar results in that total FBRM counts did not correlate well with solid fraction, tapering off at high particle concentrations. Such can be explained as follows. When there is a higher concentration of solids, a smaller volume of the system is sampled, as the laser beam is blocked by more solids. Since the sample size in the 5-g seeds system is smaller, a smaller number of particles are reflected in the FBRM statistics. Also notable in Table 5-5 is the difference in the median value. A higher median was registered for the smaller seed mass. In view that the agitation speed was the same in both cases, a plausible explanation would be that a greater number of bigger particles were suspended near the FBRM window in the case of the smaller seed mass.

(a)

(b)
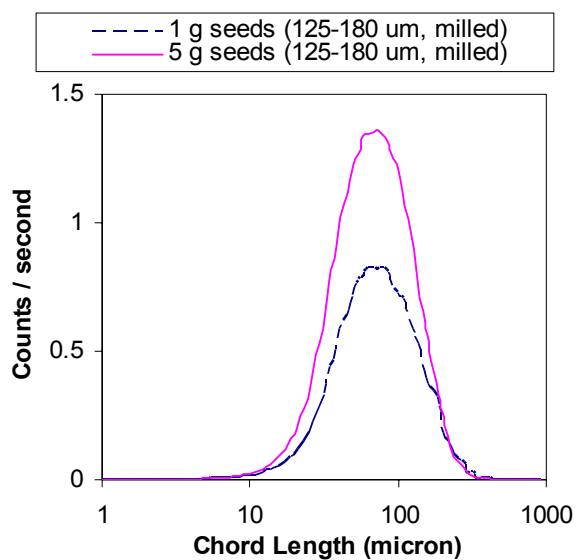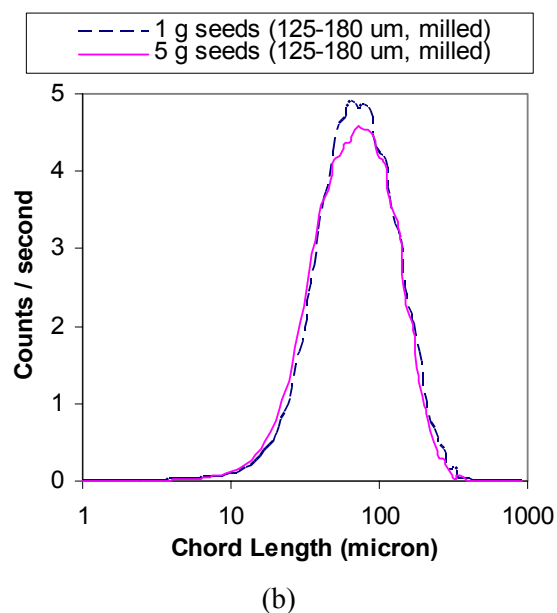
Figure 5-28: (a) Square-weighted and (b) Normalised square-weight CLDs of 1 and 5 g of seeds (125-212 μm) for glycine system.

Table 5-5: Glycine system: FBRM statistics (in the 1-1000 μm range) for initial CLDs of similar seeds (product crystals in sieve fraction of 125-212 μm) in different masses.

FBRM Statistic	Weighting	1-g seeds	5-g seeds
Counts per Second	Non-Weighted	621.04	1173.83
Median	Non-Weighted	27.06	25.44
Mean	Square-Weighted	86.90	83.44
Standard Deviation	Non-Weighted	29.23	27.56
Standard Deviation	Square-Weighted	52.65	51.27

In view of this, it is noteworthy that the magnitude of the FBRM statistic not be taken as an absolute value, but only as an observation of the trend in the system.

Another experiment was carried out to further investigate the significance of the FBRM data. Using seeds of two different size ranges (product crystals in the

sieve fraction range of 300-355 µm and 125-212 µm) in two separate experiments, an attempt was made to add sufficient amounts of seeds such that the counts per second statistic as registered by the FBRM are similar. 10 g of 300-355 µm seeds were needed to match 4 g of 125-212 µm seeds in terms of particle counts recorded by FBRM. Calculation of the ratio of the surface area of the two seed batches added revealed that they have similar total surface area, which implies these two batches of seeds are comparably as effective as seeds. For the same surface area, bigger seeds have larger masses, hence a larger mass of seeds were added for the bigger seeds. As previously stated, the area under the square-weighted CLD is correlated to the mass of the particles in the system. The area under the CLD for the batch of 4 g of 125-212 µm seeds is clearly smaller than the other seed batch (Figure 5-29(a)), hence re-affirming our claim. The normalized CLDs in Figure 5-29(b) show clearly a shift of the CLD along the chord length axis between the different seed batch, a reflection of the different seed sizes. The FBRM statistics in Table 5-6 shows a distinct difference in the mean sizes of the seeds in the systems. The median of the larger sized seeds is presumed to be larger than that for the smaller ones, but unexpectedly, the medians of the two seed batches are similar. Again, both these systems were at the same agitation speed. Hence, it can be explained similarly as before that in the case of the bigger mass of bigger seeds, only the smaller particles are suspended near the FBRM window. Heath et al. (2002) pointed out that the probability of a particle being detected is proportional to its diameter, introducing a bias. Also, although the seed range of 300-355 µm is smaller than 125-212 µm,

both the non-weighted and square-weighted standard deviation of the latter is greater. In view of the fact that glycine crystals are not fragile and hence abrasion of the crystals by the impeller is not significant, the only plausible reason for the disparity is again due to the same agitation speed used in both cases.
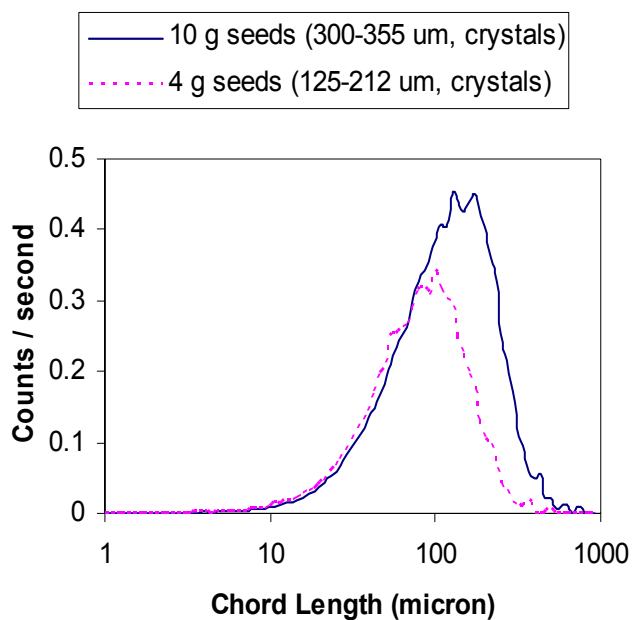
(a)
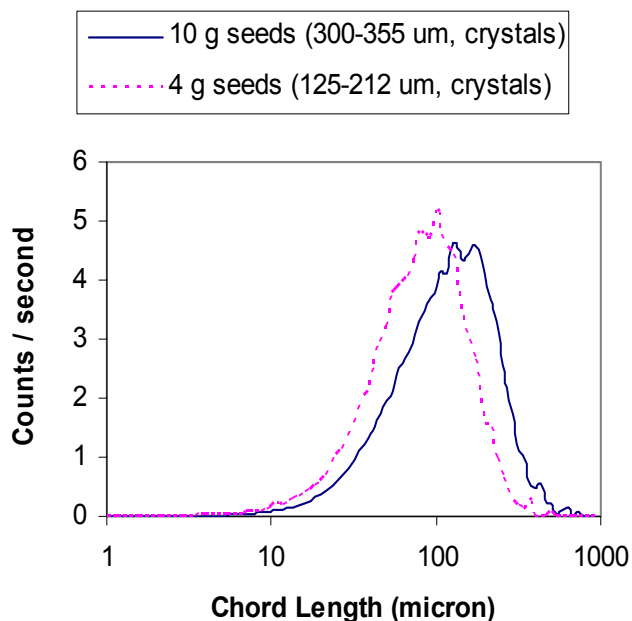
(b)

Figure 5-29: (a) Square-weighted and (b) Normalized square-weighted CLDs of different masses of seeds of different sizes for glycine system.

Table 5-6: Glycine system: FBRM statistics (in the 1-1000 μm range) for initial CLDs of different seed masses of different sizes.

FBRM Statistic	Weighting	300-355 μm (10 g)	125-212 μm (4 g)
Counts per Second	Non-Weighted	500.26	475.78
Median	Non-Weighted	23.51	23.34
Mean	Square-Weighted	142.91	97.50
Standard Deviation	Non-Weighted	42.86	32.06
Standard Deviation	Square-Weighted	91.78	57.83

Taking these into account, a caveat is that comparing different systems based on FBRM data is not conclusive. FBRM data can be used for comparison analysis only for the same system, as differences in shape and size results in bias in the data.

5.17) Summary

With the use of in-line instrumentations as per the PAT initiative, several control strategies for batch cooling crystallization were investigated.

Current common measurement techniques include the use of the ATR-FTIR, FBRM, and PVM. Further improvements of such instruments promise breakthrough of the present bottleneck, allowing greater precision and more information of the crystallization process. The choice of the control approach may dramatically influence the performances of a certain crystallization process. The purpose of this thesis is to evaluate the benefits of new methods of controlling crystallization against conventional ones, thereby providing a useful guide for the crystallization control community in the choice of the appropriate control strategy.

Most of the previous control studies have dealt with finding the open-loop temperature versus time trajectory that optimizes some characteristics of the desired crystal size distribution. Such an approach requires the development of a detailed model with accurate growth and nucleation kinetics, which is time-consuming and inaccurate due to varying process conditions. An alternative control approach is to control the solution concentration as a function of temperature, so that the crystallizer follows a preset supersaturation curve in the metastable zone. The metastable zone is bounded by the solubility and the metastable curves. The setpoint supersaturation curve is the result of the

compromise between the desire of fast crystal growth rate that occurs near the metastable curve and low nucleation rate which takes place near the solubility curve. The advantage of this approach is that, unlike to the first approach, it does not require the derivation of accurate growth and nucleation kinetics. Hence, it can be easily implemented based on the practical determination of the solubility and metastable curves of a certain crystallization process.

Closed-loop feedback S-control was implemented on glycine-water system, and found not to give any significant benefits over simple T-control for seeded systems. The insignificant difference between the effectiveness of S-control and T-control may be due to the fast growth rate of glycine. The average linear growth rate at cooling rate of 0.3 $^{\circ}$C/min is estimated to be 62 nm/s by optical microscopy, and that is equivalent to at least 124 molecules being incorporated onto the crystal per second. As a result, the controlling factor in glycine crystallization is the nucleation step. Once nuclei are formed (or seeds are introduced), the magnitude of the cooling rate will not make a significant difference because of the rapid growth rate.

Product consistency was however not observed in unseeded systems due to the inconsistent initial seeds generated by primary nucleation, even when S-control was implemented. Hence, consistent seeding is important for glycine crystallization from water if reproducibility of product quality and process conditions are of prime concern.

In view of the constraint on the number of available vessel ports in industry, a decision often has to be made between insertion of a probe for in-line monitoring or for external seeding. An in-line probe has the advantage of enabling constant monitoring such that any off-specification instants in the entire process are pinpointed. On the other hand, primary nucleation is random and unpredictable, conferring much discrepancy in the product crystals. Hence, a trade-off exists between the two choices. A strategy is thus proposed here to use FBRM to automatically detect primary nucleation and condition the seeds so generated to achieve consistency in different unseeded runs.

The novel concept of a closed feedback loop involving FBRM was successfully implemented on the glycine-water and paracetamol-water systems. Whereas product crystal consistency could not be achieved previously for unseeded glycine-water system even with the implementation of sophisticated S-control, this technique made it possible. FBRM was first used to detect the onset of primary nucleation, after which the cooling temperature ramp in approaching nucleation was automatically halted. Subsequently, a heating ramp was initiated to dissolve the fines such that the CLDs attain a pre-determined setpoint c.v. This step ensured the achievement of consistent initial seeds generated by primary nucleation. As proven previously, consistency in the initial seeds ensured consistency in the product crystals, regardless of the ensuing temperature profile.

Table 5-7 gives the averaged FBRM statistics the system before the implementation of T-control or S-control (point B in Figure 5-8). The inconsistencies of primary nuclei are obvious in average variability (the value after the ± signs) of eight separate runs each. The enormous benefit of using FBRM monitoring and control is obvious in the significant reduction in the average variability (values after ± sign). Although external seeding still seems to be the most consistent, external seeding has its attendant problems as described earlier; hence the technique of internally generating the seeds is an advantageous option.

Table 5-7: Glycine system: Averaged FBRM statistics for various seeding methods for eight different runs each.

Averaged FBRM Statistics	Unseeded (primary nuclei)	Externally seeded	Internally generated seeds
Mean	122.76 ± 35.75	99.10 ± 1.61	149.80 ± 6.02
Standard Deviation	106.49 ± 40.28	61.45 ± 2.36	103.96 ± 5.47

6) Overall Conclusion and Future Opportunities

6.1) Conclusions

- The novel concept of using FBRM in a feedback loop in the control of batch cooling crystallization has been successfully implemented.

- Two techniques involving this closed loop have been proposed.

    - To detect the onset of primary nucleation.

    - To achieve consistent internally generated seeds in unseeded systems, hence providing a viable alternative to external seeding.

- A successful control strategy for unseeded crystallization systems involves the following procedure:

    1. Monitor the onset of primary nucleation using FBRM.

    2. Adjust the system c.v. derived from FBRM statistics to achieve consistent internally generated 'seeds'.

    3. Implement T-control or S-control.

- Internally generated seeds are as reproducible as external seeds.

- Techniques have been proven to work for glycine-water and paracetamol-water systems.

6.2) Future Opportunities

There are a few compelling trends in the field of solution crystallization research.

The first is crystallization control. The vast majority of papers on crystallization control have investigated the control of some characteristic (e.g., weight mean size) of the CSD. The aim is of obtaining better quality crystals in terms of shape, size distribution, purity etc by means of measuring supersaturation and crystal sizes in-line. "Good crystalline product" can mean a pure product, a special size distribution or a good filterable product. In addition, the process should also be optimized, which means low energy consumption, small volume, easily handled products, and no unusable batches (Ulrich, 2003). Most crystallization processes are batch processes, and it is essential to operate them with a controlled temperature program, taking into account the need to adjust the supersaturation level to optimize growth rate. Furthermore, the crystallization must start at the right moment in the middle of the MZW (Fujiwara et al., 2005). It is also important to know the MZW in relation to process conditions.

Sensor development is hence the prime issue. Despite the urgent need for progress in the measurement of accurate and reliable process data, available

sensors are lagging far behind the progress in software for computer simulations of crystallization processes (Ulrich and Jones, 2004). To control crystal growth at an optimum level requires constant information regarding the position of the process with respect to both the supersaturation of the system and the MZW under the pertinent process conditions. Since the MZW is dependent partly on impurities and these are increasing in concentration in process time, only a control by means of a sensor for the metastability of the system can provide a complete control (Ulrich, 2003). New sensors have been developed, for example using infrared spectrometer (refer to Chapter 3.2) and as an ultrasound technique (Ruecroft et al., 2005; Gracin et al., 2005; Guo et al., 2005; Kim et al., 2003; Sayan and Ulrich, 2002; Hipp et al., 2000; Cains et al., 1998). Additionally, there are control algorithms and powerful software tools available. Other concepts involve observing the evolution of the CSD and using this as sensor information for the control of the crystallizer, as is done in this work.

The second trend is the molecular modeling of crystals, to achieve a better understanding and control of crystal shapes and the effects of additives and solvents. The focus is on finding "tailor made additives" by computer simulations. The additive should influence the crystal shape to help the post crystallization operations like solid-liquid separation or the solid handling. The computer simulation should save time and lower laboratory costs. The initiation and progress of this research arena is due to the fast development of hardware and software in computer science in the last 20 years.

The main idea is first to simulate the crystal behavior of the pure compound from fundamental data, then to simulate what an impurity molecule does to the crystal. The commercially available software packages still cannot simulate everything due to the incorporated model assumptions and additional algorithms are required (Simons et al., 2004; Cue et al., 2001; Bellies et al., 2001; Chen et al., 1994). In the near future, the screening of substances in order to find one which can change the crystals from needles or plates to more bulky bodies will be possible at the computer level rather than in the laboratory (Ulrich et al., 2003). The progress in the last few years must be sustained in the years to come, so that much money and time can be saved by this way of searching.

The third trend is for a more detailed insight and control of polymorphism and pseudo polymorphism of the crystal products. There has been a rapid growth of experimental literature devoted to the study of polymorphism, with the desired objective being to produce one polymorph while avoiding others. Unexpected or undesired polymorphic transformation of pharmaceutical is often observed during manufacturing processes including crystallization, which has serious consequences in terms of U.S. Food and Drug Administration (FDA) approval of the drug use in human subjects (Morris et al., 2001). The increase in crystallization research in this field has shown a marked increase, as it is important to the food and pharmaceuticals industries. To ensure consistent production of the desired polymorph, better control over the crystallization

process is needed. Strategies for obtaining the desired polymorphs include seeding, choice of solvents, and crystal engineering (see (Beckmann, 2000; Threlfall, 2000; Yu et al., 2000) and references therein). Although the theoretical framework for solvent-mediated polymorphic transformation (Davey et al., 1986) is available, it is still difficult to predict and control during pharmaceutical crystallization (Rodrigues-Hornedo and Murphy, 1999). In a high-throughput evaluation of various crystallization conditions for paracetamol polymorphs, some irreproducibility was observed, consistent with the known intractable nature of the polymorphic transformation (Peterson et al., 2002). For the efficient design of robust and reliable crystallization processes, a more integrated approach based on underlying physical mechanisms is desired rather than trial-and-error. Fujiwara et al. (2005) believe that controlling polymorphic transformation during pharmaceutical crystallization is an area where the implementation of more advanced modeling and control strategies can make a great impact.

Another area where modeling and control strategies can be beneficial is macromolecular crystallization. Due to recent developments in genomics and proteomics, there has been an increasing demand in protein crystallization for structure-based drug design. For faster protein structure determination, high-throughput approaches have been developed for rapid screening of numerous crystallization conditions that result in protein crystal formation (Fujiwara et al., 2005). Because many of the protein crystals produced this way are not of diffraction quality, there is a need for optimization of high-throughput protein

crystallization process to produce large high quality crystals for structural analysis (Chayen and Saridakis, 2002). It has been shown that larger crystals of several model proteins, such as lysozyme and aprotinin, can be obtained by controlling the supersaturation level by changing the temperature or the ionic strength of the solution (Tamagawa et al., 2002; Schall et al., 1996; Jones et al., 2001). This strategy or a more advanced control strategy could be used in combination with a high-throughput technique to improve protein crystal growth. Protein crystallization is also important in manufacture of biopharmaceuticals. Therapeutic proteins require different crystal characteristics, where small uniform crystals with narrow distribution are preferred (Merkle and Jen, 2002). Also, they are produced at a much larger scale than proteins for structural studies. In this respect, a better understanding of issues associated with scale-up, such as the effect of mixing on protein crystallization, is desired. Currently, insulin is the only therapeutic protein commonly produced in crystalline form (Shenoy et al., 2001). Recently it was shown that some crystalline proteins exhibited increased stability compared to the amorphous form, suggesting that an increasing number of therapeutic proteins may be produced in the crystalline form in formulation (Shenoy et al., 2001). These recent developments in drug delivery and biotechnology open many opportunities to apply advanced control strategies in the crystallization of proteins and other biomolecules.

Solution crystallization has much to offer to continuing research. If the speed of research can be maintained, more prediction based knowledge rather than

experience and experiments can be expected in the future and will make crystallization an even more interesting technology for purification and particle design.

References

1.   Abbas, A.; Nobbs, D.; Romagnoli, J. A., Investigation of on-line optical particle characterization in reaction, and cooling crystallization systems. Current state of the art. *Measurement Science & Technology* **2002,** 13, (3), 349-356.

2.   Agarwal, P.; Berglund, K. A., In situ monitoring of calcium carbonate polymorphs during batch crystallization in the presence of polymeric additives using Raman spectroscopy. *Crystal Growth & Design* **2003,** 3, (6), 941-946.

3.   Alander, E. M.; Uusi-Penttila, M. S.; Rasmuson, A. C., Agglomeration of paracetamol during crystallization in pure and mixed solvents. *Industrial & Engineering Chemistry Research* **2004,** 43, (2), 629-637.

4.   Alander, E. M.; Uusi-Penttila, M. S.; Rasmuson, A. C., Characterization of paracetamol agglomerates by image analysis and strength measurement. *Powder Technology* **2003,** 130, (1-3), 298-306.

5.   Aldridge, P. K.; Evans, C. L.; Ward, H. W.; Colgan, S. T.; Boyer, N.; Gemperline, P. J., Near-IR detection of polymorphism and process-related substances. *Analytical Chemistry* **1996,** 68, (6), 997-1002.

6.   Alfano, J. C.; Carter, P. W.; Dunham, A. J.; Nowak, M. J.; Tubergen, K. R., Polyelectrolyte-induced aggregation of microcrystalline cellulose: Reversibility and shear effects. *Journal of Colloid and Interface Science* **2000,** 223, (2), 244-254.

7.   Al-Zoubi, N.; Kachrimanis, K.; Malamataris, S., Effects of harvesting and cooling on crystallization and transformation of orthorhombic paracetamol in ethanolic solution. *European Journal of Pharmaceutical Sciences* **2002,** 17, (1-2), 13-21.

8.   Attarakih, M. M.; Bart, H. J.; Faqir, N. M., Numerical solution of the spatially distributed population balance equation describing the hydrodynamics of interacting liquid-liquid dispersions. *Chemical Engineering Science* **2004,** 59, (12), 2567-2592.

9.   Bagusat, F.; Bohme, B.; Schiller, P.; Mogel, H. J., Shear induced periodic structure changes in concentrated alumina suspensions at constant shear rate monitored by FBRM. *Rheologica Acta* **2005,** 44, (3), 313-318.

10.   Barrera, M. D.; Evans, L. B., Optimal-Design and Operation of Batch Processes. *Chemical Engineering Communications* **1989,** 82, 45-66.

11.   Barrett, P., Selecting in-process particle-size analyzers. *Chemical Engineering Progress* **2003,** 99, (8), 26-32.

12.   Barrett, P.; Glennon, B., Characterizing the metastable zone width and solubility curve using lasentec FBRM and PVM. *Chemical Engineering Research & Design* **2002,**

80, (A7), 799-805.

13.   Barrett, P.; Glennon, B., In-line FBRM monitoring of particle size in dilute agitated suspensions. *Particle & Particle Systems Characterization* **1999,** 16, (5), 207-211.

14.   Barrett, P.; Smith, B.; Worlitschek, J.; Bracken, V.; O'Sullivan, B.; O'Grady, D., A review of the use of process analytical technology for the understanding and optimization of production batch crystallization processes. *Organic Process Research & Development* **2005,** 9, (3), 348-355.

15.   Barrett, P. B.; Becker, R., Nucleation, solubility, and polymorph identification: The interrelationship as monitored with lasentec FBRM. *Abstracts of Papers of the American Chemical Society* **2002,** 223, U641-U642.

16.   Barrett, P. B.; Ward, J. A., Case study: Tracking a polymorphic transition using FBRM, PVM, Raman, FTIR and calorimetry. *Abstracts of Papers of the American Chemical Society* **2003,** 225, U960-U960.

17.   Barthe, S.; Rousseau, R. W., Utilization of focused beam reflectance measurement in the control of crystal size distribution in a batch cooled crystallizer. *Chemical Engineering & Technology* **2006,** 29, (2), 206-211.

18.   Beckmann, W., Seeding the desired polymorph: Background, possibilities, limitations, and case studies. *Organic Process Research & Development* **2000,** 4, (5), 372-383.

19.   Beilles, S.; Cardinael, P.; Ndzie, E.; Petit, S.; Coquerel, G., Preferential crystallisation and comparative crystal growth study between pure enantiomer and racemic mixture of a chiral molecule: 5-ethyl-5-methylhydantoin. *Chemical Engineering Science* **2001,** 56, (7), 2281-2294.

20.   Benesch, T.; Meier, U.; John, E.; Blatter, F.; Schutz, W., Influences of physicochemical parameters on the separation of colloidal organics. *Filtration & Separation* **2004,** 41, (8), 35-40.

21.   Birch, M.; Fussell, S. J.; Higginson, P. D.; McDowall, N.; Marziano, I., Towards a PAT-Based strategy for crystallization development. *Organic Process Research & Development* **2005,** 9, (3), 360-364.

22.   Black, S. N.; Quigley, K.; Parker, A., A well-behaved crystallisation of a pharmaceutical compound. *Organic Process Research & Development* **2006,** 10, (2), 241-244.

23.   Bloemen, H. H. J.; De Kroon, M. G. M., Transformation of chord length distributions into particle size distributions using least squares techniques. *Particulate Science and Technology* **2005,** 23, (4), 377-386.

24.   Borissova, A.; Dashova, Z.; Lai, X.; Roberts, K. J., Examination of the semi-batch

crystallization of benzophenone from saturated methanol solution via aqueous antisolvent drowning-out as monitored in-process using ATR FTIR spectroscopy. *Crystal Growth & Design* **2004,** 4, (5), 1053-1060.

25. Braatz, R. D., Advanced control of crystallization processes. *Annual Reviews in Control* **2002,** 26, (1), 87-99.

26. Braatz, R. D.; Fujiwara, M.; Ma, D. L.; Togkalidou, T.; Tafti, D. K., Simulation and new sensor technologies for industrial crystallization: A review. *International Journal of Modern Physics B* **2002,** 16, (1-2), 346-353.

27. Buckton, G.; Yonemochi, E.; Hammond, J.; Moffat, A., The use of near infra-red spectroscopy to detect changes in the form of amorphous and crystalline lactose. *International Journal of Pharmaceutics* **1998,** 168, (2), 231-241.

28. Cains, P. W.; Martin, P. D.; Price, C. J., The use of ultrasound in industrial chemical synthesis and crystallization. 1. Applications to synthetic chemistry. *Organic Process Research & Development* **1998,** 2, (1), 34-48.

29. Cerreta, M.; Liebel, J. In *Crystal Size Distribution Control During Batch Crystallization*, Lasentec Users' Forum 2000, Orlando, 2000; Orlando, 2000.

30. Chayen, N. E.; Saridakis, E., Protein crystallization for genomics: towards high-throughput optimization techniques. *Acta Crystallographica Section D-Biological Crystallography* **2002,** 58, 921-927.

31. Chen, B. D.; Garside, J.; Davey, R. J.; Maginn, S. J.; Matsuoka, M., Growth of M-Chloronitrobenzene Crystals in the Presence of Tailor-Made Additives - Assignment of the Polar Axes from Morphological Calculations. *Journal of Physical Chemistry* **1994,** 98, (12), 3215-3221.

32. Chew, C. M.; Ristic, R. I.; Dennehy, R. D.; De Yoreo, J. J., Crystallization of paracetamol under oscillatory flow mixing conditions. *Crystal Growth & Design* **2004,** 4, (5), 1045-1052.

33. Choi, Y. C.; Morgenroth, E., Monitoring biofilm detachment under dynamic changes in shear stress using laser-based particle size analysis and mass fractionation. *Water Science and Technology* **2003,** 47, (5), 69-76.

34. Chung, S. H.; Ma, D. L.; Braatz, R. D., Optimal seeding in batch crystallization. *Canadian Journal of Chemical Engineering* **1999,** 77, (3), 590-596.

35. Clarke, M. A.; Bishnoi, P. R., Determination of the intrinsic kinetics of CO2 gas hydrate formation using in situ particle size analysis. *Chemical Engineering Science* **2005,** 60, (3), 695-709.

36. Clarke, M. A.; Bishnoi, P. R., Determination of the intrinsic rate constant and activation energy of CO2 gas hydrate decomposition using in-situ particle size analysis.

Chemical Engineering Science **2004,** 59, (14), 2983-2993.

37.   Cue, C. C.; Salvador, A. R. R.; Morales, S. A.; Rodriguez, F. L. F.; Gonzalez, P. P., Raffinose-sucrose crystal interaction modelling. *Journal of Crystal Growth* **2001,** 231, (1-2), 280-289.

38.   Custers, J. P. A.; Hersmis, M. C.; Meuldijk, J.; Vekemans, J. A. J. M.; Hulshof, L. A., 3,4,5-Tri-dodecyloxybenzoic acid: Combining reaction engineering and chemistry in the development of an attractive tool to assist scaling up solid-liquid reactions. *Organic Process Research & Development* **2002,** 6, (5), 645-651.

39.   Davey, R. J.; Cardew, P. T.; Mcewan, D.; Sadler, D. E., Rate Controlling Processes in Solvent-Mediated Phase-Transformations. *Journal of Crystal Growth* **1986,** 79, (1-3), 648-653.

40.   De Clercq, B.; Lant, P. A.; Vanrolleghem, P. A., Focused beam reflectance technique for in situ particle sizing in wastewater treatment settling tanks. *Journal of Chemical Technology and Biotechnology* **2004,** 79, (6), 610-618.

41.   del Rio, R. M.; Rousseau, R. W., Batch and tubular-batch crystallization of paracetamol: Crystal size distribution and polymorph formation. *Crystal Growth & Design* **2006,** 6, (6), 1407-1414.

42.   Deneau, E.; Steele, G., An in-line study of oiling out and crystallization. *Organic Process Research & Development* **2005,** 9, (6), 943-950.

43.   Doki, N.; Seki, H.; Takano, K.; Asatani, H.; Yokota, M.; Kubota, N., Process control of seeded batch cooling crystallization of the metastable alpha-form glycine using an in-situ ATR-FTIR spectrometer and an in-situ FBRM particle counter. *Crystal Growth & Design* **2004,** 4, (5), 949-953.

44.   Dowding, P. J.; Goodwin, J. W.; Vincent, B., Factors governing emulsion droplet and solid particle size measurements performed using the focused beam reflectance technique. *Colloids and Surfaces a-Physicochemical and Engineering Aspects* **2001,** 192, (1-3), 5-13.

45.   Dunham, A. J.; Tubergen, K. R.; Govoni, S. T.; Alfano, J. C., The effects of dissolved and colloidal substances on flocculation of mechanical pulps. *Journal of Pulp and Paper Science* **2000,** 26, (3), 95-101.

46.   Dunuwila, D. D.; Berglund, K. A., ATR FTIR spectroscopy for in situ measurement of supersaturation. *Journal of Crystal Growth* **1997,** 179, (1-2), 185-193.

47.   Dunuwila, D. D.; Berglund, K. A., Identification of infrared spectral features related to solution structure for utilization in solubility and supersaturation measurements. *Organic Process Research & Development* **1997,** 1, (5), 350-354.

48.   Dunuwila, D. D.; Carroll, L. B.; Berglund, K. A., An Investigation of the Applicability

of Attenuated Total-Reflection Infrared-Spectroscopy for Measurement of Solubility and Supersaturation of Aqueous Citric-Acid Solutions. *Journal of Crystal Growth* **1994,** 137, (3-4), 561-568.

49.   Eaton, J. W.; Rawlings, J. B., Feedback-Control of Chemical Processes Using Online Optimization Techniques. *Computers & Chemical Engineering* **1990,** 14, (4-5), 469-479.

50.   Femioyewo, M. N.; Spring, M. S., Studies on Paracetamol Crystals Produced by Growth in Aqueous-Solutions. *International Journal of Pharmaceutics* **1994,** 112, (1), 17-28.

51.   Feng, L. L.; Berglund, K. A., Application of ATR-FTIR in controlled cooling batch crystallization. *Abstracts of Papers of the American Chemical Society* **2002,** 223, U641-U641.

52.   Fevotte, G., New perspectives for the on-line monitoring of pharmaceutical crystallization processes using in situ infrared spectroscopy. *International Journal of Pharmaceutics* **2002,** 241, (2), 263-278.

53.   Fujiwara, M.; Chow, P. S.; Ma, D. L.; Braatz, R. D., Paracetamol crystallization using laser backscattering and ATR-FTIR spectroscopy: Metastability, agglomeration, and control. *Crystal Growth & Design* **2002,** 2, (5), 363-370.

54.   Fujiwara, M.; Nagy, Z. K.; Chew, J. W.; Braatz, R. D., First-principles and direct design approaches for the control of pharmaceutical crystallization. *Journal of Process Control* **2005,** 15, (5), 493-504.

55.   Gahn, C.; Mersmann, A., The Brittleness of Substances Crystallized in Industrial-Processes. *Powder Technology* **1995,** 85, (1), 71-81.

56.   Garcia, E.; Hoff, C.; Veesler, S., Dissolution and phase transition of pharmaceutical compounds. *Journal of Crystal Growth* **2002,** 237, 2233-2239.

57.   Garcia, E.; Veesler, S.; Boistelle, R.; Hoff, C., Crystallization and dissolution of pharmaceutical compounds - An experimental approach. *Journal of Crystal Growth* **1999,** 199, 1360-1364.

58.   Garside, J.; Mersmann, A.; Nyvlt, J., *Measurement of Crystal Growth and Nucleation Rates.* Institution of Chemical Engineers (IChemE): 2002.

59.   Ge, X. M.; Zhang, L.; Bai, F. W., Impacts of yeast floc size distributions on their observed rates for substrate uptake and product formation. *Enzyme and Microbial Technology* **2006,** 39, (2), 289-295.

60.   Gracin, S.; Uusi-Penttila, M.; Rasmuson, A. C., Influence of ultrasound on the nucleation of polymorphs of p-aminobenzoic acid. *Crystal Growth & Design* **2005,** 5, (5), 1787-1794.

61.   Granberg, R. A.; Bloch, D. G.; Rasmuson, A. C., Crystallization of paracetamol in acetone-water mixtures. *Journal of Crystal Growth* **1999,** 199, 1287-1293.

62.   Granberg, R. A.; Rasmuson, A. C., Crystal growth rates of paracetamol in mixtures of water plus acetone plus toluene. *Aiche Journal* **2005,** 51, (9), 2441-2456.

63.   Groen, H.; Roberts, K. J., An examination of the crystallization of urea from supersaturated aqueous and aqueous-methanol solutions as monitored in-process using ATR FTIR spectroscopy. *Crystal Growth & Design* **2004,** 4, (5), 929-936.

64.   Groen, H.; Roberts, K. J., Nucleation, growth, and pseudo-polymorphic behavior of citric acid as monitored in situ by attenuated total reflection Fourier transform infrared spectroscopy. *Journal of Physical Chemistry B* **2001,** 105, (43), 10723-10730.

65.   Gron, H.; Borissova, A.; Roberts, K. J., In-process ATR-FTIR spectroscopy for closed-loop supersaturation control of a batch crystallizer producing monosodium glutamate crystals of defined size. *Industrial & Engineering Chemistry Research* **2003,** 42, (1), 198-206.

66.   Gunawan, R.; Ma, D. L.; Fujiwara, M.; Braatz, R. D., Identification of kinetic parameters in multidimensional crystallization processes. *International Journal of Modern Physics B* **2002,** 16, (1-2), 367-374.

67.   Guo, Z.; Zhang, M.; Li, H.; Wang, J.; Kougoulos, E., Effect of ultrasound on anti-solvent crystallization process. *Journal of Crystal Growth* **2005,** 273, (3-4), 555-563.

68.   Heath, A. R.; Bahri, P. A.; Fawell, P. D.; Farrow, J. B., Polymer flocculation of calcite: Experimental results from turbulent pipe flow. *Aiche Journal* **2006,** 52, (4), 1284-1293.

69.   Heath, A. R.; Bahri, P. A.; Fawell, P. D.; Farrow, J. B., Polymer flocculation of calcite: Relating the aggregate size to the settling rate. *Aiche Journal* **2006,** 52, (6), 1987-1994.

70.   Heath, A. R.; Fawell, P. D.; Bahri, P. A.; Swift, J. D., Estimating average particle size by focused beam reflectance measurement (FBRM). *Particle & Particle Systems Characterization* **2002,** 19, (2), 84-95.

71.   Hendriksen, B. A.; Grant, D. J. W.; Meenan, P.; Green, D. A., Crystallisation of paracetamol (acetaminophen) in the presence of structurally related substances. *Journal of Crystal Growth* **1998,** 183, (4), 629-640.

72.   Hentschel, M. L.; Page, N. W., Selection of descriptors for particle shape characterization. *Particle & Particle Systems Characterization* **2003,** 20, (1), 25-38.

73.   Hipp, A. K.; Walker, B.; Mazzotti, M.; Morbidelli, M., In-situ monitoring of batch crystallization by ultrasound spectroscopy. *Industrial & Engineering Chemistry Research* **2000,** 39, (3), 783-789.

74.		Hu, Q.; Rohani, S.; Jutan, A., Modelling and optimization of seeded batch crystallizers. *Computers & Chemical Engineering* **2005,** 29, (4), 911-918.

75.		Hu, S. Y. B.; Wiencek, J. M.; Arnold, M. A., Application of near-infrared spectra on temperature-controlled protein crystallization - A simulation study. *Applied Biochemistry and Biotechnology* **2001,** 94, (2), 179-196.

76.		Hukkanen, E. J.; Braatz, R. D., Measurement of particle size distribution in suspension polymerization using in situ laser backscattering. *Sensors and Actuators B-Chemical* **2003,** 96, (1-2), 451-459.

77.		Jeffers, P.; Raposo, S.; Lima-Costa, M. E.; Connolly, P.; Glennon, B.; Kieran, P. M., Focussed beam reflectance measurement (FBRM) monitoring of particle size and morphology in suspension cultures of Morinda citrifolia and Centaurea calcitrapa. *Biotechnology Letters* **2003,** 25, (23), 2023-2028.

78.		Jones, A. G., *Crystallization Process Systems*. 1st ed.; Butterworth-Heinemann: Oxford, 2002.

79.		Jones, A. G., Optimal operation of a batch cooling crystallizer. *Chemical Engineering Science* **1974,** 29, (5), 1075-1087.

80.		Jones, A. G.; Mullin, J. W., Programmed cooling crystallization of potassium sulphate solutions. *Chemical Engineering Science* **1974,** 26, 369-377.

81.		Jones, W. F.; Wiencek, J. M.; Darcy, P. A., Improvements in lysozyme crystal quality via temperature-controlled growth at low ionic strength. *Journal of Crystal Growth* **2001,** 232, (1-4), 221-228.

82.		Kim, K. J.; Mersmann, A., Estimation of metastable zone width in different nucleation processes. *Chemical Engineering Science* **2001,** 56, (7), 2315-2324.

83.		Kim, K. J.; Ryu, S. K., Nucleation of thiourea adduct crystals with cyclohexane-methylcyclopentane system. *Chemical Engineering Communications* **1997,** 159, 51-66.

84.		Kim, S. J.; Wei, C. K.; Kiang, S., Crystallization process development of an active pharmaceutical ingredient and particle engineering via the use of ultrasonics and temperature cycling. *Organic Process Research & Development* **2003,** 7, (6), 997-1001.

85.		Kim, Y. S.; Del Rio, J. R. M.; Rousseau, R. W., Solubility and prediction of the heat of solution of sodium naproxen in aqueous solutions. *Journal of Pharmaceutical Sciences* **2005,** 94, (9), 1941-1948.

86.		Kougoulos, E.; Jones, A. G.; Jennings, K. H.; Wood-Kaczmar, M. W., Use of focused beam reflectance measurement (FBRM) and process video imaging (PVI) in a modified mixed suspension mixed product removal (MSMPR) cooling crystallizer. *Journal of Crystal Growth* **2005,** 273, (3-4), 529-534.

87.   Kougoulos, E.; Jones, A. G.; Wood-Kaczmar, M. W., Estimation of crystallization kinetics for an organic fine chemical using a modified continuous cooling mixed suspension mixed product removal (MSMPR) crystallizer. *Journal of Crystal Growth* **2005,** 273, (3-4), 520-528.

88.   Kougoulos, E.; Jones, A. G.; Wood-Kaczmar, M. W., A hybrid CFD compartmentalization modeling framework for the scaleup of batch cooling crystallization processes. *Chemical Engineering Communications* **2006,** 193, (8), 1008-1023.

89.   Kougoulos, E.; Jones, A. G.; Wood-Kaczmar, M. W., Modelling particle disruption of an organic fine chemical compound using Lasentec focussed beam reflectance monitoring (FBRM) in agitated suspensions. *Powder Technology* **2005,** 155, (2), 153-158.

90.   Lahav, M.; Leiserowitz, L., The effect of solvent on crystal growth and morphology. *Chemical Engineering Science* **2001,** 56, (7), 2245-2253.

91.   Lewiner, F.; Fevotte, G.; Klein, J. P.; Puel, F., Improving batch cooling seeded crystallization of an organic weed-killer using on-line ATR FTIR measurement of supersaturation. *Journal of Crystal Growth* **2001,** 226, (2-3), 348-362.

92.   Lewiner, F.; Klein, J. P.; Puel, F.; Fevotte, G., On-line ATR FTIR measurement of supersaturation during solution crystallization processes. Calibration and applications on three solute/solvent systems. *Chemical Engineering Science* **2001,** 56, (6), 2069-2084.

93.   Li, M.; Wilkinson, D.; Patchigolla, K., Comparison of particle size distributions measured using different techniques. *Particulate Science and Technology* **2005,** 23, (3), 265-284.

94.   Li, M. Z.; Wilkinson, D., Determination of non-spherical particle size distribution from chord length measurements. Part 1: Theoretical analysis. *Chemical Engineering Science* **2005,** 60, (12), 3251-3265.

95.   Li, M. Z.; Wilkinson, D.; Patchigolla, K., Determination of non-spherical particle size distribution from chord length measurements. Part 2: Experimental validation. *Chemical Engineering Science* **2005,** 60, (18), 4992-5003.

96.   Li, T. L.; Morris, K. R.; Park, K., Influence of solvent and crystalline supramolecular structure on the formation of etching patterns on acetaminophen single crystals: A study with atomic force microscopy and computer simulation. *Journal of Physical Chemistry B* **2000,** 104, (9), 2019-2032.

97.   Li, T. L.; Morris, K. R.; Park, K., Influence of tailor-made additives on etching patterns of acetaminophena single crystals. *Pharmaceutical Research* **2001,** 18, (3), 398-402.

98.   Liotta, V.; Sabesan, V., Monitoring and feedback control of supersaturation using ATR-FTIR to produce an active pharmaceutical ingredient of a desired crystal size. *Organic Process Research & Development* **2004,** 8, (3), 488-494.

99. Loan, M.; Parkinson, G.; Newman, M.; Farrow, J., Iron oxy-hydroxide crystallization in a hyd ro metallurgical residue. *Journal of Crystal Growth* **2002,** 235, (1-4), 482-488.

100. Ma, D. L.; Braatz, R. D., Robust identification and control of batch processes. *Computers & Chemical Engineering* **2003,** 27, (8-9), 1175-1184.

101. Ma, D. L.; Chung, S. H.; Braatz, R. D., Worst-case performance analysis of optimal batch control trajectories. *Aiche Journal* **1999,** 45, (7), 1469-1476.

102. Ma, D. L.; Chung, S. H.; Braatz, R. D., Worst-case performance analysis of optimal batch control trajectories. *Aiche Journal* **1999,** 45, (7), 1469-1476.

103. Madras, G.; McCoy, B. J., Transition from nucleation and growth to Ostwald ripening. *Chemical Engineering Science* **2002,** 57, (18), 3809-3818.

104. Masy, J. C.; Cournil, M., Using a Turbidimetric Method to Study the Kinetics of Agglomeration of Potassium-Sulfate in a Liquid-Medium. *Chemical Engineering Science* **1991,** 46, (2), 693-701.

105. Matthews, H. B.; Miller, S. M.; Rawlings, J. B., Model identification for crystallization: Theory and experimental verification. *Powder Technology* **1996,** 88, (3), 227-235.

106. Mayrhofer, B.; Nyvlt, J., Programmed Cooling of Batch Crystallizers. *Chemical Engineering and Processing* **1988,** 24, (4), 217-220.

107. McDonald, K. A.; Jackman, A. P.; Hurst, S., Characterization of plant suspension cultures using the focused beam reflectance technique. *Biotechnology Letters* **2001,** 23, (4), 317-324.

108. Merkle, H. P.; Jen, A., A crystal clear solution for insulin delivery. *Nature Biotechnology* **2002,** 20, (8), 789-790.

109. Mersmann, A., Supersaturation and nucleation. *Chemical Engineering Research & Design* **1996,** 74, (A7), 812-820.

110. Mersmann, A.; Bartosch, K., How to predict the metastable zone width. *Journal of Crystal Growth* **1998,** 183, (1-2), 240-250.

111. Miller, S. M.; Rawlings, J. B., Model Identification and Control Strategies for Batch Cooling Crystallizers. *Aiche Journal* **1994,** 40, (8), 1312-1327.

112. Monnier, O.; Fevotte, G.; Hoff, C.; Klein, J. P., Model identification of batch cooling crystallizations through calorimetry and image analysis. *Chemical Engineering Science* **1997,** 52, (7), 1125-1139.

113. Morris, K. R.; Griesser, U. J.; Eckhardt, C. J.; Stowell, J. G., Theoretical

approaches to physical transformations of active pharmaceutical ingredients during manufacturing processes. *Advanced Drug Delivery Reviews* **2001,** 48, (1), 91-114.

114. Moscosa-Santillan, M.; Bals, O.; Fauduet, H.; Porte, C.; Delacroix, A., Study of batch crystallization and determination of an alternative temperature-time profile by on-line turbidity analysis - application to glycine crystallization. *Chemical Engineering Science* **2000,** 55, (18), 3759-3770.

115. Muller, M.; Meier, U.; Wieckhusen, D.; Beck, R.; Pfeffer-Hennig, S.; Schneeberger, R., Process development strategy to ascertain reproducible API polymorph manufacture. *Crystal Growth & Design* **2006,** 6, (4), 946-954.

116. Mullin, J. W., *Crystallization.* 4th ed.; Butterworth-Heinemann: Oxford ; Boston, 2001; p xv, 594 p.

117. Mullin, J. W.; Jancic, S. J., Interpretation of metastable zone width. *Chemical Engineering Research and Design* **1979**, (57), 188.

118. Mullin, J. W.; Nyvlt, J., Programmed cooling of batch crystallizers. *Chemical Engineering Science* **1971,** 26, (3), 369-377.

119. Nagy, Z. K.; Braatz, R. D., Open-loop and closed-loop robust optimal control of batch processes using distributional and worst-case analysis. *Journal of Process Control* **2004,** 14, (4), 411-422.

120. Nagy, Z. K.; Braatz, R. D., Robust nonlinear model predictive control of batch processes. *Aiche Journal* **2003,** 49, (7), 1776-1786.

121. Negro, C.; Sanchez, L. M.; Fuente, E.; Blanco, A.; Tijero, J., Polyacrylamide induced flocculation of a cement suspension. *Chemical Engineering Science* **2006,** 61, (8), 2522-2532.

122. Norris, T.; Aldridge, P. K.; Sekulic, S. S., Near-infrared spectroscopy. *Analyst* **1997,** 122, (6), 549-552.

123. Nyvlt, J., Kinetics of nucleation in solutions. *Journal of Crystal Growth* **1968,** 3/4, 377.

124. Nyvlt, J., Nucleation and Growth Rate in Mass Nucleation. *Progress in Crystal Growth and Characterization* **1984,** 9, 335-370.

125. Nyvlt, J.; Rychly, R.; Gottfrid, J.; Wurzelova, J., Metastable zone width of some aqueous solutions. *Journal of Crystal Growth* **1970,** 6, 151.

126. Ono, T.; ter Horst, J. H.; Jansens, P. J., Quantitative measurement of the polymorphic transformation of L-glutamic acid using in-situ Raman spectroscopy. *Crystal Growth & Design* **2004,** 4, (3), 465-469.

127.   O'Sullivan, B.; Barrett, P.; Hsiao, G.; Carr, A.; Glennon, B., In situ monitoring of polymorphic transitions. *Organic Process Research & Development* **2003,** 7, (6), 977-982.

128.   O'Sullivan, B.; Glennon, B., Application of in situ FBRM and ATR-FTIR to the monitoring of the polymorphic transformation of D-mannitol. *Organic Process Research & Development* **2005,** 9, (6), 884-889.

129.   Otte, X.; Lejeune, R.; Thunus, L., Fourier Transform Infrared Spectrometry (FTIR) for qualitative and quantitative analysis of azodicarboxamide and its potential impurities. *Analytica Chimica Acta* **1997,** 355, (1), 7-13.

130.   Owen, A. T.; Fawell, P. D.; Swift, J. D.; Farrow, J. B., The impact of polyacrylamide flocculant solution age on flocculation performance. *International Journal of Mineral Processing* **2002,** 67, (1-4), 123-144.

131.   Pacek, A. W.; Moore, I. P. T.; Nienow, A. W.; Calabrese, R. V., Video Technique for Measuring Dynamics of Liquid-Liquid Dispersion during Phase Inversion. *Aiche Journal* **1994,** 40, (12), 1940-1949.

132.   Parsons, A. R.; Black, S. N.; Colling, R., Automated measurement of metastable zones for pharmaceutical compounds. *Chemical Engineering Research & Design* **2003,** 81, (A6), 700-704.

133.   Patience, D. B.; Rawlings, J. B., Particle-shape monitoring and control in crystallization processes. *Aiche Journal* **2001,** 47, (9), 2125-2130.

134.   Paulaime, A. M.; Seyssiecq, I.; Veesler, S., The influence of organic additives on the crystallization and agglomeration of gibbsite. *Powder Technology* **2003,** 130, (1-3), 345-351.

135.   Pearson, A. P.; Glennon, B.; Kieran, P. M., Comparison of morphological characteristics of Streptomyces natalensis by image analysis and focused beam reflectance measurement. *Biotechnology Progress* **2003,** 19, (4), 1342-1347.

136.   Pearson, A. P.; Glennon, B.; Kieran, P. M., Monitoring of cell growth using the focused beam reflectance method. *Journal of Chemical Technology and Biotechnology* **2004,** 79, (10), 1142-1147.

137.   Peterson, M. L.; Morissette, S. L.; McNulty, C.; Goldsweig, A.; Shaw, P.; LeQuesne, M.; Monagle, J.; Encina, N.; Marchionna, J.; Johnson, A.; Gonzalez-Zugasti, J.; Lemmo, A. V.; Ellis, S. J.; Cima, M. J.; Almarsson, O., Iterative high-throughput polymorphism studies on acetaminophen and an experimentally derived structure for form III. *Journal of the American Chemical Society* **2002,** 124, (37), 10958-10959.

138.   Pollanen, K.; Hakkinen, A.; Reinikainen, S. P.; Louhi-Kultanen, M.; Nystrom, L., ATR-FTIR in monitoring of crystallization processes: comparison of indirect and direct OSC methods. *Chemometrics and Intelligent Laboratory Systems* **2005,** 76, (1), 25-35.

139.   Pollanen, K.; Hakkinen, A. W.; Reinikainen, S. P.; Louhi-Kultanen, A.; Nystrom, L., A study on batch cooling crystallization of sulphathiazole - Process monitoring using ATR-FTIR and product characterization by automated image analysis. *Chemical Engineering Research & Design* **2006,** 84, (A1), 47-59.

140.   Prasad, K. V. R.; Ristic, R. I.; Sheen, D. B.; Sherwood, J. N., Crystallization of paracetamol from solution in the presence and absence of impurity. *International Journal of Pharmaceutics* **2001,** 215, (1-2), 29-44.

141.   Prasad, K. V. R.; Ristic, R. I.; Sheen, D. B.; Sherwood, J. N., Dissolution kinetics of paracetamol single crystals. *International Journal of Pharmaceutics* **2002,** 238, (1-2), 29-41.

142.   Profir, V. M.; Furusjo, E.; Danielsson, L. G.; Rasmuson, A. C., Study of the crystallization of mandelic acid in water using in situ ATR-IR spectroscopy. *Crystal Growth & Design* **2002,** 2, (4), 273-279.

143.   Puel, F.; Fevotte, G.; Klein, J. P., Simulation and analysis of industrial crystallization processes through multidimensional population balance equations. Part 1: a resolution algorithm based on the method of classes. *Chemical Engineering Science* **2003,** 58, (16), 3715-3727.

144.   Puel, F.; Marchal, P.; Klein, J., Habit transient analysis in industrial crystallization using two dimensional crystal sizing technique. *Chemical Engineering Research & Design* **1997,** 75, (A2), 193-205.

145.   Qiu, Y. F.; Rasmuson, A. C., Estimation of Crystallization Kinetics from Batch Cooling Experiments. *Aiche Journal* **1994,** 40, (5), 799-812.

146.   Ravnjak, D.; Fuente, E.; Negro, C.; Blanco, A., Flocculation of pulp fractions induced by fluorescently-labelled PDADMAC. *Cellulose Chemistry and Technology* **2006,** 40, (1-2), 77-85.

147.   Rawlings, J. B.; Miller, S. M.; Witkowski, W. R., Model Identification and Control of Solution Crystallization Processes - a Review. *Industrial & Engineering Chemistry Research* **1993,** 32, (7), 1275-1296.

148.   Rawlings, J. B.; Witkowski, W. R.; Eaton, J. W., Modeling and Control of Crystallizers. *Powder Technology* **1992,** 69, (1), 3-9.

149.   Richmond, W. R.; Jones, R. L.; Fawell, P. D., The relationship between particle aggregation and rheology in mixed silica-titania suspensions. *Chemical Engineering Journal* **1998,** 71, (1), 67-75.

150.   Rodriguez-Hornedo, N.; Murphy, D., Significance of controlling crystallization mechanisms and kinetics in pharmaceutical systems. *Journal of Pharmaceutical Sciences* **1999,** 88, (7), 651-660.

151.   Rohani, S.; Horne, S.; Murthy, K., Control of product quality in batch crystallization of pharmaceuticals and fine chemicals. Part 1: Design of the crystallization process and the effect of solvent. *Organic Process Research & Development* **2005,** 9, (6), 858-872.

152.   Rohani, S.; Horne, S.; Murthy, K., Control of product quality in batch crystallization of pharmaceuticals and fine chemicals. Part 2: External control. *Organic Process Research & Development* **2005,** 9, (6), 873-883.

153.   Ruecroft, G.; Hipkiss, D.; Ly, T.; Maxted, N.; Cains, P. W., Sonocrystallization: The use of ultrasound for improved industrial crystallization. *Organic Process Research & Development* **2005,** 9, (6), 923-932.

154.   Ruf, A.; Worlitschek, J.; Mazzotti, M., Modeling and experimental analysis of PSD measurements through FBRM. *Particle & Particle Systems Characterization* **2000,** 17, (4), 167-179.

155.   Salari, A.; Young, R. E., Application of attenuated total reflectance FTIR spectroscopy to the analysis of mixtures of pharmaceutical polymorphs. *International Journal of Pharmaceutics* **1998,** 163, (1-2), 157-166.

156.   Sayan, P.; Ulrich, J., The effect of particle size and suspension density on the measurement of ultrasonic velocity in aqueous solutions. *Chemical Engineering and Processing* **2002,** 41, (3), 281-287.

157.   Schall, C. A.; Riley, J. S.; Li, E.; Arnold, E.; Wiencek, J. M., Application of temperature control strategies to the growth of hen egg-white lysozyme crystals. *Journal of Crystal Growth* **1996,** 165, (3), 299-307.

158.   Scholl, J.; Bonalumi, D.; Vicum, L.; Mazzotti, M.; Muller, M., In situ monitoring and modeling of the solvent-mediated polymorphic transformation of L-glutamic acid. *Crystal Growth & Design* **2006,** 6, (4), 881-891.

159.   Scholl, J.; Vicum, L.; Muller, M.; Mazzotti, M., Precipitation of L-glutamic acid: Determination of nucleation kinetics. *Chemical Engineering & Technology* **2006,** 29, (2), 257-264.

160.   Schwartz, A. M.; Berglund, K. A., In situ monitoring and control of lysozyme concentration during crystallization in a hanging drop. *Journal of Crystal Growth* **2000,** 210, (4), 753-760.

161.   Schwartz, A. M.; Berglund, K. A., The use of Raman spectroscopy for in situ monitoring of lysozyme concentration during crystallization in a hanging drop. *Journal of Crystal Growth* **1999,** 203, (4), 599-603.

162.   Scott, C.; Black, S., In-line analysis of impurity effects an crystallisation. *Organic Process Research & Development* **2005,** 9, (6), 890-893.

163.   Shaikh, A. A.; Salman, A. D.; Mcnamara, S.; Littlewood, G.; Ramsay, F.; Hounslow,

M. J., In situ observation of the conversion of sodium carbonate to sodium carbonate monohydrate in aqueous suspension. *Industrial & Engineering Chemistry Research* **2005,** 44, (26), 9921-9930.

164.   Shenoy, B.; Wang, Y.; Shan, W. Z.; Margolin, A. L., Stability of crystalline proteins. *Biotechnology and Bioengineering* **2001,** 73, (5), 358-369.

165.   Sherwood, J. N.; Ristic, R. I., The influence of mechanical stress on the growth and dissolution of crystals. *Chemical Engineering Science* **2001,** 56, (7), 2267-2280.

166.   Shi, B.; Frederick, W. J.; Rousseau, R. W., Effects of calcium and other ionic impurities on the primary nucleation of burkeite. *Industrial & Engineering Chemistry Research* **2003,** 42, (12), 2861-2869.

167.   Simons, S. J. R.; Pratola, Y.; Jones, A. G.; Brunsteiner, M.; Price, S. L., Towards a fundamental understanding of the mechanics of crystal agglomeration: A microscopic and molecular approach. *Particle & Particle Systems Characterization* **2004,** 21, (4), 276-283.

168.   Sistare, F.; Berry, L. S. P.; Mojica, C. A., Process analytical technology: An investment in process knowledge. *Organic Process Research & Development* **2005,** 9, (3), 332-336.

169.   Skrdla, P. J.; Antonucci, V.; Crocker, L. S.; Wenslow, R. M.; Wright, L.; Zhou, G., A simple quantitative FT-IR approach for the study of a polymorphic transformation under crystallization slurry conditions. *Journal of Pharmaceutical and Biomedical Analysis* **2001,** 25, (5-6), 731-739.

170.   Starbuck, C.; Spartalis, A.; Wai, L.; Wang, J.; Fernandez, P.; Lindemann, C. M.; Zhou, G. X.; Ge, Z. H., Process optimization of a complex pharmaceutical polymorphic system via in situ Raman spectroscopy. *Crystal Growth & Design* **2002,** 2, (6), 515-522.

171.   Swift, J. D.; Simic, K.; Johnston, R. R. M.; Fawell, P. D.; Fartow, J. B., A study of the polymer flocculation reaction in a linear pipe with a focused beam reflectance measurement probe. *International Journal of Mineral Processing* **2004,** 73, (2-4), 103-118.

172.   Tadayyon, A.; Rohani, S., Control of fines suspension density in the fines loop of a continuous KCl crystallizer using transmittance measurement and an FBRM (R) probe. *Canadian Journal of Chemical Engineering* **2000,** 78, (4), 663-673.

173.   Tai, C. Y.; Wu, J. F.; Rousseau, R. W., Interfacial Supersaturation, Secondary Nucleation, and Crystal-Growth. *Journal of Crystal Growth* **1992,** 116, (3-4), 294-306.

174.   Takiyama, H.; Shindo, K.; Matsuoka, M., Effects of undersaturation on crystal size distribution in cooling type batch crystallization. *Journal of Chemical Engineering of Japan* **2002,** 35, (11), 1072-1077.

175.   Tamagawa, R. E.; Miranda, E. A.; Berglund, K. A., Raman spectroscopic

monitoring and control of aprotinin supersaturation in hanging-drop crystallization. *Crystal Growth & Design* **2002,** 2, (4), 263-267.

176. Tamagawa, R. E.; Miranda, E. A.; Berglund, K. A., Simultaneous monitoring of protein and (NH4)(2)SO4 concentrations in aprotinin hanging-drop crystallization using Raman spectroscopy. *Crystal Growth & Design* **2002,** 2, (6), 511-514.

177. Tavare, N. S., Batch Crystallizers. *Reviews in Chemical Engineering* **1991,** 7, (3-4), 211-355.

178. Tavare, N. S., *Industrial crystallization : process simulation analysis and design.* Plenum Press: New York, 1995; p xxviii, 527 p.

179. Threlfall, T., Crystallisation of polymorphs: Thermodynamic insight into the role of solvent. *Organic Process Research & Development* **2000,** 4, (5), 384-390.

180. Togkalidou, T.; Braatz, R. D.; Johnson, B. K.; Davidson, O.; Andrews, A., Experimental design and inferential modeling in pharmaceutical crystallization. *Aiche Journal* **2001,** 47, (1), 160-168.

181. Togkalidou, T.; Fujiwara, M.; Patel, S.; Braatz, R. D. In *Crystal shape distribution using FBRM and PVM instrumentation*, Lasentec FBRM Users' Forum, Barcelona, Spain, 2001; Barcelona, Spain, 2001.

182. Togkalidou, T.; Fujiwara, M.; Patel, S.; Braatz, R. D., Solute concentration prediction using chemometrics and ATR-FTIR spectroscopy. *Journal of Crystal Growth* **2001,** 231, (4), 534-543.

183. Togkalidou, T.; Tung, H. H.; Sun, Y.; Andrews, A. T.; Braatz, R. D., Parameter estimation and optimization of a loosely bound aggregating pharmaceutical crystallization using in situ infrared and laser backscattering measurements. *Industrial & Engineering Chemistry Research* **2004,** 43, (19), 6168-6181.

184. Togkalidou, T.; Tung, H. H.; Sun, Y. K.; Andrews, A.; Braatz, R. D., Solution concentration prediction for pharmaceutical crystallization processes using robust chemometrics and ATR FTIR spectroscopy. *Organic Process Research & Development* **2002,** 6, (3), 317-322.

185. Ulrich, J., Growth-Rate Dispersion - a Review. *Crystal Research and Technology* **1989,** 24, (3), 249-257.

186. Ulrich, J., Solution crystallization - Developments and new trends. *Chemical Engineering & Technology* **2003,** 26, (8), 832-835.

187. Ulrich, J.; Jones, M. J., Industrial crystallization - Developments in research and technology. *Chemical Engineering Research & Design* **2004,** 82, (A12), 1567-1570.

188. Ulrich, J.; Strege, C., Some aspects of the importance of metastable zone width

and nucleation in industrial crystallizers. *Journal of Crystal Growth* **2002,** 237, 2130-2135.

189.   Wang, X. J.; Ching, C. B., A systematic approach for preferential crystallization of 4-hydroxy-2-pyrrolidone: Thermodynamics, kinetics, optimal operation and in-situ monitoring aspects. *Chemical Engineering Science* **2006,** 61, (8), 2406-2417.

190.   Wang, Z. Z.; Wang, J. K.; Dang, L. P., Nucleation, growth, and solvated behavior of erythromycin as monitored in situ by using FBRM and PVM. *Organic Process Research & Development* **2006,** 10, (3), 450-456.

191.   Ward, J. D.; Mellichamp, D. A.; Doherty, M. F., Choosing an operating policy for seeded batch crystallization. *Aiche Journal* **2006,** 52, (6), 2046-2054.

192.   Warstat, A.; Ulrich, J., Seeding during batch cooling crystallization - An initial approach to heuristic rules. *Chemical Engineering & Technology* **2006,** 29, (2), 187-190.

193.   Winn, D.; Doherty, M. F., Modeling crystal shapes of organic materials grown from solution. *Aiche Journal* **2000,** 46, (7), 1348-1367.

194.   Workman, J.; Veltkamp, D. J.; Doherty, S.; Anderson, B. B.; Creasy, K. E.; Koch, M.; Tatera, J. F.; Robinson, A. L.; Bond, L.; Burgess, L. W.; Bokerman, G. N.; Ullman, A. H.; Darsey, G. P.; Mozayeni, F.; Bamberger, J. A.; Greenwood, M. S., Process analytical chemistry. *Analytical Chemistry* **1999,** 71, (12), 121R-180R.

195.   Worlitschek, J.; Hocker, T.; Mazzotti, M., Restoration of PSD from chord length distribution data using the method of projections onto convex sets. *Particle & Particle Systems Characterization* **2005,** 22, (2), 81-98.

196.   Worlitschek, J.; Mazzotti, M., Choice of the focal point position using lasentec FBRM. *Particle & Particle Systems Characterization* **2003,** 20, (1), 12-17.

197.   Worlitschek, J.; Mazzotti, M., Model-based optimization of particle size distribution in batch-cooling crystallization of paracetamol. *Crystal Growth & Design* **2004,** 4, (5), 891-903.

198.   Wynn, E. J. W., Relationship between particle-size and chord-length distributions in focused beam reflectance measurement: stability of direct inversion and weighting. *Powder Technology* **2003,** 133, (1-3), 125-133.

199.   Yin, Q. X.; Wang, J. K.; Zhang, M. J.; Wang, Y. L., Influence of nucleation mechanisms on the multiplicity patterns of agglomeration-controlled crystallization. *Industrial & Engineering Chemistry Research* **2001,** 40, (26), 6221-6227.

200.   Yoon, S. Y.; Deng, Y. L., Flocculation and reflocculation of clay suspension by different polymer systems under turbulent conditions. *Journal of Colloid and Interface Science* **2004,** 278, (1), 139-145.

201.   Yu, L.; Reutzel-Edens, S. M.; Mitchell, C. A., Crystallization and polymorphism of

conformationally flexible molecules: Problems, patterns, and strategies. *Organic Process Research & Development* **2000,** 4, (5), 396-402.

202.   Yu, L. X.; Lionberger, R. A.; Raw, A. S.; D'Costa, R.; Wu, H. Q.; Hussain, A. S., Applicatlons of process analytical technology to crystallization processes. *Advanced Drug Delivery Reviews* **2004,** 56, (3), 349-369.

203.   Yu, Z. Q.; Chow, P. S.; Tan, R. B. H., Application of attenuated total reflectance-Fourier transform infrared (ATR-FTIR) technique in the monitoring and control of anti-solvent crystallization. *Industrial & Engineering Chemistry Research* **2006,** 45, (1), 438-444.

204.   Yu, Z. Q.; Tan, R. B. H.; Chow, P. S., Effects of operating conditions on agglomeration and habit of paracetamol crystals in anti-solvent crystallization. *Journal of Crystal Growth* **2005,** 279, (3-4), 477-488.

205.   Zhou, G. X.; Fujiwara, M.; Woo, X. Y.; Rusli, E.; Tung, H. H.; Starbuck, C.; Davidson, O.; Ge, Z. H.; Braatz, R. D., Direct design of pharmaceutical antisolvent crystallization through concentration control. *Crystal Growth & Design* **2006,** 6, (4), 892-898.